Summary (English)

The project is motivated by the goal of increasing the wind penetration in the danish grid from 20% to 50% by 2020. However as wind power is an intermittent resource, it is necessary to be able to consume power when it is available and lower the consumption when the production is lower. In other words, to allow for a larger amount of wind power in the power grid, a more flexible power consumption is needed. Several smart grid project have therefore been initialized to make the grid more flexible.

One such project which sets out to do this is the "Styr din varmepumpe" (Control your heat pump) project. This project allows an aggregator to control a the heat pumps of a large number of houses. By allowing this aggregator to bid in the energy markets it can bid on behalf on many houses and simply distribute the power to the houses that are most in need. If however the aggregator bids for more or less power than the houses consumes it is punished monetarily. This means that it is necessary with some sort of prediction tool which will accurately predict the combined power consumption of the houses over some period.

In this project this is done by developing a model of an average house which can predict the indoor temperature based on the outside temperature, the solar intensity and the heat pump. As a large amount of data is available from the "Styr din varmepumpe" project model identification can be used to design a model which corresponds with the generated data. The problem with this is, however, that the houses are inhabited. This means that not only are the measurements contaminated with unpredictable noise from human behavior, they are also running in a closed loop setting. Closed loop identification is notoriously difficult as the noise and the input can no longer be assumed independent. However, methods exist that allow for closed loop model identification. One of these is the Hansen Scheme.

The Hansen Scheme turns the problem of identifying a closed loop system into the problem of estimating the open loop error between some nominal system and the real system. For this to be done the system must be factorized into coprime factorizations. Coprime factorizations of a linear time invariant system with proportional controllers are well known, while coprime factorizations with integral control and feedforward are less so. These factorizations are therefore derived and analytically and experimentally proven.

The nominal model of a house is constructed by taking the average values for different parameters for a number of houses along with some educated estimations. The structure of the controller is designed and the values of it are generated using linear quadratic methods. This gives a nominal system which is used in model identification. The initial model identification shows significant improvements over the nominal model but also highlights where the nominal model is lacking. Using this information the nominal model is revised and a new identification is attempted. The results are dramatically better than the initial model. The conclusion of this is that the method of model identification works and is capable of identifying a model which may be used in prediction of power use.

Resumé (Dansk)

Projektet er motiveret af målet om at øge vind energi delen i det danske elnet fra 20% til 50% i 2020. Idet vindenergi er en uregelmæssig ressource, er det nødvendigt at kunne forbruge strøm, når den er tilgængelig og sænke forbruget, når produktionen er lavere. Med andre ord, for at give mulighed for en større mængde vindenergi i el-nettet, er der behov for et mere fleksibelt energiforbrug. Adskillige smart grid-projekteter er derfor blevet startet for at gøre energinettet mere fleksibelt.

Et af disse projekter er, "styr din varmepumpe". Dette projekt giver en aggregator mulighed for at styre varmepumperne i en lang række af huse. Ved at give aggregatoren mulighed for at byde på energimarkederne kan han byde på vegne af mange huse og blot distribuere energien til de huse, der har størst behov. Hvis aggregatoren byder på mere eller mindre energi en husene forbruger tilsammen bliver han straffet økonomisk. Det er derfor nødvendigt med en metode der er istand til at forudsige hvor meget energi husene vil forbruge over et givet tidsperiode.

Det er i dette projekt gjort ved at udvikle en model for et gennemsnitligt hus der kan forudsige indetemperature udfra ude-temperaturen, sol intensiteten og energiindtaget fra varmepumpen. Det er muligt at bruge model identifikation da der er en stor mængde data tilgængeligt fra, "styr din varmepumpe" projektet. At bruge dette data medføre dog problemet at mange huse er beboede. Al data er derfor ikke kun belagt støj fra bla. menneskelig adfærd, men systemet kører også i lukket sløjfe. Lukke sløjfe identifikation er betydeligt mere besværligt da støj og input ikke kan ses som uafhængige. Der findes dog metoder til lukket sløjfe identifikation. En sådan metode er Hansen Scheme.

Hansen Scheme laver lukket sløjfe identifikation af anlægget om til en åben sløjfe identifikation af åben sløjfe fejlen imellem et start gæt og det faktiske anlæg. For at gøre dette bruge man indbyrdes primiske faktoriseringer. Primiske faktoriseringer af en lineær tidsinvariant-system med proportional regulatorer er velkendte, mens indbyrdes primisk faktoriseringer med integreret kontrol og feedforward er mindre. Disse faktoriseringer er derfor afledt samt analytisk og eksperimentelt bevist.

Den nominelle model af et hus er konstrueret ved at tage de gennemsnitlige værdier for forskellige parametre for en række af huse sammen med nogle kvalificerede skøn. Strukturen af regulatoren konstrueret og værdierne af denne designes ved brug af lineær kvadratiske metoder. Dette giver et nominelt system, der anvendes i modelidentifikationen. Den oprindelige model identifikation viser signifikante forbedringer i forhold til den nominelle model, men fremhæver også, hvad den nominelle model mangler. Ved at bruge denne information er den nominelle model blevet revideret, og en ny identifikation er forsøgt. Dette resultere i en dramatisk forbedring i forhold til den oprindelige model. Konklusionen af dette er, at fremgangsmåden ifølge modelidentifikationen virker og er i stand til at identificere en model, som kan anvendes i forudsigelse af strømforbrug.

Closed loop model identification using the Hansen Scheme: Thermal modeling of occupied houses

AALBORG UNIVERSITY
DENMARK

Frederik Juul & André Krabdrup Sekunda

Master Thesis

AALBORG UNIVERSITY
DENMARK

Title:
Closed loop model identification using the Hansen Scheme:
Thermal modeling of occupied houses.

Theme:
Master Thesis

Project period:
Control and Automation 4, Spring 2014

Project group:
Frederik Juul & André Krabdrup Sekunda

Supervisor:
Jan Dimon Bendtsen
Palle Andersen

External Supervisor:
Per Dahlgaard Pedersen

Copies: 5

Pages: 83

Appendix: 6

Project finished: 4-6-2014

All figures generated using Ti*k*Z.

Abstract: In this project model identification of a thermal closed loop system is investigated. The plant is analyzed using first principles and the behavior of the controller is investigated. This leads to nominal model for plant and controller which is used for model identification. The Hansen Scheme method of identifying a plant is explained. The Hansen Scheme necessitates coprime factorizations of the system which are not widely available for PI-controllers with reference feedforward. Coprime factorizations for a such a controller are analytically found and a model identification technique using these factorizations is given. Using this technique on data from the "Styr din varmepumpe"-project a closed loop identification is performed.

Frederik Juul

André Krabdrup Sekunda

Nomenclature

Abbreviations

AAU	Aalborg Universitet
DMI	Danmarks Meteorologiske Institut
PSO	Public Service Obligation
TSO	Transmission System Operator
NRMSE	Normalized Root Mean Square Error

Notation

$\dot{}$	Derivative with respect to time
$\tilde{}$	Right Coprime
$\bar{}$	Left Coprime
$\hat{}$	Estimation

Contents

Nomenclature **v**

1 Introduction **1**
1.1 Energy Markets . . . 1
1.2 Prediction . . . 2

2 Problem Description **5**

3 System Analysis **7**
3.1 House Analysis . . . 7
3.2 Heat Pump Analysis . . . 8

4 Identification Techniques **11**
4.1 Basic Identification . . . 11
4.2 Hansen Scheme . . . 12
4.3 Bezout's Identity . . . 12
4.4 The Hansen Scheme Explained . . . 13
4.5 System Identification Block (S) . . . 15

5 House Model **17**
5.1 Input Parameters and Noise . . . 17
5.2 Model Structure . . . 18
5.3 Initial guess of house model . . . 22

6 Controller Structure **23**
6.1 Controller Design . . . 23
6.2 Observer Design . . . 24
6.3 Closed loop system . . . 25
6.4 Reference feedforward . . . 26

7 Youla-Kucera Parameterization **29**
7.1 Factorizations . . . 30
7.1.1 Right Coprime Factorization of Plant . . . 31
7.1.2 Left Coprime Factorization of Plant . . . 33
7.1.3 Right Coprime Factorization of Controller . . . 35
7.1.4 Left Coprime Factorization of Controller . . . 36
7.2 Algorithm Example . . . 39

8 Model Identification **43**
8.1 Experiment Design . . . 43
8.2 Identification of S . . . 44
8.3 Observations and Results . . . 47

9 Conclusion **51**

10 Discussion **53**

Bibliography **55**

A Energy Flow Check **57**
A.1 Objective . . . 57
A.2 Procedure . . . 57
A.3 Results . . . 58

B Coefficient of Performance **61**
B.1 Objective . . . 61
B.2 Procedure . . . 61
B.3 Results . . . 61

C Identification Data **63**
C.1 Objective . . . 63
C.2 Procedure . . . 63
C.3 Results . . . 64

D Coprime Expansion **65**

E Simulation Example **71**
E.1 Coprime Factorization . . . 75
E.2 Error Calculation . . . 76
E.3 Identification . . . 77
E.4 Model Reduction . . . 78

F Coprime Factorizations **83**

Introduction 1

The danish energy sector is supposed to increase the wind power produced from 20 % to 50 % of the energy usage in Denmark by 2020 [1]. However as windpower is an intermittent resource, it is necessary to be able to consume power when it is available and lower the consumption when the production is lower. In other words, to allow for a larger amount of wind power in the power grid, a more flexible power consumption is needed. Several smart grid project have therefore been initialized to make the grid more flexible [2].

One such project which sets out to do this is the "Styr din varmepumpe" (Control your heat pump) project [3], supported under the ForskEL program. This project allows for a large amount of residential heat pumps to be centrally controlled and monitored, to investigate the amount of power that can be shifted as well as the economic impact of shifting and the wear and tear of the heat pump due to centralized control. This project has generated large amounts of data which can be used to further analyze the differences between different heat pump installations and control strategies.

Heat pumps used to heat up houses is a growing market and already around 27,000 heat pumps are installed in houses in Denmark [4], with a potential of 205,000 households. Being able to control the heat pumps to heat up houses when energy is abundant can therefore lead to a tremendous reduction in peak energy usage.

Since a large supply of wind energy in the grid means a lower price for the energy, this can be a motivating factor for consumers to allow their heat pump to be controlled such that the consumption follows the production. However a major factor in successfully doing so is to keep the indoor temperature within some comfort bounds acceptable to the consumer. This can be hard as the task of both precisely modeling every house in the program and reacting to noise while following a strict preset program may lead to imprecise predictions of power consumption for the individual house.

However, for a centralized aggregator, such as the case with "Styr din varmepumpe", it may be possible to buy a large amount of power, the sum of the expected power consumed, and then distribute this across a large amount of houses. This largely replaces the problem of having a preset amount of power needed to be consumed by the individual heat pump and changes it to one of scheduling the power in the most efficient way.

A consequence of controlling a large portfolio of heat pumps is that it allows the aggregator to participate in the wholesale energy market, buying the energy in bulk and further lowering the prices for the participants. In Denmark this is the Nord Pool Spot market.

1.1 Energy Markets

The Nord Pool Spot market is the market in which the wholesale electricity for the Nordic and Baltic countries is traded. The market covers Denmark, Finland, Sweden, Norway, Estonia and Lithuania [5].

Electricity markets usually consist of a number of producers and retailers. Retailers are often local utilities who participate in the markets on behalf of end-users, who then pay a fixed price for their services. However very large end-users such as large companies may also participate in these markets.

Several different markets exists - For the purpose of this explanation three of them are especially interesting: The bulk power day ahead, the intraday and the regulation market.

The bulk power market is, as the name suggests, concerned with trading bulk power, not unlike how other commodities are traded but with the important distinction that the energy cannot be stored.

Retailers bid for hourly production one day ahead. All bids must be done by 12:00 every day, after which the price is published. This price for power then depend on the supply and demand of the electricity in a given hour. This means that some hours will be cheaper than other hours and that any shiftable consumption should then ideally be moved to the hours with the lowest price, to achieve the lowest total price.

If a retailer agrees to buy a given amount of power for an hour they must use that amount of power. Any discrepancy between the bought and the used amount is by definition sold to or bought from the grid operator, usually at a loss for the retailer.

The intraday market is used to trade bulk power between suppliers and retailers up to two hours before actually needing the power. This means that wind park operators may buy production from someone else to be able to meet their bulk commitment, if the park is producing less than predicted. Similarly, if the temperature is significantly hotter than predicted, a heat pump aggregator may not be able to consume the bulk power bought and would then need to sell the excess power on the intraday market.

The regulation market on the other hand is used for trading regulation capacity. This capacity is the amount of power that the seller must be able to deliver at any given time and is used when there are inconsistencies between the expected and the realized power. This is where the grid operator buys or sells the aforementioned power discrepancy. If everyone is able to *precisely* meet their bulk purchase and production, no amount of regulation power is needed.

Proper prediction is therefore of key importance when participating in the energy markets.

1.2 Prediction

Predicting the behavior of a system necessitates a model. However the behavior of a inhabited house can be extremely hard to model as the behavior of people can be very unpredictable. As the number of people in a house change so does the dynamics. Further, entering and leaving a house often means opening and closing doors, which introduce altered dynamics, just as turning on the stove or fire place introduces new inputs. This noise may dominate the behavior of the system.

The energy use of a very large group of people can however be somewhat predictable - If the door of a single house is opened it doesn't change much in terms of energy consumption for the entire portfolio. Because human behavior can be considered nondeterministic, as one house might need more energy than expected another may use less.

Extending this idea it may be possible to model the behavior of a collection of houses in such a way that the fluctuations of a single house do not dominate the behavior of the collective system.

Such a lumped model could be useful in determining large scale usage predictions, useful in day ahead energy bids.

One problem with the lumped approach is how the system should be modeled. An initial guess would likely be some sort of average value of the different houses that are to be considered, but an in-depth analysis of every house would be not only time consuming but costly as well. Furthermore, even with precise measurements of modeling parameters these could be time variant. Also, the model would ultimately have to be fitted to the measurements from the real houses. Instead, model identification techniques could be employed to both lighten the necessary workload to find a lumped model but also be useful in fitting the model to the measurements.

For this a preliminary analysis of how the system behaves is necessary.

Problem Description 2

When purchasing energy in the day ahead market it is necessary with a prediction of the usage for the following day. Because the indoor temperature and thus the energy usage of a house is heavily dependent on the behavior of its inhabitants this can be difficult to predict. As the amount of houses in the system increases the computational complexity of the algorithm becomes increasingly important for single house modeling. It is therefore desirable that the complete model is computationally simple while still being capable of giving a precise estimate of the heat pumps energy usage. However, when one house use more energy than expected another may use less because of the unknown disturbances, such as external heating sources, change in number of inhabitants and so forth. While this human behavior might be possible to model with a complex noise model, a lumped model capturing a large amount of houses can be expected to lessen the impact of each individuals behavior which may simplify the model.

A top-down approach using a simple first order model was attempted in [4]. While the results were promising, more precise prediction may be made by further considering the thermal characteristics of the houses. Such a method can be used without increasing the complexity of the model above the desired threshold.

Individual versus lumped model

Modeling of heating pumps in houses have been done in several ways. In [6, 7] thermal models of individual houses were designed to predict how the indoor temperature changes with the energy usage of the heat pump. For these models of individual houses it have been shown extremely hard to predict the changes in temperature due to noise such as other heating instruments, human behavior etc. However [7] shows it is possible to design a simple physical model that can predict the indoor temperature for an house with a mean square error of less than 0.1 when all inputs are known. It is therefore believed possible to design a model that capture the characteristics of the house when disregarding the noise. An other approach is to model several houses as one using a lumped model. In [4] a first order model of a group of houses is made, and it is shown that by adding more houses the noise gets easier to model. The first order model used in [4], disregarded the thermal properties of the house to simplify the identification procedure. It is therefore believed possible to improve the results from [4] with a thermal model of several houses, while keeping the model feasible to use for estimation of hourly energy demand in households.

In this project the desired outcome of the model is to give an estimate of the average indoor temperature and thus not needed to predict the changes in the temperature of the individual households. An aggregated model is therefore preferred, which makes it possible to better predict the total energy and reduces the computational effort needed.

It is difficult to obtain data for a system running in open loop when accessing data on the indoor temperature of houses, as data obtained from the "Styr din varmepumpe" project is only available in closed loop. The identification method therefore needs to be able to handle that the data is obtained with a certain controller being part of the system. In this project the focus is on designing a method for modeling of the indoor temperature of houses using data obtained from a closed loop system. The method designed is therefore needed to be able to identify the plant with a specific type of controller applied.

System Analysis 3

To identify the system it is necessary to know some basic characteristics about how a house is heated and cooled. In this chapter the primary facilitators of energy flow through the house are presented and the behavior of these are analyzed. Further the behavior and control laws of a common heat pump are analyzed.

3.1 House Analysis

When it's colder outside than it is inside, any house will lose energy to the outside. During the day, additional energy is put into the house by the sun. However, to keep a comfortable indoor temperature it is necessary to replenish the lost energy and control the inflow of energy. For this, different heating techniques can be used. The focus of this project is houses with heat pump floor heating.

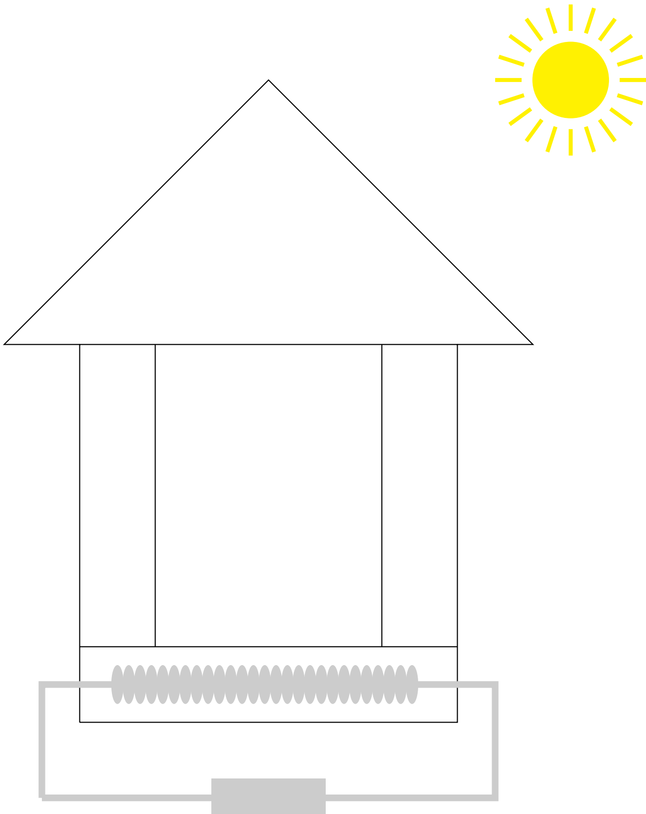

Fig. 3.1: The heat pump, as well as the sun, transfers energy into the houses. The houses lose energy to the outside when the outside temperature is lower then the inside temperature.

While the most basic behavior of the temperature in a house is readily understood, the basic behavior of a heat pump can be more challenging, as both the governing characteristics as well as the specific control laws of a heat pumps are not common knowledge. It is therefore necessary with a deeper analysis of the behavior of a heat pump.

3.2 Heat Pump Analysis

Heat pumps work by moving heat from a heat source to a heat sink. The source is often outside, with effectively infinite energy, while the sink is often inside a contained space, such as a house. The same principle is exploited in refrigerators where the desirable outcome is cooling of a contained space, switching the sink and the source.

Because the heat pump moves energy, rather than generates it, the energy which enters into the sink is greater than the amount of energy expended by the pump itself. This ratio between the energy expended by the pump and the energy transferred to the sink is known as the Coefficient of Performance (COP). This coefficient is dependant on the temperature of both the source and the sink and will vary during use, as the temperature of the source and sink changes.

Condensing Cycle

The energy is moved by exploiting the physical properties of the evaporation / condensing cycle of a refrigerant through the ideal gas law. The refrigerant is compressed and circulated through the system by a compressor. The compressed liquid enters a condenser where energy is released to the sink. The refrigerant then enters and expansion valve where it is expanded and cools down. The cooled down refrigerant then enters the evaporator where energy is absorbed from the source, after which it enters the compressor and the cycle begins anew. This cycle is illustrated on Fig. 3.2.

For the heat pump to function the fluid must be hotter than the sink when in the condenser, while it must be colder than the source when in the evaporator.

Since the heat pump is a closed system, i.e. the amount of fluid remains constant, this simplifies the ideal gas law, $PV = nRT$, to only have two variables - the pressure and the temperature. That means that if the pressure falls, as after the expansion valve, the temperature must fall as well to obey the ideal gas law. The inverse is true as well: An increase in pressure, as seen after the compressor, necessitates an increase in temperature.

Control

To avoid speaking in too general terms, this analysis is based on the DHP series from Danfoss[1]. These heatpumps are considered representative of how the average heatpump works.

According to [8] the heat pumps operate in accordance to their heat demand which is defined as the integrated error between a set temperature and the measured temperature. As this heat demand reach specific set point values, $A1$ and $A2$, the compressor and auxiliary heating unit will turn on to supply heat to the system. When the temperature of the system is above it's reference temperature the integrator value will increase. When the heat demand reaches 0 the compressor turns off. As the temperature is still higher than the reference the integrator value will still increase until the temperature decreases below the reference temperature.

This means that the temperature will constantly, though slowly, fluctuate around its reference temperature.

If however the temperature of the water entering the house, T1, decreases too much compared to the calculated necessary temperature, T2, the integral value changes to the value needed to activate the heat pump, as seen on Fig. 3.4.

[1] DHP-H Opti Pro, DHP-H, DHP-C, DHP-L, DHP-A, DHP-AL

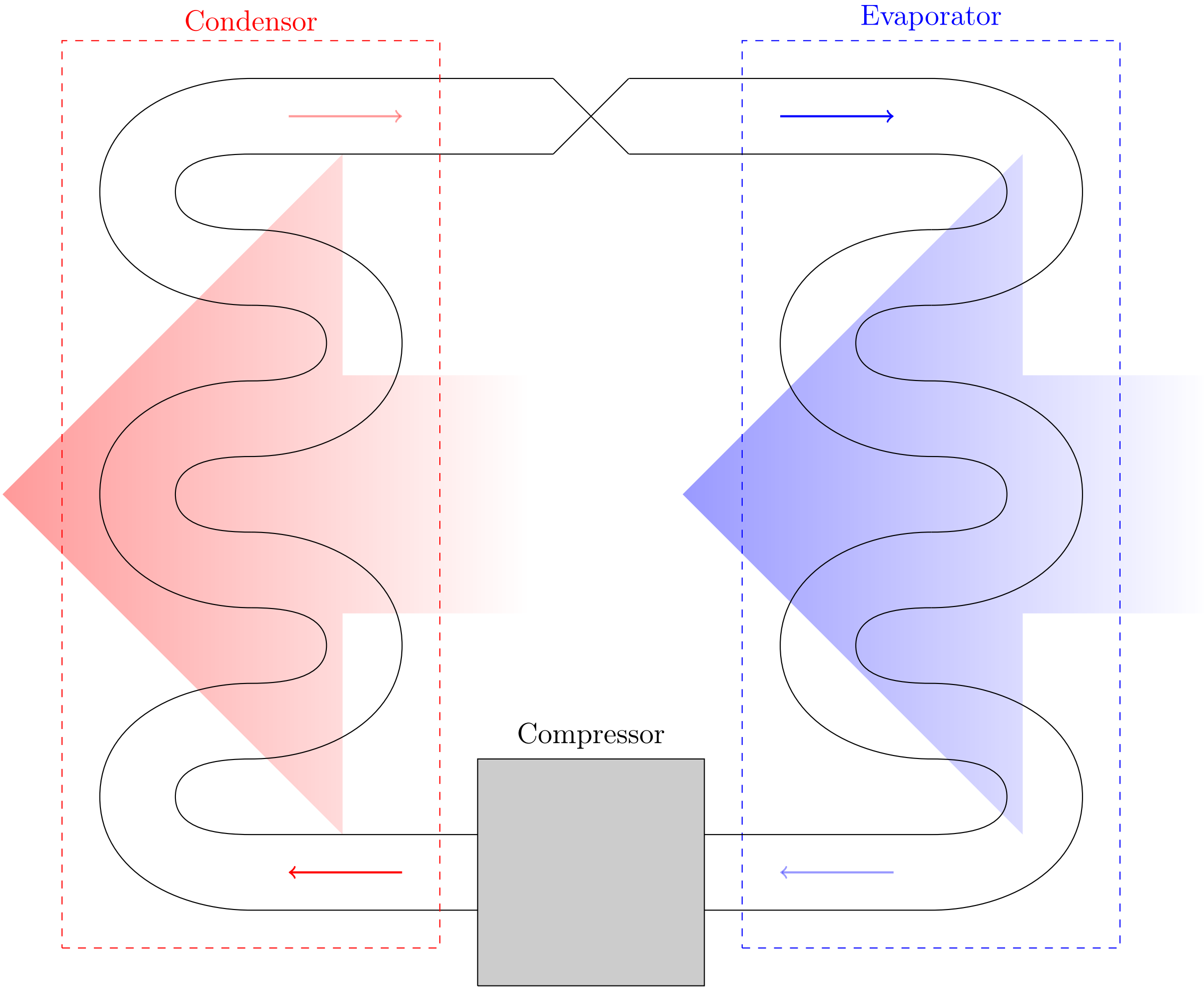

Fig. 3.2: Energy from the source enters the evaporator, heating the refrigerant. This energy is then released to the sink through the condensor.

In other words this regulation scheme is dependent on a proportional error and an integrated error and is in that way similar to how a PI controller works. It is therefore assumed that the behavior of the controller can be approximated by that of a PI controller.

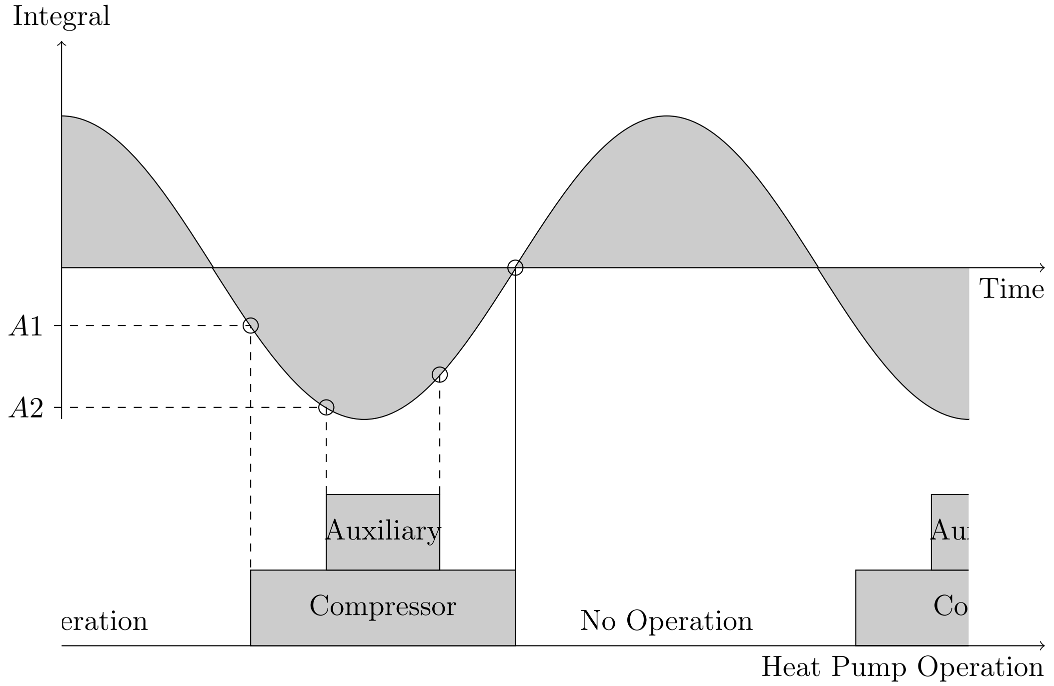

Fig. 3.3: The error between set point and actual temperature is integrated. When this integration reaches a certain value, $A1$, the heat pump is turned on. If the integrator reaches $A2$ the auxiliary heater is turned on as well. These will stay on until predefined shut off values are reached.

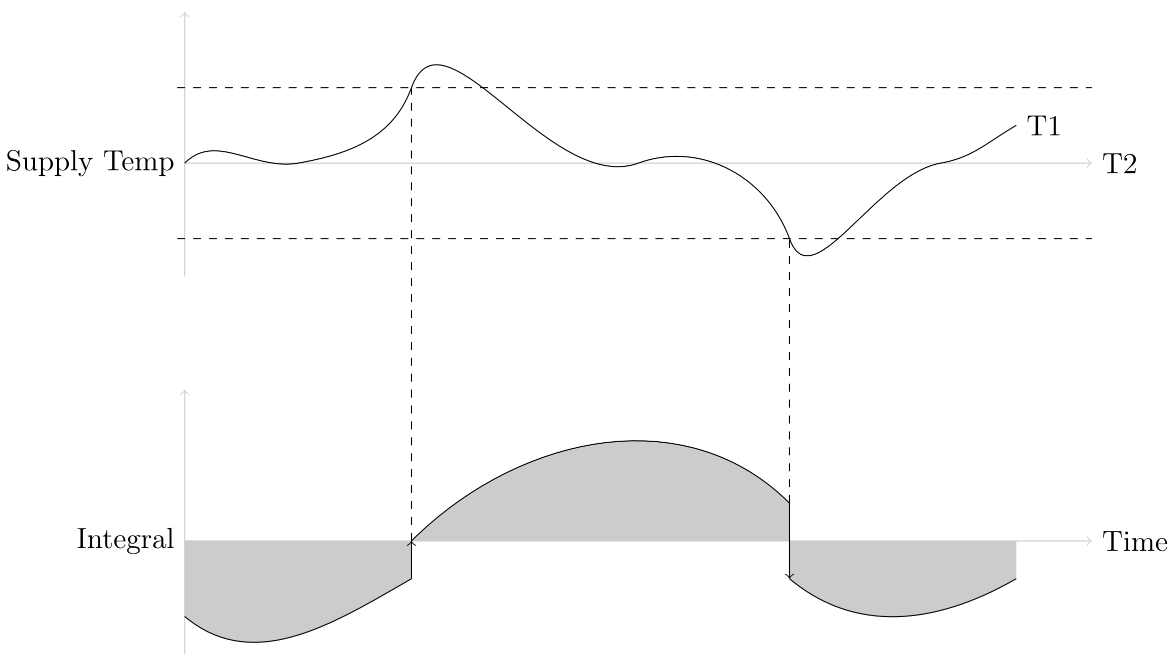

Fig. 3.4: If the difference between the actual and expected supply temperature, T1 and T2, exceed some predefined value the integral value is changed to active or disable the heat pump.

Identification Techniques 4

In this chapter the identification method used for the project will be stated. First the difficulties of some common identification methods are shown and the idea of the Hansen scheme explained. Then the identification method using the Hansen Scheme is derived. Lastly a definition of the plant using the identification method is given.

4.1 Basic Identification

For system identification the goal is to identify the system from the input, u, to the output, y. For an open loop system this task corresponds to Fig. 4.1a, where the task is to identify P with the noise, n, applied to the output signal. To do this task the noise and input signals are assumed independent and the identification can therefore be formulated as in Eq. (4.1).

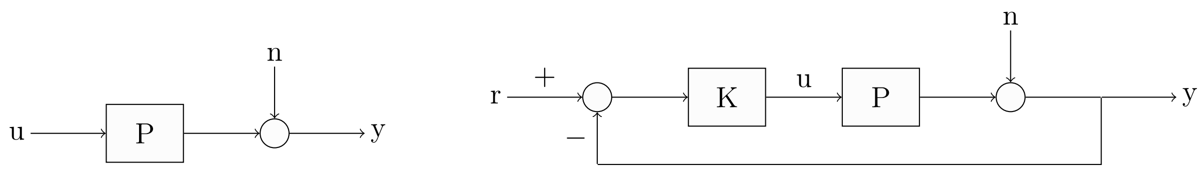

(a) Open loop identification problem

(b) Closed loop identification problem

Fig. 4.1

$$y = Pu + n \tag{4.1}$$

There is a large number of open loop system identification solvers for matlab, such as `n4sid`, `idss` and `ssest`. Open loop identification has received a lot of attention over the years, most notably by Lennart Ljung in [9].

For an open loop system the input and noise are assumed independent which makes the identification straightforward. As explained in [10] the relationship between the input and output does not stay independent of the output noise, n, for a closed loop system. It is therefore much more difficult to identify closed loop systems. However many systems are not possible to model as being open loop. There can be several reasons for why an open loop identification is impossible to perform. It could be because the plant is stabilized by the controller and it is simply impossible to get data from the plant without a controller implemented, the performance might not be acceptable without a controller, or the feedback might simply not be possible to remove [11] [12].

The data used in this project is obtained from a plant being in a closed loop as shown on Fig. 4.1b. It is therefore needed to perform a closed loop identification. The Hansen scheme is one such method, first introduced in [13] and further elaborated in [10].

4.2 Hansen Scheme

The Hansen Scheme transforms a closed loop identification problem into an open loop identification problem by block manipulation. The system is represented as shown on Fig. 4.2 which is equivalent to Fig. 4.1b. On Fig. 4.2 $\tilde{X}\tilde{Y}^{-1}$ is a right coprime factorization of the controller, $\bar{Y}^{-1}\bar{X}$ is the left coprime factorization of the controller and $\tilde{N}\tilde{D}^{-1}$ is the right coprime factorization of the nominal plant. A coprime factorization means that the system have been divided into two subsystems where the greatest common divisor is identity. A more thorough explanation of left and right coprime factorization is given in chapter 7 together with how they are derived in this work.

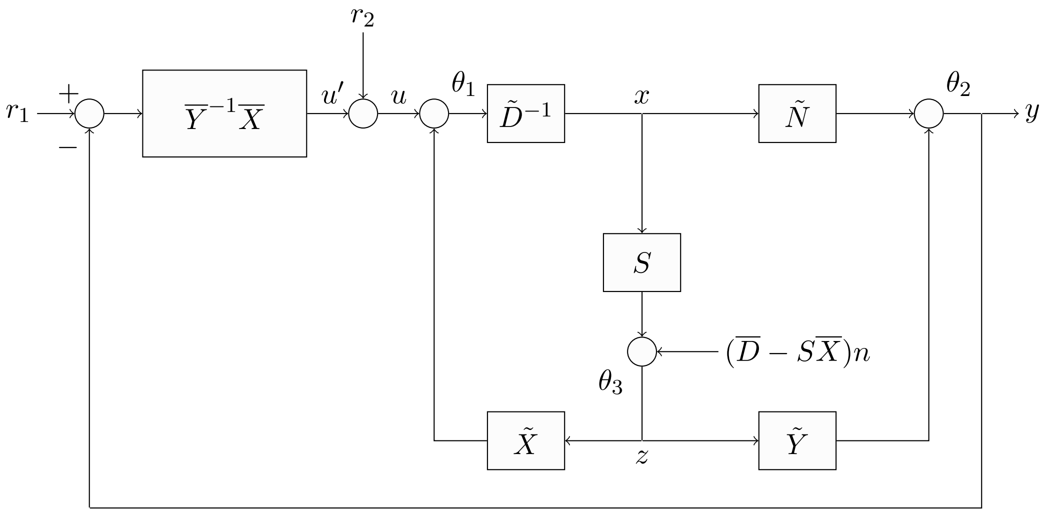

Fig. 4.2: Closed loop system with fractional representation.

4.3 Bezout's Identity

For the Hansen Scheme to hold the polynomials, $\tilde{D}, \tilde{N}, \tilde{Y}$, and $\tilde{X}$, have to satisfy the Bezout Identity. According to Bezouts lemma, for any two polynomials a, b with greatest common divisor g, there exists two other polynomials x, y such that $ax + by = g$. The special case $g = 1$ means that the two polynomials a, b are coprime. For matrices this can be written $\bar{X}\tilde{N} + \bar{Y}\tilde{D} = \bar{N}\tilde{X} + \bar{D}\tilde{Y} = I$. This is known as Bezout's Identity. Therefore a factorization being a coprime factorization is equivalent to it fulfilling the Bezout Identity. Equivalently, this can be written as equation (4.2).

$$\begin{bmatrix} \bar{Y} & \bar{X} \end{bmatrix} \begin{bmatrix} \tilde{D} \\ \tilde{N} \end{bmatrix} = I, \begin{bmatrix} \bar{N} & \bar{D} \end{bmatrix} \begin{bmatrix} \tilde{X} \\ \tilde{Y} \end{bmatrix} = I,$$
$$\begin{bmatrix} -\bar{N} & \bar{D} \end{bmatrix} \begin{bmatrix} \tilde{D} \\ \tilde{N} \end{bmatrix} = 0, \begin{bmatrix} \bar{Y} & \bar{X} \end{bmatrix} \begin{bmatrix} -\tilde{X} \\ \tilde{Y} \end{bmatrix} = 0 \tag{4.2}$$

These four equations can be combined to arrive at what is known as Bezout's Double Identity, as seen in equation (4.3).

$$\begin{bmatrix} \bar{Y} & \bar{X} \\ -\bar{N} & \bar{D} \end{bmatrix} \begin{bmatrix} \tilde{D} & -\tilde{X} \\ \tilde{N} & \tilde{Y} \end{bmatrix} = \begin{bmatrix} I & 0 \\ 0 & I \end{bmatrix} \tag{4.3}$$

4.4 The Hansen Scheme Explained

The main idea is to estimate from x to z instead of estimating from u to y on Fig. 4.1b. To make this estimate possible a relation from r_1 and r_2 to x is needed. From Fig. 4.2 it is easy to see that Eq. (4.4) must be fulfilled at θ_1 and that x can be expressed using Eq. (4.5).

$$\theta_1 = \tilde{X}(Sx + (\bar{D} - S\bar{X})n) + u \tag{4.4}$$
$$x = \tilde{D}^{-1}\theta_1 \tag{4.5}$$

By isolating θ_1 in Eq. (4.5) and substituting into Eq. (4.4) a relation with only x, n and u is found as shown in Eq. (4.6).

$$\tilde{D}x = \tilde{X}(Sx + (\bar{D} - S\bar{X})n) + u \tag{4.6}$$

As stated earlier the input, u, and noise are not independent in a close loop setting, and an expression of u using r_1 and r_2 is therefore found in Eq. (4.7).

$$u = r_2 + (\bar{Y}^{-1}\bar{X})(r_1 - y) \tag{4.7}$$

The input signal is therefore substituted in Eq. (4.6) with Eq. (4.7). Eq. (4.8) shows the point x given with regards to the noise, references and output.

$$\tilde{D}x = \tilde{X}(Sx + (\bar{D} - S\bar{X})n) + r_2 + (\bar{Y}^{-1}\bar{X})(r_1 - y) \tag{4.8}$$
$$(\tilde{D} - \tilde{X}S)x = \tilde{X}(\bar{D} - S\bar{X})n + r_2 + \bar{Y}^{-1}\bar{X}r_1 - \bar{Y}^{-1}\bar{X}y \tag{4.9}$$

Furthermore an expression for θ_2 is needed, which can be seen in Eq. (4.10).

$$\begin{aligned} y &= \tilde{N}x + \tilde{Y}(Sx + (\bar{D} - S\bar{X})n) \\ y &= (\tilde{N} + \tilde{Y}S)x + \tilde{Y}(\bar{D} - S\bar{X})n \end{aligned} \tag{4.10}$$

By multiplying with $\bar{X}$ from the left side in Eq. (4.10) and with $\bar{Y}$ from the left side in Eq. (4.9) we get Eq. (4.11) and Eq. (4.12).

$$\bar{Y}\tilde{X}(\bar{D} - S\bar{X})n = \bar{Y}(\tilde{D} - \tilde{X}S)x - \bar{Y}r_2 - \bar{X}r_1 + \bar{X}y \tag{4.11}$$
$$\bar{X}\tilde{Y}(\bar{D} - S\bar{X})n = \bar{X}y - \bar{X}(\tilde{N} + \tilde{Y}S)x \tag{4.12}$$

To further reduce Eq. (4.11) and Eq. (4.12) 4 equalities given by the Bézout double identity are needed which are shown in Eq. (4.13) to (4.16) and further explained in section 4.3.

$$\bar{Y}\tilde{D} + \bar{X}\tilde{N} = I \tag{4.13}$$
$$\bar{D}\tilde{N} - \bar{N}\tilde{D} = 0 \tag{4.14}$$
$$\bar{X}\tilde{Y} - \bar{Y}\tilde{X} = 0 \tag{4.15}$$
$$\bar{D}\tilde{Y} + \bar{N}\tilde{X} = I \tag{4.16}$$

Because of the Bézout double identity $\bar{Y}\tilde{X}$ must be equal to $\bar{X}\tilde{Y}$ and Eq. (4.12) can therefore be substituted into Eq. (4.11) as shown in Eq. (4.17). Some more manipulation is done in Eq. (4.18) to make further use of the Bézout double identity.

$$\begin{aligned} \bar{X}y - \bar{X}(\tilde{N} + \tilde{Y}S)x &= \bar{Y}(\tilde{D} - \tilde{X}S)x - \bar{Y}r_2 - \bar{X}r_1 + \bar{X}y && (4.17)\\ (\bar{Y}\tilde{D} + \bar{X}\tilde{N})x + (\bar{X}\tilde{Y} - \bar{Y}\tilde{X})Sx &= \bar{Y}r_2 + \bar{X}r_1 && (4.18)\end{aligned}$$

With the use of Eq. (4.13) and Eq. (4.15) the expression can be reduced to Eq. (4.19).

$$x = \bar{X}r_1 + \bar{Y}r_2 \tag{4.19}$$

Using Eq. (4.19) it is possible to calculate the point x with only the knowledge of r_1 and r_2 which are independent of the noise. For the identification procedure the point z also needs to be determined. It can be seen on Fig. 4.2 that θ_1 can also be exspressed as in Eq. (4.20), and θ_2 can also be expressed as in Eq. (4.21).

$$\begin{aligned} \tilde{D}x &= u + \tilde{X}z && (4.20)\\ \tilde{N}x &= y - \tilde{Y}z && (4.21)\end{aligned}$$

By multiplying with $\bar{N}$ in Eq. (4.20) and $\bar{D}$ in Eq. (4.21) and use that $\bar{D}\tilde{N} = \bar{N}\tilde{D}$ have to be fulfilled due to the Bézout double identity, Eq. (4.22) can be found and z can be isolated as in Eq. (4.23).

$$\begin{aligned} \bar{D}y - \bar{D}\tilde{Y}z &= \bar{N}u + \bar{N}\tilde{X}z && (4.22)\\ (\bar{N}\tilde{X} + \bar{D}\tilde{Y})z &= z = \bar{D}y - \bar{N}u && (4.23)\end{aligned}$$

A relationship between z and x is needed for the identification procedure. By inspecting Fig. 4.2 the relationship can also be found as seen in Eq. (4.24), and since x was determined only with variables independent of the noise, the problem of determining S is an open loop problem.

$$z = Sx + (\bar{D} - S\bar{X})n \tag{4.24}$$

The problem is thus changed from identification of the real plant to identification of the S block. The main advantage from this parametrization method is that the identification problem have been reformulated into an open loop identification problem which there are many well known methods to solve. However the Hansen Scheme also add some demands to the system identified. For the coprime factorization to be possible the system must have as many inputs as outputs. This is easy to see from chapter 7 where the coprime factorizations have been derived. Furthermore the procedure needs prior knowledge of the controller and a model of the plant.

4.5 System Identification Block (S)

In this section the S block on Fig. 4.2 is explained. To see how S affect the plant a transfer function from u to y is found. An expression for θ_1 and θ_2 are found in (4.25) and (4.26) respectively. It is important to note that the noise, n, have been set to 0 to explore the impact of S on the noiseless plant.

$$\theta_1 = u + \tilde{X}Sx = \tilde{D}x \Rightarrow x = (\tilde{D} - \tilde{X}S)^{-1}u \quad (4.25)$$

$$\theta_2 = \tilde{N}x + \tilde{Y}Sx = (\tilde{N} + \tilde{Y}S)x = y \quad (4.26)$$

By isolating x in Eq. (4.25) and substitute it into Eq. (4.26) a relationship between u and y can be found as in Eq. (4.27).

$$y = (\tilde{N} + \tilde{Y}S)(\tilde{D} - \tilde{X}S)^{-1}u \quad (4.27)$$

Eq. (4.27) corresponds to the plant in open loop and since $\tilde{N}\tilde{D}^{-1}$ is the nominal plant, S can be seen as a measure of the open loop error between u and y. This is most easily seen as when S is 0, the nominal plant simply corresponds to the true plant and as S increases the true plant will deviate more from the nominal plant.

House Model 5

In this chapter a dynamic model of the indoor temperature of a house heated by a heatpump will be given. First a simple themal model of the house using 3 states is given, then a state space representation is introduced which will be used for parameter estimation and using different techniques in later chapters. An initial guess on the model parameters are given to be used for the model identification.

Nomenclature

A nomenclature is added to look up all abbreviations used in the following chapter. Abbreviations will be explained first time they are used, to keep redundancy is kept at a minimum.

Notation	Description	Units
E_a	Total energy of the air in the house	J
E_w	Total energy stored in the walls	J
E_f	Total energy stored in the floor	J
COP	Coefficient of performance of the heat pump	$-$
P_p	Electrical energy used by the heat pump	W
$P_{p,f}$	Power transfer from the heat pump to the floor	W
$P_{f,a}$	Power transfer from the floor to the air	W
$P_{o,w}$	Power transfer from the outside to the wall	W
$P_{s,f}$	Power transfer from the sun to the floor	W
$P_{s,w}$	Power transfer from the sun to the wall	W
$P_{w,a}$	Power transfer from the wall to the air inside the house	W
$\alpha_{f,a}$	Heat transfer from floor to the air	W/K
$\alpha_{o,w}$	Heat transfer from the outside to the wall	W/K
$\alpha_{w,a}$	Heat transfer from the wall to the air	W/K
$T_{w,i}$	Temperature of water at inflow	K
$T_{w,o}$	Temperature of the water at the outflow	K
T_f	Temperature of the floor	K
T_a	Temperature of the air inside the house	K
T_w	Temperature of the wall	K
T_o	Temperature of the air outside the house	K
M_a	Total mass of the air in the house	Kg
M_w	Total mass of the wall	Kg
M_f	Total mass of the floor	Kg
c_a	Heat capacity of the air in the house	$J/(Kg \cdot K)$
c_f	Heat capacity of the floor	$J/(Kg \cdot K)$
c_w	Heat capacity of the water in the floor heating	$J/(L \cdot K)$
c_{wall}	Heat capacity of the walls of the house	$J/(Kg \cdot K)$
q_w	Flow rate of water through the heat pump	L/s

5.1 Input Parameters and Noise

Before introducing the thermal model it is needed to decide what is defined as inputs to the model, and what should be disregarded as noise. The model is verified with data provided by the ForskEL project and data collection is therefore constrained to data received from the ForskEl project.

The goal of the model is not to be able to control the specific heat pump, but simply to give an estimate of the indoor temperature. For this the only controllable input is the energy put into the heat pumps, while a prediction of the outdoor temperature and the sun intensity are known uncontrollable inputs. The final goal is to make a lumped model representing several houses, however to do this a model able to fit an average house is developed. Any input which is not covered by the heat pump, sun intensity and outdoor temperature are regarded as noise.

5.2 Model Structure

The model is inspired by the house model found in [6] where it was attempted to create a model of the indoor temperature of a single house. For the model the house is considered to consist of a single room without any kind of furniture. The house is therefore modeled as 3 control volumes, the wall temperature, the floor temperature and the indoor air temperature. All 3 control volumes are modeled as lumped masses with a uniform mass and heat capacity. The energy transfers of the model can be seen on Fig. 5.1, where arrows shows which direction have been chosen to be positive for the respective flows. All energy flows not represented on Fig. 5.1 are defined as being noise, which will be looked into using a stochastic model later on. The 3 control volumes are given as seen in 5.2, 5.2 and 5.2, and in 5.2 the respective state equations are given.

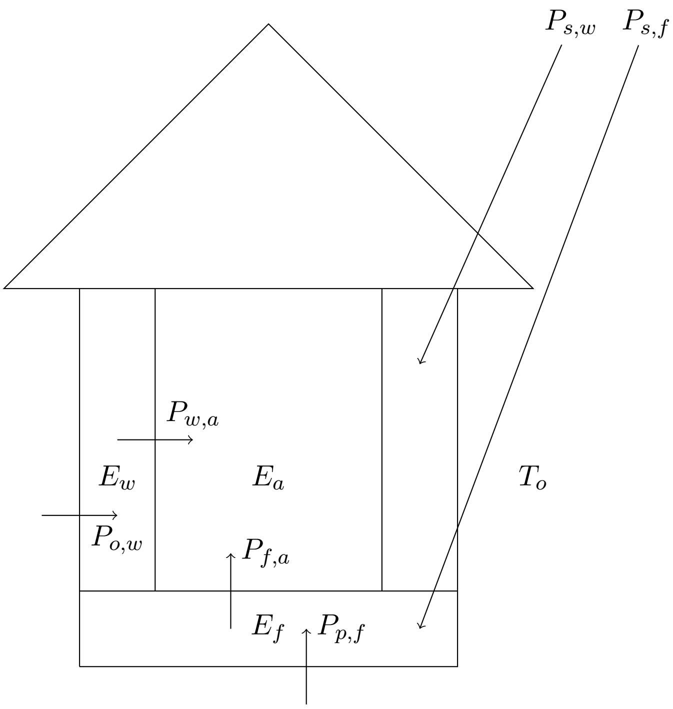

Fig. 5.1: Energy flow through the house

The relations between the different control volumes and inputs can be seen in Fig. 5.2.

Solar radiation model

The intensity of electromagnetic radiation the Sun delivers per square meter at a distance of roughly 1 AU is known as the solar constant, $I_0 = 1353\frac{\mathrm{W}}{\mathrm{m}^2}$. Since the AU is defined as the

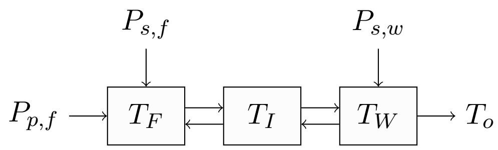

Fig. 5.2: The relations between the control volumes and the different inputs.

mean distance between the earth and the sun, this is also roughly the amount of electromagnetic radiation that hits the earth. However as it is necessary for this light to travel through the atmosphere before hitting the Earth the intensity is less when hitting the house. This is largely dependent on the angle of the sun and weather. The solar radiation at surface level, I_s, is in this project obtained using data from DMI.

From this it is possible to calculate the wattage the sun delivers to a house with a given surface, A. Since the sun shines through the windows of a house some of the energy is delivered to the wall while the rest is delivered to the floor. This is reflected by the β parameter which distributes the power between the floor and the wall.

$$P_{s,w} = I_s \cdot A \cdot \beta \tag{5.1}$$
$$P_{s,f} = I_s \cdot A \cdot (1 - \beta) \tag{5.2}$$

Where I_s is the electromagnetic radiation per square meter at ground level $[\frac{w}{m^2}]$
A is the area the house covers $[m^2]$
β is the ratio between solar radiation on the wall and on the floor [-]

While the model could easily be expanded to include additional parameters such as reflection, it is limited to include only A and β as it is desirable to limit the number of parameters which are necessary to estimate.

Lumped floor model

The energy transfer using the pump is the only controllable part and is subject to a loss due to friction in the pump, heating of the pipes etc. The transformation efficiency is given by the COP constant which can be measured using the flow of the water through the heat pumps, the change in the temperature of the water and the heat capacity. The COP is defined as in equation (5.3).

$$COP = \frac{q_w \cdot c_w \cdot (T_{w,i} - T_{w,o})}{P_p} \tag{5.3}$$

When determining the COP factor the temperature of the water let into the system and the temperature of the house are seen as constant to simplify the COP factor. The COP factor is therefore only dependent on how fast the water flows through the tubes. The COP of the houses are found in appendix B, with the use of data from the ForskEL project. With the COP factor determined the energy put into the floor using the heat pump can be expressed as in Eq. (5.4).

$$P_{p,f} = P_p \cdot COP \tag{5.4}$$

The balance equation of the floor is expressed in Eq. (5.5), where the floor is considered one lumped mass, and the energy is transfered from the pump to the floor, and from the floor to the air.

$$\dot{E}_f = M_f \cdot c_f \cdot \dot{T}_f = P_{p,f} - P_{f,a} = P_p \cdot COP - \alpha_{f,a}(T_f - T_a) \tag{5.5}$$

Using Eq. (5.5) it is possible to calculate the energy delivered to the house by the heat pump.

Lumped wall model

With the balance equation for the floor and the radiation from the sun described, the dissipation of energy through the walls needs to be looked into as well. The dissipation is due to the difference in heat on each side of the wall, since the temperature dissipation is slower through the wall than through the air. The wall therefore imposes a time delay to the dissipation speed. Eq. (5.6) describes how the dissipation is estimated using the available data.

$$\dot{E}_w = M_w \cdot c_w \cdot \dot{T}_w = P_{o,w} - P_{w,a} = \alpha_{o,w}(T_o - T_w) - \alpha_{w,a}(T_w - T_a) \tag{5.6}$$

Lumped air model

It is assumed that the air inside the house is connected only to the wall and the floor of the house. With the air inside the house only connected to the wall and floor the inside temperature can be found as a energy balance between the energy inside the house, the energy transfer between the wall and the inside and the energy transfer between the floor. and the inside. The changes of the energy inside the house can therefore be expressed as in eq. (5.7)

$$\dot{E}_a = M_a \cdot c_a \cdot \dot{T}_a = P_{w,a} + P_{f,a} = \alpha_{w,a}(T_w - T_a) + \alpha_{f,a}(T_f - T_a) \tag{5.7}$$

State Equations

With all states of the system described a state space model can be derived, with the temperature of the wall, the indoor air and the floor as states, as seen in Eq. (5.8).

$$\mathbf{x} = \begin{bmatrix} T_a \\ T_w \\ T_f \end{bmatrix} \tag{5.8}$$

Given the state matrix in Eq. (5.8) the system matrix can be constructed as in Eq. (5.9).

$$\mathbf{A} = \begin{bmatrix} -\frac{\alpha_{f,a}+\alpha_{w,a}}{M_a \cdot c_a} & \frac{\alpha_{w,a}}{M_a \cdot c_a} & \frac{\alpha_{f,a}}{M_a \cdot c_a} \\ \frac{\alpha_{w,a}}{M_w \cdot c_w} & -\frac{\alpha_{o,w}+\alpha_{w,a}}{M_w \cdot c_w} & 0 \\ \frac{\alpha_{f,a}}{M_f \cdot c_f} & 0 & -\frac{\alpha_{f,a}}{M_f \cdot c_f} \end{bmatrix} \tag{5.9}$$

As seen the values on the diagonal are all negative. This fits with the notion that the temperature of an object will fall if it has the highest temperature in the system. Further it can be seen that the wall and the floor only affect each other through the air, which is as desired.

With the solar radiation, the pump power and the outside temperature as inputs, the input vector can be written as in Eq. (5.10).

$$\mathbf{u} = \begin{bmatrix} P_p \\ I_s \\ T_o \end{bmatrix} \tag{5.10}$$

With this the input matrix is found in Eq. (5.11).

$$\mathbf{B} = \begin{bmatrix} 0 & 0 & 0 \\ 0 & A \cdot \beta & \frac{\alpha_{o,w}}{M_w c_w} \\ \frac{COP}{M_f c_f} & A \cdot (1-\beta) & 0 \end{bmatrix} \tag{5.11}$$

From this it can be seen that no input directly affects the indoor air temperature, as was expected from Fig. 5.1.

Since only the indoor air temperature is of interest, the output matrix is simply given as Eq. (5.12).

$$\mathbf{C} = \begin{bmatrix} 1 & 0 & 0 \end{bmatrix} \tag{5.12}$$

With the D matrix simply defined as Eq. (5.13), the system is described in state space form.

$$\mathbf{D} = \begin{bmatrix} 0 & 0 & 0 \end{bmatrix} \tag{5.13}$$

To verify that the states behave as expected under different inputs, the model is tested in appendix A

Square system

The model as described in (5.9), (5.11), (5.12) and (5.13) is a system with 3 inputs and one output. This model is however not suitiable for the parametrization method used for identification purposes. The models must have the same number of inputs and outputs for the Youla-Kucera parametrization. It is therefore chosen to use the uncontrollable inputs as outputs as well, which changes the **C** and **D**. The new **C** matrix is shown in Eq. (5.14) where it is extended with zeros, since none of the states have any impact on the two new outputs.

$$\mathbf{C} = \begin{bmatrix} 1 & 0 & 0 \\ 0 & 0 & 0 \\ 0 & 0 & 0 \end{bmatrix} \tag{5.14}$$

The **D** matrix is extended to directly feed the two uncontrollable inputs to the output. The extended **D** matrix can be seen in Eq. (5.15).

$$\mathbf{D} = \begin{bmatrix} 0 & 0 & 0 \\ 0 & 1 & 0 \\ 0 & 0 & 1 \end{bmatrix} \tag{5.15}$$

5.3 Initial guess of house model

An initial guess on the parameters of the house model is necessary for the identification method. For the initial guess it is assumed that the standard house consists of one room, with 4 walls being 30 cm thick each, a flat roof that adds zero mass and that energy can't go through and a floor that is 30 cm. The impact of doors and windows has been disregarded from the initial guess. The heat transfer constants between the outside and the wall has been found using the suggestion in [14] for how to build houses while the heat transfer coefficient between the wall and the inside and the heat transfer coefficient between the floor and the inside were found as suggestions in [15]. The initial values for the heat transfer coefficients can be seen in (5.16), (5.17) and (5.18).

$$\alpha_{w,a} = 3.3 \cdot A_{wall} = 3.3 \cdot 4 \cdot 196^{0.5} \cdot 3 = 554.4 \tag{5.16}$$

$$\alpha_{f,a} = 2.3 \cdot A_{floor} = 2.3 \cdot 196 = 450.8 \tag{5.17}$$

$$\alpha_{o,w} = 0.7 \cdot A_{wall} = 0.7 \cdot 4 \cdot 196^{0.5} \cdot 3 = 117.6 \tag{5.18}$$

Where A_{wall} is the area of the wall segments $[m^2]$
A_{floor} is the area of the floor $[m^2]$

A guess on the mass of the different objects is made by the use of density estimation given in [14] and using the average size of houses participating in the project. The average size of a house participating is 196 m^2 as seen in appendix C, the height is estimated to 3 meter and the initial estimate for the mass of the wall, floor and air can then be calculated as in Eq. (5.19), Eq. (5.20) and Eq. (5.21) respectively.

$$M_w = A_{wall} \cdot L_{wall} \cdot \rho_w = 4 \cdot 196^{0.5} \cdot 3 \cdot 0.3 \cdot 1744 = 87897.6Kg \tag{5.19}$$

$$M_f = A_{floor} \cdot L_{floor} \cdot \rho_f = 196 \cdot 0.3 \cdot 1300 = 76440Kg \tag{5.20}$$

$$M_a = A_{floor} \cdot h \cdot \rho_a = 196 \cdot 3 \cdot 1.3 = 764.4Kg \tag{5.21}$$

Where L_{wall} is the thickness of the wall segments $[m]$
L_{floor} is the thickness of the floor segments $[m]$
h is the height inside the house $[m]$

Lastly the heat capacity of each individual part is needed. The heat capacity of all commonly used materials for walls and floor is close to 1 which is the same for air [16]. All heat capacity constants are therefore guessed to be 1.

Controller Structure 6

As concluded in chapter 4 the identification method demands the controller to be known. It was found in section 3.2 that the controller can be approximated by a PI controller. For state space systems this is equivalent to a state feedback controller with integral output control. However, since the states are not directly observable, an observer is necessary for state feedback control to work. Further, assuming that state feedback and and integral gain should work toward the same reference, it is necessary with a feedforward reference gain.

6.1 Controller Design

Integral control is implemented by extending the state vector x with an integral state, x_i, with derivative, $\dot{x}_i = r - y = r - (Cx + Du)$. This extended vector is called x_e.

The extended system can then be described as in Eq. (6.1) and Eq.(6.2).

$$\begin{bmatrix} \dot{x} \\ \dot{x}_i \end{bmatrix} = \begin{bmatrix} A & 0 \\ -C & 0 \end{bmatrix} \begin{bmatrix} x \\ x_i \end{bmatrix} + \begin{bmatrix} B \\ -D \end{bmatrix} u + \begin{bmatrix} 0 \\ 1 \end{bmatrix} r \tag{6.1}$$

$$y = \begin{bmatrix} C & 0 \end{bmatrix} \begin{bmatrix} x \\ x_i \end{bmatrix} + \begin{bmatrix} D \end{bmatrix} u \tag{6.2}$$

With this extended system the controller can be designed using standard Linear Quadratic methods, such as the `lqr` command in matlab. However, since only one input is controllable, the designed controller must only be able to affect this single input. To do this B and u are split into a controllable and an uncontrollable part, $B = \begin{bmatrix} B_c & B_u \end{bmatrix}$, $u = \begin{bmatrix} u_c \\ u_u \end{bmatrix}$.

A controller, F_c, is then designed for B_c, such that $\text{eig}(A + B_c F_c) < 0$. The designed controller is thus only mapping from the output to the controllable input and the zero correlation between the feedback and the uncontrollable inputs have to be added manually.The final controller is therefore the extended matrix $F = \begin{bmatrix} F_c \\ 0 \end{bmatrix}$, such that $BFx_e = B_c F_c x_e + B_u 0 x_e = B_c F_c x_e$. Naturally such a controller will consist of a state feedback part, F_x, and an integral feedback part, F_i, such that $Fx_e = \begin{bmatrix} F_x & F_i \\ 0 & 0 \end{bmatrix} \begin{bmatrix} x \\ x_i \end{bmatrix}$.

This gives the closed loop system seen in Eq. (6.3) and Eq. (6.4) and can be illustrated as on Fig. 6.1, where state feedback and integral control is implemented.

$$\begin{bmatrix} \dot{x} \\ \dot{x}_i \end{bmatrix} = \begin{bmatrix} A + BF_x & BF_i \\ -(C + DF_x) & -DF_i \end{bmatrix} \begin{bmatrix} x \\ x_i \end{bmatrix} + \begin{bmatrix} 0 \\ 1 \end{bmatrix} r \tag{6.3}$$

$$y = \begin{bmatrix} -(C + DF_x) & -DF_i \end{bmatrix} \begin{bmatrix} x \\ x_i \end{bmatrix} \tag{6.4}$$

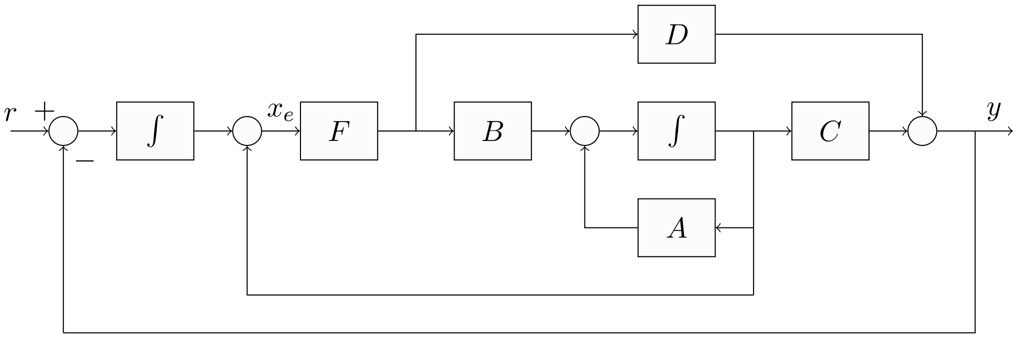

Fig. 6.1: A plant in standard state space representation with state feedback and integral control.

6.2 Observer Design

As the system is designed as a state space feedback controller it is necessary with an observer for all unmeasurable states. The system is extended with a full order observer as seen on Fig. 6.2.

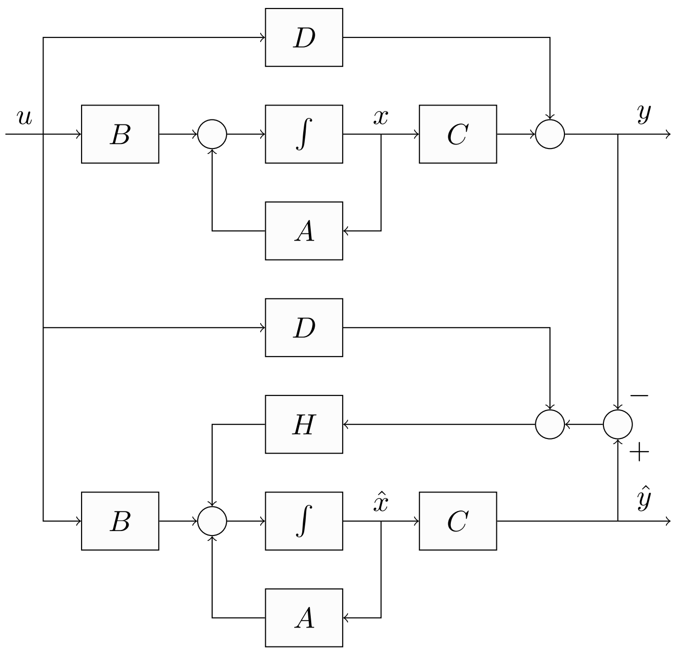

Fig. 6.2: A plant in standard state space representation with a full order observer.

The purpose of the observer is to estimate the states of the system by reacting to the error between the expected output and the actual output. From the figure the definition of the estimated states, $\hat{x}$, can be found as Eq. (6.5) and Eq. (6.6).

$$\begin{aligned}\dot{\hat{x}} &= A\hat{x} + (B+HD)u + H(C\hat{x} - y) \\ &= A\hat{x} + (B+HD)u + HC(\hat{x} - x) = (A+HC)\hat{x} + (B+HD)u - HCx \qquad (6.5)\end{aligned}$$

$$\hat{y} = C\hat{x} + Du \qquad (6.6)$$

Defining the error signal $e = \hat{x} - x$ and $\dot{e} = \dot{\hat{x}} - \dot{x}$

$$\dot{e} = A\hat{x} + BF\hat{x} + HDF\hat{x} + H(C\hat{x} - y) - (Ax + BF\hat{x}) \tag{6.7}$$
$$= A(\hat{x} - x) + HC(\hat{x} - x) + HDF\hat{x} - HDF\hat{x} \tag{6.8}$$
$$= (A + HC)e \tag{6.9}$$

The observer is designed such that the system is stable, $\text{eig}(A + HC) < 0$.

However, as the observer only attempts to estimate the states, it has no influence on the actual system unless coupled with a controller. In accordance with the separation principle this controller can be designed without regard to the observer and the resulting poles are simply the combination of the poles added by both the controller and the observer.

6.3 Closed loop system

Combining the observer and controller gives the total system as seen on Fig. 6.3.

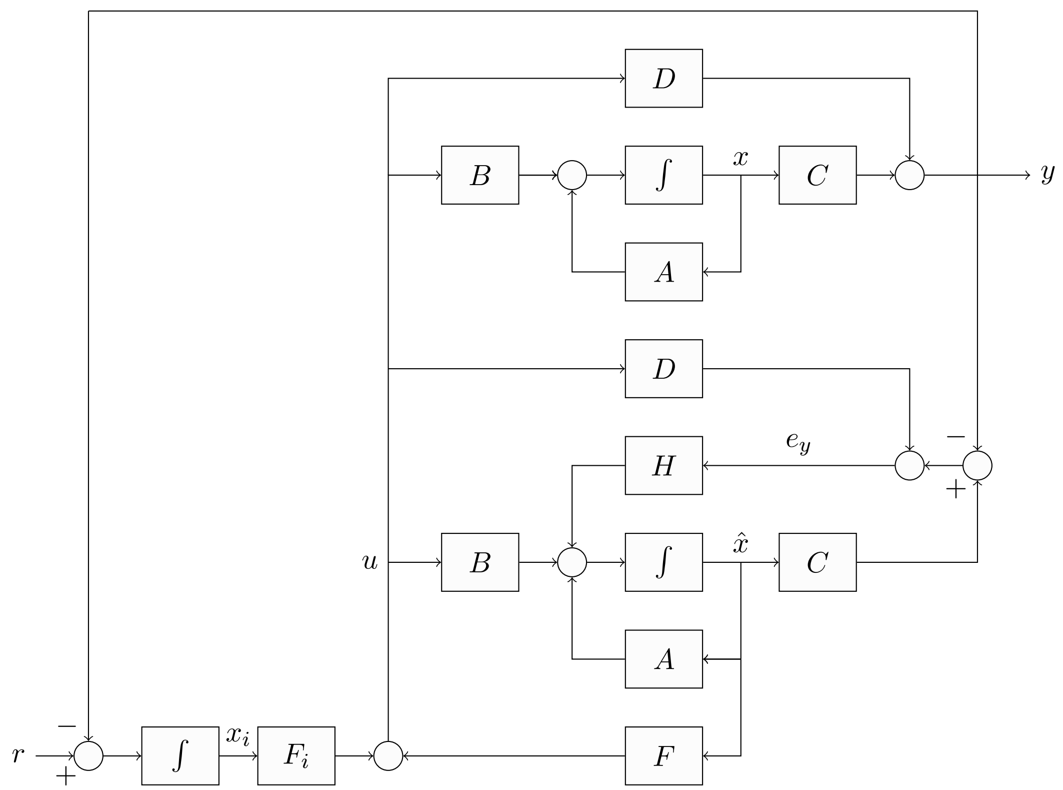

Fig. 6.3: A plant in standard state space representation with integral control and a full order observer.

Further, combining both the actual system states, the integral states and the observed states the governing equations for the system can be found in Eq. (6.10) and Eq. (6.11).

$$
\begin{bmatrix} \dot{x} \\ \dot{\hat{x}} \\ \dot{x}_i \end{bmatrix} = \begin{bmatrix} A & BF_x & BF_i \\ -HC & A + BF_x + HC & BF_i \\ -C & -DF_x & -DF_i \end{bmatrix} \begin{bmatrix} x \\ \hat{x} \\ x_i \end{bmatrix} + \begin{bmatrix} 0 \\ 0 \\ I \end{bmatrix} r \tag{6.10}
$$

$$
y = \begin{bmatrix} C & DF_x & DF_i \end{bmatrix} \begin{bmatrix} x \\ \hat{x} \\ x_i \end{bmatrix} \tag{6.11}
$$

With the governing equations for the full system given as in Eq. (6.10) and Eq. (6.11) the final controller will have to be given as in (6.12). This result will be used in chapter 7 when the controller factorizations have to be validated.

$$
K = \left[\begin{array}{cc|c} A + HC + BF_x + HDF_x & BF_i + HDF_i & -H \\ 0 & 0 & -I \\ \hline F_x & F_i & 0 \end{array}\right] \tag{6.12}
$$

6.4 Reference feedforward

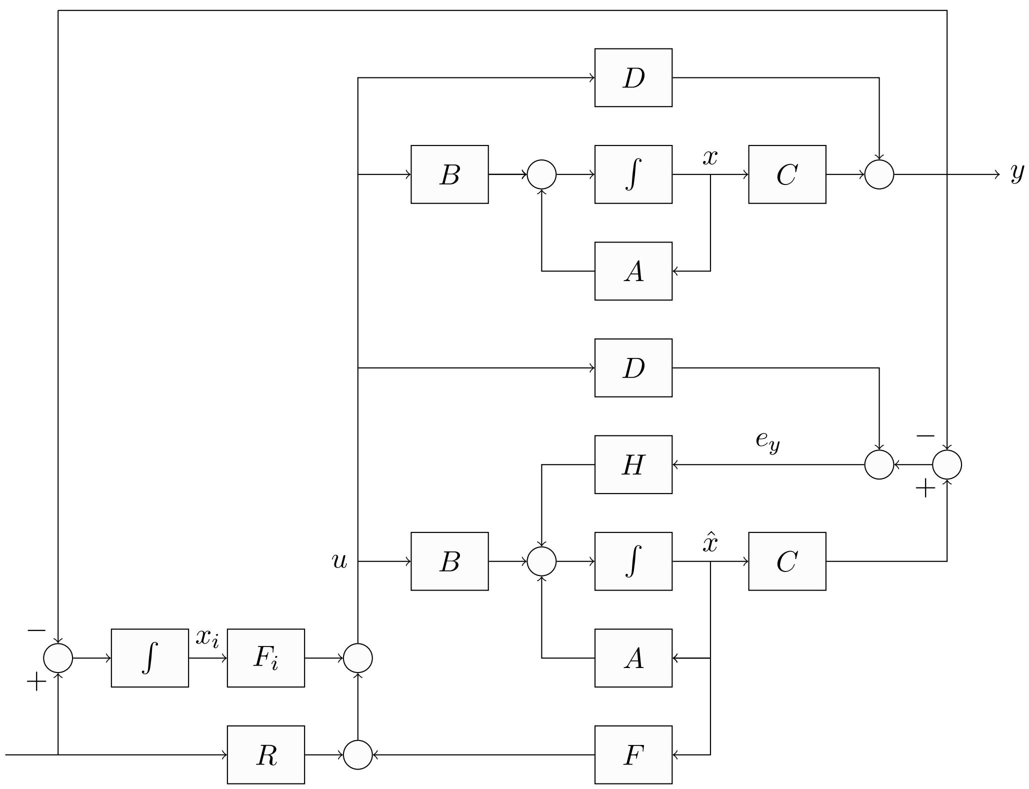

Fig. 6.4: System with reference added.

For the model to be as close as possible to the system tried to represent the reference is added to the system. The reference is added to the input using an feed forward that ensures the DC-gain from reference to output is 1. With the reference added as shown on Fig. 6.4 the closed loop system, input and output matrices are as seen in Eq. (6.13).

$$
\begin{aligned}
\begin{bmatrix} \dot{x} \\ \dot{\hat{x}} \\ \dot{x}_i \end{bmatrix} &= \begin{bmatrix} A & BF_{\hat{x}} & BF_i \\ -HC & A + BF_{\hat{x}} + HC & BF_i \\ -C & -DF_x & -DF_i \end{bmatrix} \begin{bmatrix} x \\ \hat{x} \\ x_i \end{bmatrix} + \begin{bmatrix} BR \\ BR \\ I \end{bmatrix} r \\
y &= \begin{bmatrix} C & DF_x & DF_i \end{bmatrix} \begin{bmatrix} x \\ \hat{x} \\ x_i \end{bmatrix} + \begin{bmatrix} DR \end{bmatrix} r
\end{aligned} \tag{6.13}
$$

The gain from the reference to the output can be calculated as in Eq. (6.14). It is important to notice that the unity gain is calculated without the integral state which will make sure any imperfections in the model are drawn towards a steady state gain of 1.

$$
\begin{aligned}
y &= (C \cdot -A^{-1} \cdot B + D) \cdot r \\
&= \left(\begin{bmatrix} C & 0 \end{bmatrix} \cdot - \begin{bmatrix} A & BF_{\hat{x}} \\ -HC & A + BF_{\hat{x}} + HC \end{bmatrix}^{-1} \cdot \begin{bmatrix} BR \\ BR \end{bmatrix} + \begin{bmatrix} DR \end{bmatrix} \right) \cdot r
\end{aligned} \tag{6.14}
$$

$$
\frac{y}{r} = 1 = \left(\begin{bmatrix} C & 0 \end{bmatrix} \cdot - \begin{bmatrix} A & BF_{\hat{x}} \\ -HC & A + BF_{\hat{x}} + HC \end{bmatrix}^{-1} \cdot \begin{bmatrix} B \\ B \end{bmatrix} + D \right) \cdot R \tag{6.15}
$$

From Eq. (6.15) it is easy to see that R must be the inverse of the transfer function from the input to the output. The feed forward block, R, is therefore calculated as seen in Eq. (6.16).

$$
R = \left(\begin{bmatrix} C & 0 \end{bmatrix} \cdot - \begin{bmatrix} A & BF_{\hat{x}} \\ -HC & A + BF_{\hat{x}} + HC \end{bmatrix}^{-1} \cdot \begin{bmatrix} B \\ B \end{bmatrix} + D \right)^{-1} \tag{6.16}
$$

7 Youla-Kucera Parameterization

Youla-Kucera Parameterization necessitates that both the model and the controller can be divided into coprime factorizations. While the factorizations for a system with an observer based state feedback controller are well known, the coprime factorizations of a system with integral feedback and feedforward reference gain are less so. In this chapter these factorizations are derived and analytically proven. The factorizations are then verified through simulation and the algorithm for identification is explained and tested.

Feedback Basics

The basic stabilizing feedback system consists of a plant P and a controller K, as seen on Fig. 7.1.

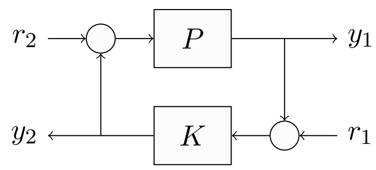

Fig. 7.1: The basic feedback system.

The output from a plant is fed into a controller, which generates a stabilizing input to the plant. The plant can be driven towards a desired state by either providing additional input to the plant or additional input to the controller. The system is controllable through r_1 and r_2 and observable through y_1 and y_2 if and only if P and K are both observable and controllable [17].

Coprime Factorization

Two integers are coprime if their greatest common divisor is 1. This concept can be extended to polynomials, where two polynomials are said to be coprime if their greatest common divisor is an invertible constant. From polynomials this concept can be extended to systems.

The concept of coprime factorization of a system was developed for rational transfer functions where a given transfer function $P(s)$ can be separated into two coprime rational stable transfer functions, $n(s)$ and $d(s)$, such that $P(s) = \frac{n(s)}{d(s)}$. The two polynomials must have no common zeros - otherwise they could be further reduced and are therefore not coprime. Further they must have no closed right half plane zeros for the transfer functions to be $Hurwitz$ [18]. The same principle can be applied to the controller, $K(s) = \frac{x(s)}{y(s)}$.

Extending this concept to state space systems it is necessary to define a left and right coprime factorization, due to the non-commutativeness of matrices.

State Space

To find the state space representation of a plant with an observer based controller it is necessary to define the equations which govern the system, as seen from different parts of the system. In particular the parts of interest are how the reference, r, and the observer-error, e, affect the input, u, and output, y, and vice versa.

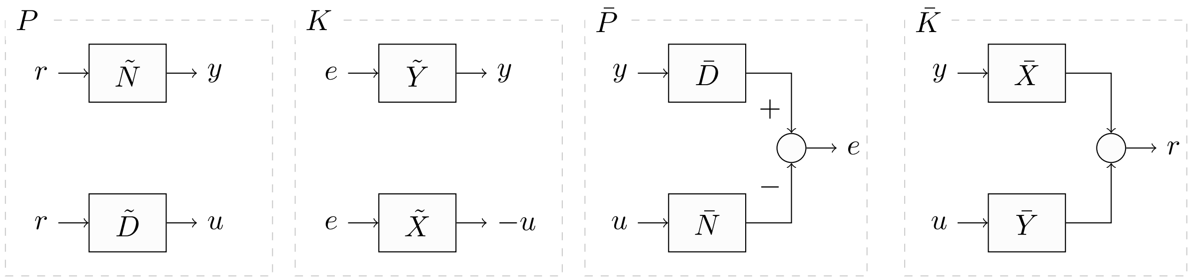

Fig. 7.2: The right and left factorizations of the plant and controller.

As the plant describes the relationship between u and y, this can be described as the relationship between u and r and r and y. From Fig. 7.2 it can be readily seen that moving through $\tilde{D}$ in the inverse direction maps from u to r, while moving through N maps from r to y. Put more succinctly:

$$y = \tilde{N}r \tag{7.1}$$
$$u = \tilde{D}r \Rightarrow r = \tilde{D}^{-1}u \tag{7.2}$$
$$y = \tilde{N}\tilde{D}^{-1}u \tag{7.3}$$
$$y = Pu \tag{7.4}$$

Again the same principle can be applied to the controller. This gives the four factorizations $P = \tilde{N}\tilde{D}^{-1} = \bar{D}^{-1}\bar{N}$ and $K = -\tilde{X}\tilde{Y}^{-1} = -\bar{Y}^{-1}\bar{X}$. This gives some obvious properties of the factorization, namely that both $\tilde{D}(s), \overline{D}(s), \tilde{Y}(s)$ and $\overline{Y}(s)$ must be non-singular. Further, since the left and right coprime factorizations of the systems are equal, this equality can also be written as Eq. (7.5).

$$\begin{bmatrix} -\overline{N} & \overline{D} \end{bmatrix} \begin{bmatrix} \tilde{D} \\ \tilde{N} \end{bmatrix} = 0, \begin{bmatrix} \overline{Y} & \overline{X} \end{bmatrix} \begin{bmatrix} -\tilde{X} \\ \tilde{Y} \end{bmatrix} = 0 \tag{7.5}$$

This is also a result of the double Bezout Identity seen in Eq. 4.3.

7.1 Factorizations

A system with observer based stabilizing state feedback, integral output feedback and feedforward reference gain has governing state equations described in Eq. (7.6).

$$\begin{aligned} \dot{x} &= Ax + Bu \\ \dot{\hat{x}} &= A\hat{x} + Bu + HC\hat{x} + HDu - Hy \\ \dot{x}_i &= r - y \\ u &= F_x\hat{x} + F_ix_i + Rr \\ y &= Cx + Du \end{aligned} \tag{7.6}$$

This can be seen on Fig. 7.3. The logic behind how the coprime factorizations can be expanded with an integral state and a reference feed forward is further explored in appendix D.

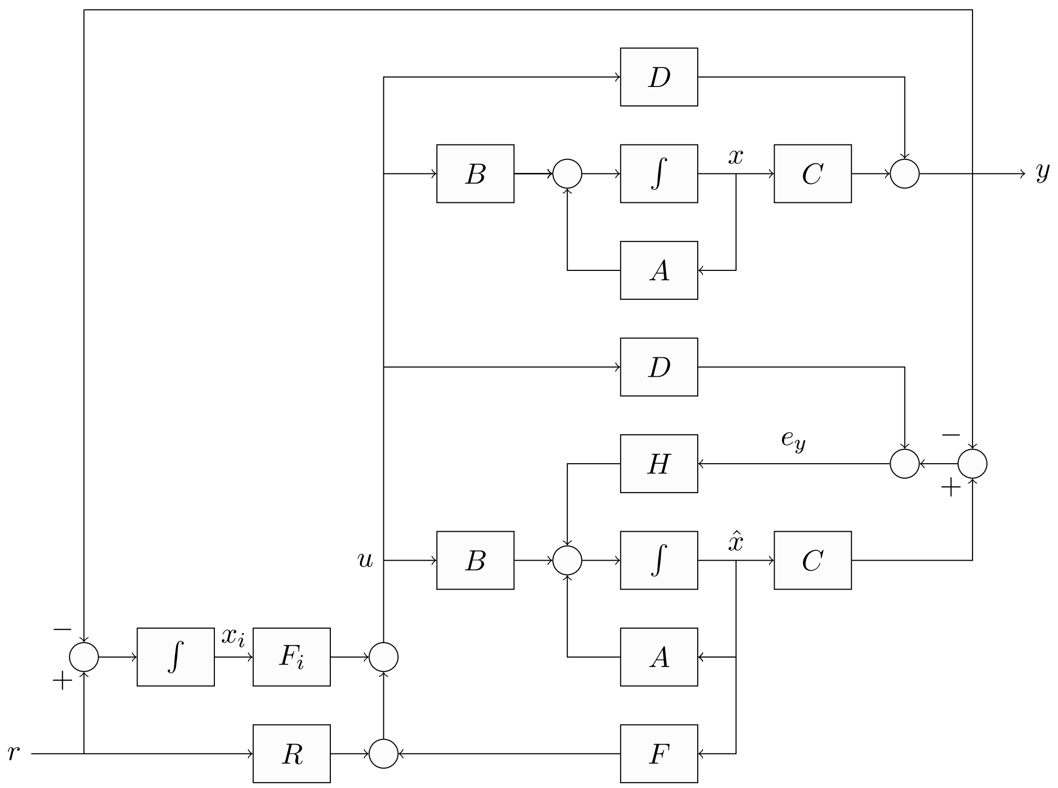

Fig. 7.3: System with observer based stabilizing feedback, integral output feedback and feedforward reference gain.

7.1.1 Right Coprime Factorization of Plant

The plant can be factorized into right coprime systems $\tilde{N}$ and $\tilde{D}$, as seen on fig. 7.4.

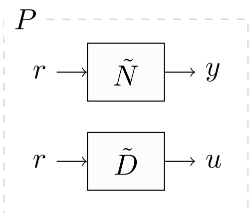

Fig. 7.4: The right coprime factorization of the plant.

To obtain a fractional description of the plant consider the the plant with stabilizing feedback $u = F_x\hat{x} + F_i x_i + Rr$, rewrite the plant with an error state rather than an observer state.

$$\dot{x} = (A + BF_x)x + BF_x e + BF_i x_i + BRr \tag{7.7}$$

$$\dot{e} = (A + HC)e \tag{7.8}$$

$$y = (C + DF_x)x + DF_x e + DF_i x_i + DRr \tag{7.9}$$

$$\dot{x}_i = r - y \tag{7.10}$$

$$= -(Cx + DF_x)x - DF_x e - DF_i x_i + (I - DR)r \tag{7.11}$$

From these the transfer function from r to y is readily found in Eq. (7.12).

$$\tilde{N} = \left[\begin{array}{ccc|c} A+BF_x & BF_x & BF_i & BR \\ 0 & A+HC & 0 & 0 \\ -C-DF_x & -DF_x & -DF_i & I-DR \\ \hline C+DF_x & DF_x & DF_i & DR \end{array}\right] = \left[\begin{array}{cc|c} A+BF_x & BF_i & BR \\ -C-DF_x & -DF_i & I-DR \\ \hline C+DF_x & DF_i & DR \end{array}\right] \tag{7.12}$$

The error state can be removed as it is stable and receives no input and will therefore always go towards 0.

The transfer function r to u as well as its inverse can then be found Eq. (7.13) and (7.14).

$$\tilde{D} = \left[\begin{array}{ccc|c} A+BF_x & BF_x & BF_i & BR \\ 0 & A+HC & 0 & 0 \\ -C-DF_x & -DF_x & -DF_I & I-DR \\ \hline F_x & F_x & F_i & R \end{array}\right] = \left[\begin{array}{cc|c} A+BF_x & BF_i & BR \\ -C-DF_x & -DF_i & I-DR \\ \hline F_x & F_i & R \end{array}\right] \tag{7.13}$$

$$\tilde{D}^{-1} = \left[\begin{array}{cc|c} A & 0 & B \\ -C-R^{-1}F_x & -R^{-1}F_i & R^{-1}-D \\ \hline -R^{-1}F_x & -R^{-1}F_i & R^{-1} \end{array}\right] \tag{7.14}$$

These two results are then multiplied as seen in Eq. (7.15).

$$\tilde{N}\tilde{D}^{-1} = \left[\begin{array}{cccc|c} A & 0 & 0 & 0 & B \\ -C-R^{-1}F_x & -R^{-1}F_i & 0 & 0 & R^{-1}-D \\ -BF_x & -BF_i & A+BF_x & BF_i & B \\ -R^{-1}F_x+DF_x & -R^{-1}F_i+DF_i & -C-DF_x & -DF_i & R^{-1}-D \\ \hline -DF_x & -DF_i & C+DF_x & DF_i & D \end{array}\right] \tag{7.15}$$

Denote the states of this system ζ_1, ζ_2, ζ_3, ζ_4.

To see that this is indeed the correct system, consider a system with the states $\xi = \zeta_1 - \zeta_3$,$\dot{\xi} = \dot{\zeta}_1 - \dot{\zeta}_3$ and $\phi = \zeta_2 - \zeta_4$,$\dot{\phi} = \dot{\zeta}_2 - \dot{\zeta}_4$, such that this system defines the difference in derivates.

$$\begin{aligned}
\dot{\xi} = \dot{\zeta}_1 - \dot{\zeta}_3 &= A\zeta_1 + BF_x\zeta_1 + BF_i\zeta_2 - A\zeta_3 - BF_x\zeta_3 - BF_i\zeta_4 + Bu - Bu && (7.16)\\
&= (A+BF_x)(\zeta_1 - \zeta_3) + BF_i(\zeta_2 - \zeta_4) && (7.17)\\
&= (A+BF_x)\xi + BF_i\phi && (7.18)\\
\dot{\phi} = \dot{\zeta}_2 - \dot{\zeta}_4 &= (-C - R^{-1}F_x)\zeta_1 - R^{-1}F_i\zeta_2 + (R^{-1}F_x - DF_x)\zeta_1 + (R^{-1}F_i - DF_i)\zeta_2 \\
&\quad + (C+DF_x)\zeta_3 + DF_i\zeta_4 + (R^{-1} - D)u - (R^{-1} - D)u && (7.19)\\
&= (-C - DF_x)(\zeta_1 - \zeta_3) - DF_i(\zeta_2 - \zeta_4) && (7.20)\\
&= (-C - DF_x)\xi - DF_i\phi && (7.21)
\end{aligned}$$

Since the output of this pseudo system is of no interest, this gives the system defined in Eq. (7.22).

$$
\left[\begin{array}{cc|c}
A + BF_x & BF_i & 0 \\
-C - DF_x & -DF_i & 0 \\
\hline
0 & 0 & 0
\end{array}\right] \tag{7.22}
$$

Since F_x, F_i is a stabilizing controller it is already known that this system is stable. Since a stable system goes towards 0 the difference between the states will always go towards 0. Further, since there is no input to excite the states, once they reach their steady state value they will stay there.

In other words, the difference in derivatives are completely dependent on the difference between the states. This means that if the states are equal they will continue to be equal, which in turn means that x can simply be chosen to be either ζ_1 or ζ_3. Since ζ_1 is independent of ζ_3 this is the easier choice. This leaves $\dot{x} = Ax + Bu$.

For the output, since $\zeta_1 = \zeta_3$ and $\zeta_2 = \zeta_4$, this gives $y = -DF_x\zeta_1 - DF_i\zeta_2 + (C + DF_x)\zeta_3 + DF_i\zeta_4 + Du = C\zeta_3 + Du = Cx + Du$.

This means that the system can be reduced to Eq. (7.23).

$$
\tilde{N}\tilde{D}^{-1} = \left[\begin{array}{c|c}
A & B \\
\hline
C & D
\end{array}\right] \tag{7.23}
$$

7.1.2 Left Coprime Factorization of Plant

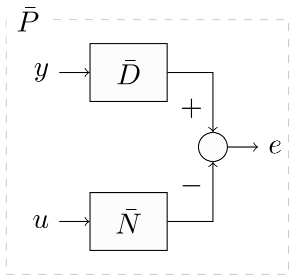

Fig. 7.5: The left coprime factorization of the plant.

To find the equations governing the relations from u to $-e$ and from y to e it is necessary to define the error $e = C\hat{x} + Du - y$. Further it is necessary to define the governing equations with inputs u and y.

$$
\begin{aligned}
\dot{x} &= Ax + Bu && (7.24)\\
\dot{\hat{x}} &= (A + HC)\hat{x} + Bu + HDu - Hy && (7.25)\\
\dot{x}_i &= r - y && (7.26)\\
&= -R^{-1}F_x\hat{x} - R^{-1}F_i x_i + R^{-1} - y && (7.27)
\end{aligned}
$$

Consider then the systems $\bar{N}$ and $\bar{D}$ which map from u and y to $-e$ and e, as seen in Eq. (7.28) through (7.30).

$$\bar{N} = \left[\begin{array}{ccc|c} A & 0 & 0 & B \\ 0 & A+HC & 0 & B+HD \\ 0 & -R^{-1}F_x & -R^{-1}F_i & R^{-1} \\ \hline 0 & -C & 0 & -D \end{array}\right] = \left[\begin{array}{cc|c} A+HC & 0 & B+HD \\ -R^{-1}F_x & -R^{-1}F_i & R^{-1} \\ \hline -C & 0 & -D \end{array}\right] \tag{7.28}$$

$$\bar{D} = \left[\begin{array}{ccc|c} A & 0 & 0 & 0 \\ 0 & A+HC & 0 & -H \\ 0 & -R^{-1}F_x & -R^{-1}F_i & -I \\ \hline 0 & C & 0 & -I \end{array}\right] = \left[\begin{array}{cc|c} A+HC & 0 & -H \\ -R^{-1}F_x & -R^{-1}F_i & -I \\ \hline C & 0 & -I \end{array}\right] \tag{7.29}$$

$$\bar{D}^{-1} = \left[\begin{array}{cc|c} A & 0 & -H \\ -R^{-1}F_x - C & -R^{-1}F_i & -I \\ \hline -C & 0 & -I \end{array}\right] \tag{7.30}$$

Coupling the systems gives Eq. (7.31).

$$\bar{D}^{-1}\bar{N} = \left[\begin{array}{cccc|c} A+HC & 0 & 0 & 0 & B+HD \\ -R^{-1}F_x & -R^{-1}F_i & 0 & 0 & R^{-1} \\ HC & 0 & A & 0 & HD \\ C & 0 & -R^{-1}F_x - C & -R^{-1}F_i & D \\ \hline C & 0 & -C & 0 & D \end{array}\right] \tag{7.31}$$

Denote the states of this system ζ_1, ζ_2, ζ_3, ζ_4.

By defining $x = \zeta_1 - \zeta_3$ and incidentally $\dot{x} = \dot{\zeta}_1 - \dot{\zeta}_3$ it is possible to see that the system can be reduced to the initial plant model.

$$\begin{aligned} \dot{x} &= \dot{\zeta}_1 - \dot{\zeta}_3 && (7.32)\\ &= (A+HC)\zeta_1 + (B+HD)u - HC\zeta_1 - A\zeta_3 - HDu && (7.33)\\ &= A(\zeta_1 - \zeta_3) + Bu && (7.34)\\ &= Ax + Bu && (7.35)\\ y &= C\zeta_1 - C\zeta_3 + Du && (7.36)\\ &= C(\zeta_1 - \zeta_3) + Du && (7.37)\\ &= Cx + Du && (7.38) \end{aligned}$$

Further it can be seen that the states ζ_2,ζ_4 are unobservable and therefore do not need to be considered.

$$\bar{D}^{-1}\bar{N} = \left[\begin{array}{c|c} A & B \\ \hline C & D \end{array}\right] \tag{7.39}$$

Consider the case of a given error, $\breve{e}$, with some given input and output signals, $\breve{u}$ and $\breve{y}$. These two signals can be generated from their right coprime parts, as a function of some reference $\breve{r}$.

As the error and the reference being independent, this reduces to 0, as seen in Eq. (7.40). This is a consequence of the Bezout identity, $(\bar{D}\tilde{N} - \bar{N}\tilde{D}) = 0$.

$$\begin{aligned} \breve{e} &= \bar{D}\breve{y} - \bar{N}\breve{u} \\ &= (\bar{D}\tilde{N} - \bar{N}\tilde{D})\breve{r} = 0 \end{aligned} \tag{7.40}$$

From this it is possible to see that $(\bar{D}\tilde{N} = \bar{N}\tilde{D})$, from which it is possible to see that the two factorizations must be equal, as per Eq. (7.41).

$$\begin{aligned} \bar{D}\tilde{N} &= \bar{N}\tilde{D} \\ \tilde{N}\tilde{D}^{-1} &= \bar{D}^{-1}\bar{N} = P \end{aligned} \tag{7.41}$$

7.1.3 Right Coprime Factorization of Controller

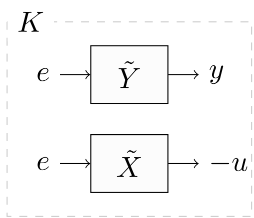

Fig. 7.6: The right coprime factorization of the controller.

To deduce the factorization of the controller observe that the output, $y = Cx + Du$ can be written as a function of the error, e, by using the observer state instead, $y = C\hat{x} + Du - e$. With the output defined as such the integral state can be rewritten to also be dependent on e.

$$\dot{x} = Ax + BF_x\hat{x} + BF_ix_i + BRr \tag{7.42}$$

$$\dot{\hat{x}} = (A + BF_x)\hat{x} + BF_ix_i + BRr + He \tag{7.43}$$

$$y = C\hat{x} + Du - e \tag{7.44}$$

$$u = F_x\hat{x} + F_ix_i + Rr \tag{7.45}$$

$$\dot{x}_i = r - y \tag{7.46}$$

$$= -(C + DF_x)\hat{x} - DF_ix_i + (I - DR)r + e \tag{7.47}$$

From this $\tilde{X}$ and $\tilde{Y}$ can be described in Eq. (7.48) through (7.50).

$$\tilde{X} = \left[\begin{array}{ccc|c} A & BF_x & BF_i & 0 \\ 0 & A + BF_x & BF_i & H \\ 0 & -C - DF_x & -DF_i & I \\ \hline 0 & F_x & F_i & 0 \end{array}\right] = \left[\begin{array}{cc|c} A + BF_x & BF_i & H \\ -C - DF_x & -DF_i & I \\ \hline -F_x & -F_i & 0 \end{array}\right] \tag{7.48}$$

$$\tilde{Y} = \left[\begin{array}{cccc|c} A & BF_x & BF_i & 0 \\ 0 & A+BF_x & BF_i & H \\ 0 & -C-DF_x & -DF_i & I \\ \hline 0 & C+DF_x & DF_i & -I \end{array}\right] = \left[\begin{array}{cc|c} A+BF_x & BF_i & H \\ -C-DF_x & -DF_i & I \\ \hline C+DF_x & DF_i & -I \end{array}\right] \tag{7.49}$$

$$\tilde{Y}^{-1} = \left[\begin{array}{cc|c} A+BF_x+HC+HDF_x & BF_i+HDF_i & -H \\ 0 & 0 & -I \\ \hline C+DF_x & DF_i & -I \end{array}\right] \tag{7.50}$$

Multiplying these then gives Eq. (7.51).

$$\tilde{X}\tilde{Y}^{-1} = \left[\begin{array}{cccc|c} A+BF_x+HC+HDF_x & BF_i+HDF_i & 0 & 0 & -H \\ 0 & 0 & 0 & 0 & -I \\ HC+HDF_x & HDF_i & A+BF_x & BF_i & -H \\ C+DF_x & DF_i & -C-DF_x & -DF_i & -I \\ \hline 0 & 0 & -F_x & -F_i & 0 \end{array}\right] \tag{7.51}$$

Exploiting the same principle as in the right coprime factorization of the plant, it is possible to see that the difference between the states, Eq. (7.52), are wholly dependent on the states and will therefore never diverge when they are equal.

$$\begin{aligned} \dot{\zeta}_1 - \dot{\zeta}_3 &= (A+BF_x)\zeta_1 + BF_i\zeta_2 - (A+BF_x)\zeta_3 - BF_i\zeta_4 \\ &= (A+BF_x)(\zeta_1-\zeta_3) + BF_i(\zeta_2-\zeta_4) \\ \dot{\zeta}_2 - \dot{\zeta}_4 &= -(C+DF_x)(\zeta_1-\zeta_3) - DF_i(\zeta_2-\zeta_4) \end{aligned} \tag{7.52}$$

This then gives the expected factorization.

$$\tilde{X}\tilde{Y}^{-1} = \left[\begin{array}{cc|c} A+BF_x+HC+HDF_x & BF_i+HDF_i & -H \\ 0 & 0 & -I \\ \hline -F_x & -F_i & 0 \end{array}\right] \tag{7.53}$$

To see that this is indeed the correct factorization of a *positive* feedback controller consider the mappings of the transfer functions $\tilde{X}$ and $\tilde{Y}$.

$$u = -\tilde{X}e \tag{7.54}$$
$$y = \tilde{Y}e \Rightarrow e = \tilde{Y}^{-1}y \tag{7.55}$$
$$u = -\tilde{X}\tilde{Y}^{-1}y \tag{7.56}$$
$$u = Ky \tag{7.57}$$

7.1.4 Left Coprime Factorization of Controller

Finally, the left coprime factorization of the controller considers the system defined by the relationship between y,u and r, as seen on Fig. 7.7.

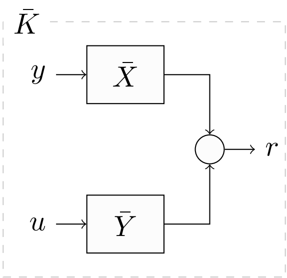

Fig. 7.7: The left coprime factorization of the controller.

$$
\begin{aligned}
\dot{x} &= Ax + Bu && (7.58)\\
\dot{\hat{x}} &= (A + HC)\hat{x} + (B + HD)u - Hy && (7.59)\\
r &= -R^{-1}F_x\hat{x} - R^{-1}F_i x_i + R^{-1}u && (7.60)\\
\dot{x}_i &= r - y && (7.61)\\
&= -R^{-1}F_x\hat{x} - R^{-1}F_i x_i + R^{-1}u - y && (7.62)
\end{aligned}
$$

The relationship between y and r, $\bar{X}$, is then defined as Eq. (7.63).

$$
\bar{X} = \left[\begin{array}{ccc|c} A & 0 & 0 & 0 \\ 0 & A+HC & 0 & -H \\ 0 & -R^{-1}F_x & -R^{-1}F_i & -I \\ \hline 0 & -R^{-1}F_x & -R^{-1}F_i & 0 \end{array}\right] = \left[\begin{array}{cc|c} A+HC & 0 & -H \\ -R^{-1}F_x & -R^{-1}F_i & -I \\ \hline -R^{-1}F_x & -R^{-1}F_i & 0 \end{array}\right] \tag{7.63}
$$

The relationship between u and r, $\bar{Y}$, and its inverse, $\bar{Y}^{-1}$, is then defined as Eq. (7.64) and (7.65).

$$
\bar{Y} = \left[\begin{array}{ccc|c} A & 0 & 0 & B \\ 0 & A+HC & 0 & B+HD \\ 0 & -R^{-1}F_x & -R^{-1}F_i & R^{-1} \\ \hline 0 & -R^{-1}F_x & -R^{-1}F_i & R^{-1} \end{array}\right] = \left[\begin{array}{cc|c} A+HC & 0 & B+HD \\ -R^{-1}F_x & -R^{-1}F_i & R^{-1} \\ \hline -R^{-1}F_x & -R^{-1}F_i & R^{-1} \end{array}\right] \tag{7.64}
$$

$$
\bar{Y}^{-1} = \left[\begin{array}{cc|c} A+HC+BF_x+HDF_x & BF_i+HDF_i & -BR-HDR \\ 0 & 0 & -I \\ \hline -F_x & -F_i & R \end{array}\right] \tag{7.65}
$$

With these two equations defined, their combined dynamics are described in Eq. (7.66).

$$
\bar{Y}^{-1}\bar{X} = \left[\begin{array}{cccc|c} A+HC & 0 & 0 & 0 & -H \\ -R^{-1}F_x & -R^{-1}F_i & 0 & 0 & -I \\ BF_x+HDF_x & BF_i+HDF_i & A+HC+BF_x+HDF_x & BF_i+HDF_i & 0 \\ R^{-1}F_x & R^{-1}F_i & 0 & 0 & 0 \\ \hline -F_x & -F_i & -F_x & -F_i & 0 \end{array}\right] \tag{7.66}
$$

Again the states are denoted ζ_1, ζ_2, ζ_3, ζ_4.

Defining $\hat{x} = \zeta_1 + \zeta_3$, $\dot{\hat{x}} = \dot{\zeta}_1 + \dot{\zeta}_3$ and $x_i = \zeta_2 + \zeta_4$, $\dot{x}_i = \dot{\zeta}_2 + \dot{\zeta}_4$, the states of the system can be simplified to Eq. (7.67),(7.68) and (7.69).

$$
\begin{aligned}
\dot{\hat{x}} &= \dot{\zeta}_1 + \dot{\zeta}_3 \\
&= (A + HC)\zeta_1 - Hy + (BF_x + HDF_x)\zeta_1 + BF_i + HDF_i\zeta_2 \\
&+ (A + HC + BF_x + HDF_x)\zeta_3 + (BF_i + HDF_i)\zeta_4 \\
&= (A + HC + BF_x + HDF_x)(\zeta_1 + \zeta_3) + (BF_i + HDF_i)(\zeta_2 + \zeta_4) - Hy \\
&= (A + HC + BF_x + HDF_x)\hat{x} + (BF_i + HDF_I)x_i - Hy && (7.67) \\
\dot{x}_i &= \dot{\zeta}_2 + \dot{\zeta}_2 \\
&= -R^{-1}F_x\zeta_1 - R^{-1}F_i\zeta_2 - y + R^{-1}F_x\zeta_1 + R^{-1}F_i\zeta_2 \\
&= -y && (7.68) \\
u &= -F_x\zeta_1 - F_i\zeta_2 - F_x\zeta_3 - F_i\zeta_4 \\
&= -F_x(\zeta_1 + \zeta_3) - F_i(\zeta_2 + \zeta_4) \\
&= -F_x\hat{x} - F_ix_i && (7.69)
\end{aligned}
$$

This completes the proof of the left coprime factorization of the controller:

$$
\bar{Y}^{-1}\bar{X} = \left[\begin{array}{cc|c} A + HC + BF_x + HDF_x & BF_i + HDF_i & -H \\ 0 & 0 & -I \\ \hline -F_x & -F_i & 0 \end{array}\right] \tag{7.70}
$$

As in the case with the left coprime factorization of the plant, consider a given reference $\breve{r}$ with some given input and output signals, $\breve{u}$ and $\breve{y}$. These two signals can be generated as a function of $\breve{e}$. As per the Bezout Identity this reduces to 0, as seen in Eq. (7.71).

$$
\begin{aligned}
\breve{r} &= \bar{X}\breve{y} + \bar{Y}\breve{u} \\
&= (\bar{X}\tilde{Y} - \bar{Y}\tilde{X})\breve{e} = 0 && (7.71)
\end{aligned}
$$

This implies that $\bar{X}\tilde{Y} = \bar{Y}\tilde{X}$, which further implies that that both factorizations are valid factorizations of the controller.

$$
\begin{aligned}
\bar{X}\tilde{Y} &= \bar{Y}\tilde{X} && (7.72) \\
\bar{Y}^{-1}\bar{X} &= \tilde{X}\tilde{Y}^{-1} && (7.73) \\
-\bar{Y}^{-1}\bar{X} &= -\tilde{X}\tilde{Y}^{-1} = K && (7.74) \\
& && (7.75)
\end{aligned}
$$

For easy reference the factorizations can be written as Eq. (7.76).

$$
\begin{aligned}
\tilde{D} &= \begin{bmatrix} F_x & F_i \end{bmatrix} \left(sI - \begin{bmatrix} A+BF_x & BF_i \\ -C-DF_x & -DF_i \end{bmatrix} \right)^{-1} \begin{bmatrix} BR \\ I-DR \end{bmatrix} + R \\
\overline{D} &= \begin{bmatrix} C & 0 \end{bmatrix} \left(sI - \begin{bmatrix} A+HC & 0 \\ -R^{-1}F_x & -R^{-1}F_i \end{bmatrix} \right)^{-1} \begin{bmatrix} -H \\ -I \end{bmatrix} - I \\
\tilde{N} &= \begin{bmatrix} C+DF_x & DF_i \end{bmatrix} \left(sI - \begin{bmatrix} A+BF_x & BF_i \\ -C-DF_x & -DF_i \end{bmatrix} \right)^{-1} \begin{bmatrix} BR \\ I-DR \end{bmatrix} + DR \\
\overline{N} &= \begin{bmatrix} -C & 0 \end{bmatrix} \left(sI - \begin{bmatrix} A+HC & 0 \\ -R^{-1}F_x & -R^{-1}F_i \end{bmatrix} \right)^{-1} \begin{bmatrix} B+HD \\ R^{-1} \end{bmatrix} - D \\
\tilde{X} &= \begin{bmatrix} -F_x & -F_i \end{bmatrix} \left(sI - \begin{bmatrix} A+BF_x & BF_i \\ -C-DF_x & -DF_i \end{bmatrix} \right)^{-1} \begin{bmatrix} H \\ I \end{bmatrix} \\
\overline{X} &= \begin{bmatrix} -R^{-1}F & -R^{-1}F_i \end{bmatrix} \left(sI - \begin{bmatrix} A+HC & 0 \\ -R^{-1}F_x & -R^{-1}F_i \end{bmatrix} \right)^{-1} \begin{bmatrix} -H \\ -I \end{bmatrix} \\
\tilde{Y} &= \begin{bmatrix} C+DF_x & DF_i \end{bmatrix} \left(sI - \begin{bmatrix} A+BF_x & BF_i \\ -C-DF_x & -DF_i \end{bmatrix} \right)^{-1} \begin{bmatrix} H \\ I \end{bmatrix} - I \\
\overline{Y} &= \begin{bmatrix} -R^{-1}F & -R^{-1}F_i \end{bmatrix} \left(sI - \begin{bmatrix} A+HC & 0 \\ -R^{-1}F_x & -R^{-1}F_i \end{bmatrix} \right)^{-1} \begin{bmatrix} B+HD \\ R^{-1} \end{bmatrix} + R^{-1}
\end{aligned}
\tag{7.76}
$$

7.2 Algorithm Example

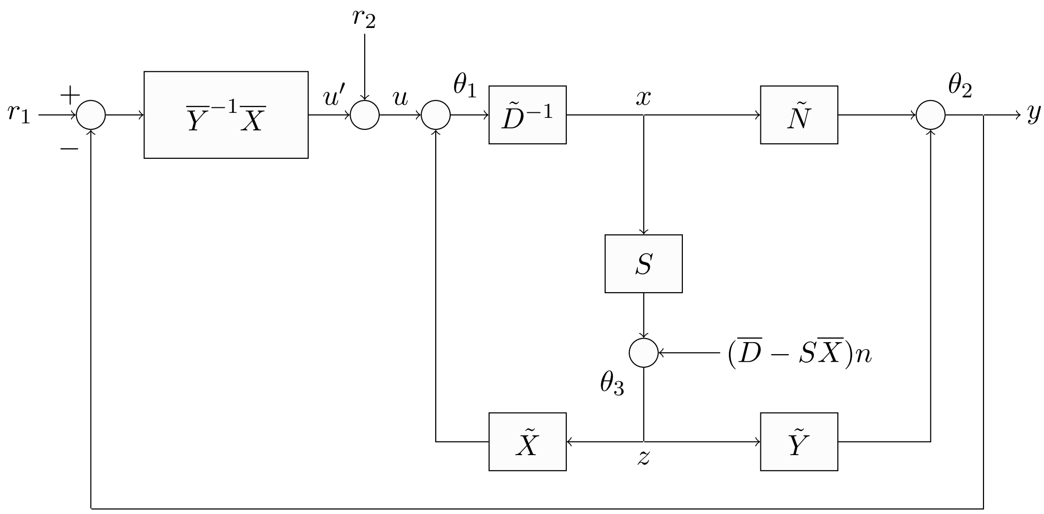

Fig. 7.8: System representation

The Youla-Kucera parametrization can be used in many different ways for different identification and control problems. For the identification performed on heat pumps, throughout this project, the method is as follows. As showed on Fig. 7.8 the output, y, and the input, u', are collected from measurements on the plant. The signal from the uncontrollable inputs are obtained using weather data. A nominal plant and controller are then proposed and the coprime factorizations are chosen as given by Eq. (7.76) to form a favorable coprime factorization. With the $\tilde{X}$, $\tilde{Y}$, $\tilde{N}$ and $\tilde{D}$ blocks determined a sequence for the point x can be calculated using Eq. (7.77) and for the point z with Eq. (7.78). The S block can then be estimated as shown in Eq. (7.79) by the use of open loop estimation software.

$$x = \bar{X}r_1 + \bar{Y}r_2 \tag{7.77}$$

$$z = \bar{D}y - \bar{N}u \tag{7.78}$$

$$z = Sx \tag{7.79}$$

A simulation example is made to validate and show how the identification method works. The full example can be seen in appendix E. The frequency response of the real plant tried to identify in the example is in Fig. 7.9 compared with the frequency response of respectively $\tilde{N}\tilde{D}^{-1}$ and $\bar{D}^{-1}\bar{N}$.

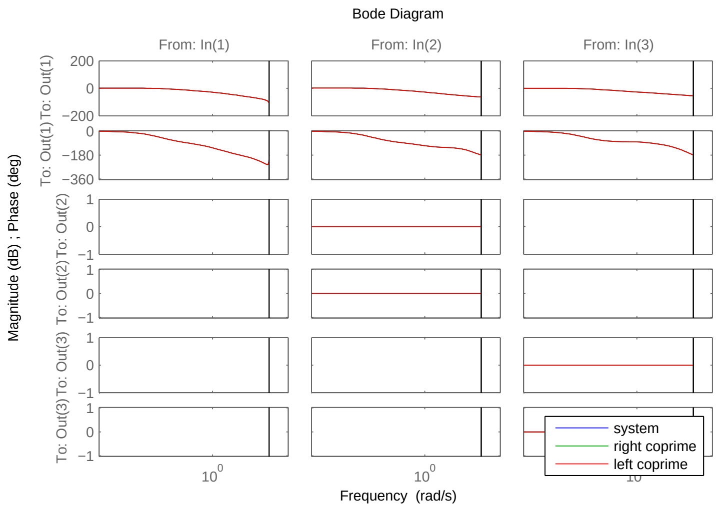

Fig. 7.9: Bode plot of the plant to be identified and the respective right and left coprime factorizations of the plant.

It is seen that the frequency responses are identical why the coprime factorization method holds. An initial plant with a chosen error compared to the real plant is used and the open loop error, S, that maps from the initial guess to the real plant is calculated. Using an open loop identification method on the data, x and z, S is identified and the identification error can be seen on Fig. 7.10.

The open loop error block, S, is not perfectly identified, but as seen on Fig. 7.11 the step response is improved. The NRMSE for the initial guess is 6 % while the right and left coprime factorized plants have an NRMSE of 67 % which is an significant improvement.

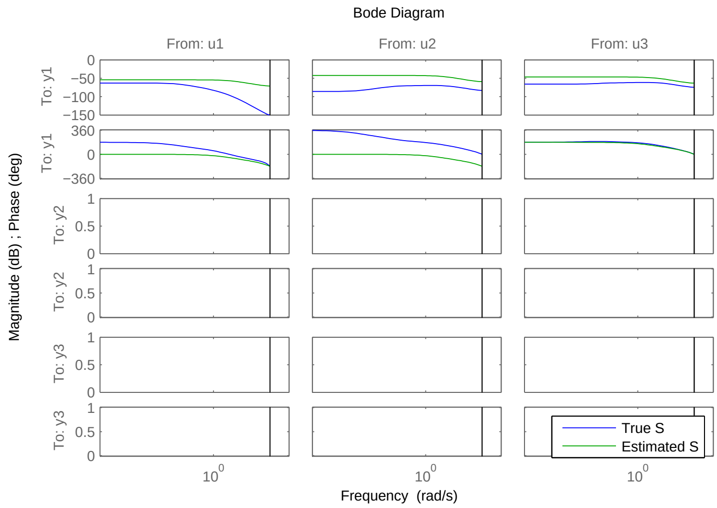

Fig. 7.10: Bode plot of the open loop error.

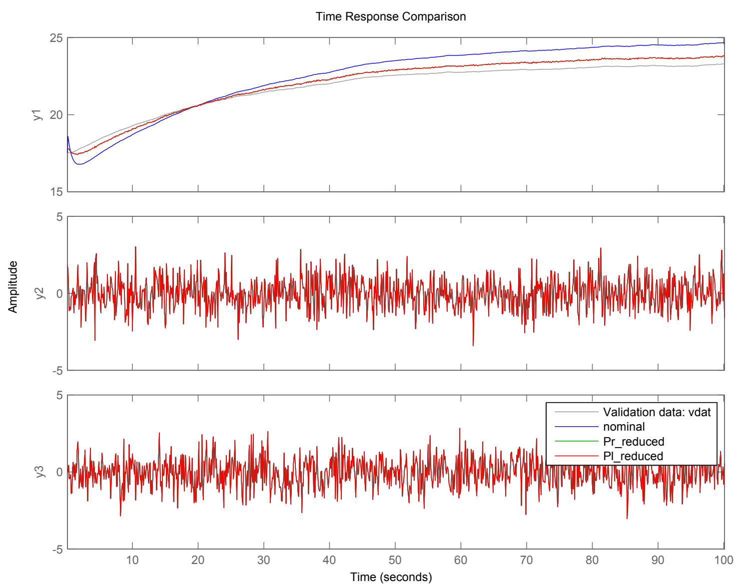

Fig. 7.11: Comparison of output for the 3 models together with the real output data.

Model Identification 8

In this chapter the Hansen Scheme model identification technique is applied to the collected data. An initial identification based on the values in section 5.3 is attempted. The method shows an improvement based on the initial guess. Based on the results of the identification, further tuning of the model is done which significantly improves the result.

8.1 Experiment Design

For identifying the model, data is collected from several houses participating in the "Styr din varmepumpe" project. Further, meteorological data such as solar intensity and outside temperature is collected for the locations from DMI. The data is presented in appendix C where the meteorological data interpolated such that the time steps for both data sources are equal.

The identification method demands that the controller applied to the system is *a priori* known. However the project scope has made it impossible to apply a known controller to the test setup. Instead a qualified guess is given of the controller. The guessed controller design can be found in chapter 6. With the use of the initial guess on the model parameters and the model derived in 5 the full observer with integral feedback is created. The observer and feedback gain are chosen using the `lqr` command in matlab. The full system can be seen on Fig. 8.1. For the identification the system block is substituted with the initial guess on the model.

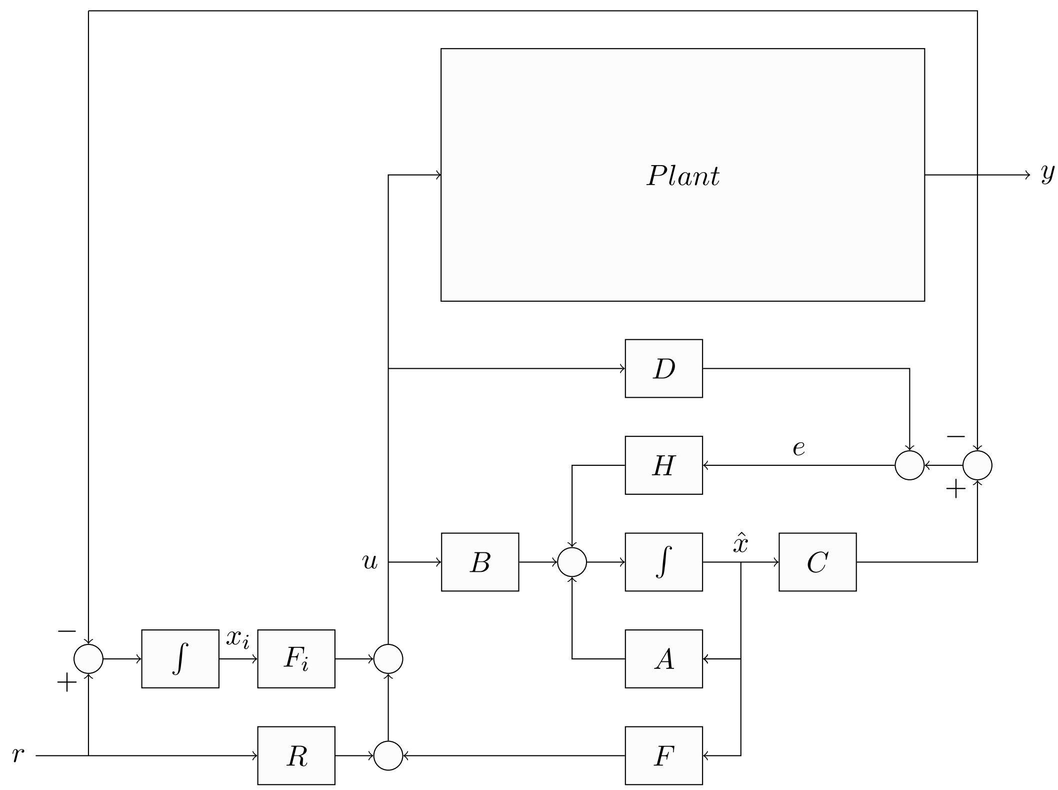

Fig. 8.1: Real plant with the initial guess on the control scheme

8.2 Identification of S

An initial analysis showed that the influence of the solar intensity had a much greater impact than expected. This was most likely due to the assumption of complete absorption of the solar energy. The absorption was reduced to 1% using a reflection coefficient on input 2.

Input sequence r_1 and r_2 are needed for the identification of the open loop error. For the system used in this project r_1 is interpreted as the reference input to the controller. The reference on the heat pump control is estimated as the average temperature in the houses over the full timespan of the data used. The r_1 sequence is found to be constant vector at each time step given in Eq. (8.1). The r_2 sequence is interpreted as the feedforward of the reference together with the two uncontrollable inputs, u_2 and u_3, which are obtained from the weather data. The r_2 sequence is calculated as seen in Eq. (8.2).

$$r_1 = \begin{bmatrix} 21.7 \\ 0 \\ 0 \end{bmatrix} \tag{8.1}$$

$$r_2 = R \begin{bmatrix} 21.7 \\ u_2 \\ u_3 \end{bmatrix} \tag{8.2}$$

With the initial guess on the plant and the proposed controller given the coprime factorizations are calculated. The open loop error, S, seen on Fig. 8.2 is then identified using the method shown in section 7.2.

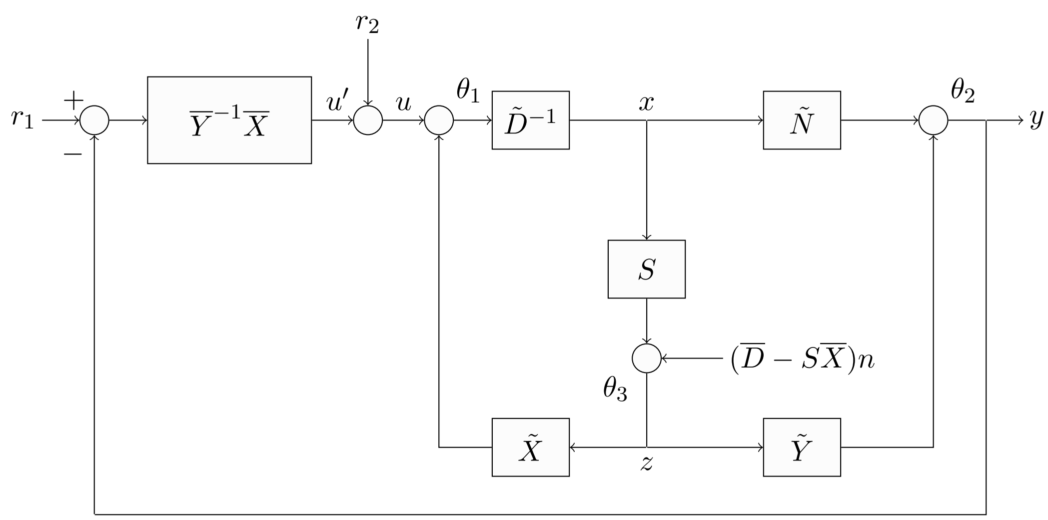

Fig. 8.2: Block representation of the Hansen Scheme

The frequency response of the identified S can be seen on Fig. 8.3. The frequency response is only shown for output 1 since the open loop error is zero from the inputs to output 2 and 3. That the error from the inputs to output 2 and 3 is zero corresponds fine with the full knowledge of the relationship between the inputs and output 2 and 3. The bode plot therefore shows a correction between all 3 inputs and output 1 which is the indoor temperature.

With the open loop error identified, the left and right coprime factorized plants are found using Eq. (8.3) and Eq. (8.4).

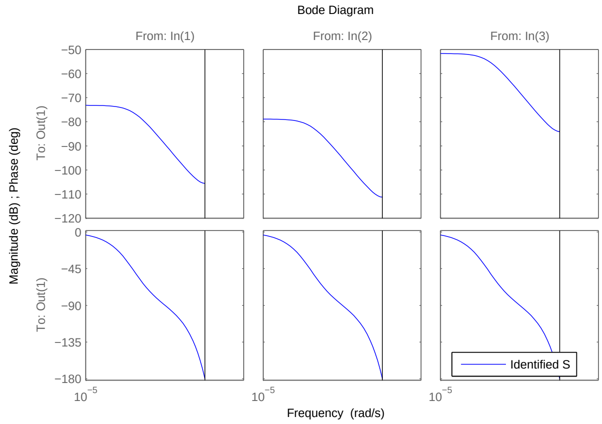

Fig. 8.3: Frequency response of the open loop error identified using the Hansen Scheme. Input 1 is the energy input from the heat pump, input two is the solar intensity, input 3 is the temperature outside and output 1 is the temperature inside the house.

$$\begin{aligned}
\tilde{P}_{identified} &= (\tilde{N} + \tilde{Y}S)(\tilde{D} - \tilde{X}S)^{-1} && (8.3)\\
\bar{P}_{identified} &= (\bar{D} - S\bar{X})^{-1}(\bar{N} + S\bar{Y}) && (8.4)\\
& && (8.5)
\end{aligned}$$

Because of the identification method the identified model is of a far higher order than the initial guess of a third order model. In this example the identified model consist of 26 states why a model reduction is in order. To determine to which order to reduce the identified models the Hankel singular values are calculated. On Fig. 8.4a the Hankel singular values for the right coprime factorized plant are shown. Because it can be very difficult to see the small energy levels of the states on a linear plot, Fig. 8.4b is made with a logarithmic y axis. Where it is only possible to distinct 3 states on Fig. 8.4a, Fig. 8.4b make it clear that no more than 4 states are needed. Using the hankel singular values the model is therefore reduced to consist of only 4 states using the **modred** function in matlab.

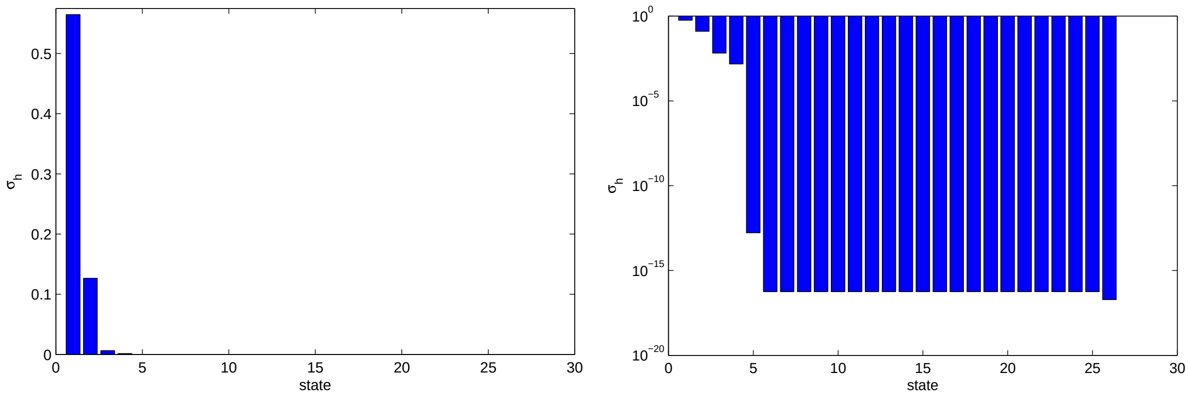

(a) Plot of the Hankel singular values for the right coprime factorized plant.

(b) Plot of the Hankel singular values for the right coprime factorized plant with a logarithmic y-scale.

The point of the model reduction is to eliminate unnecessary states without altering the overall characteristics of the plant. With the indentified plant reduced to a fourth order system the initial guess and the identified plant's are compared using a different input/output sequence.

The comparison can be seen on Fig. 8.5 which shows a significant improvement from the initial guess to the identified models.

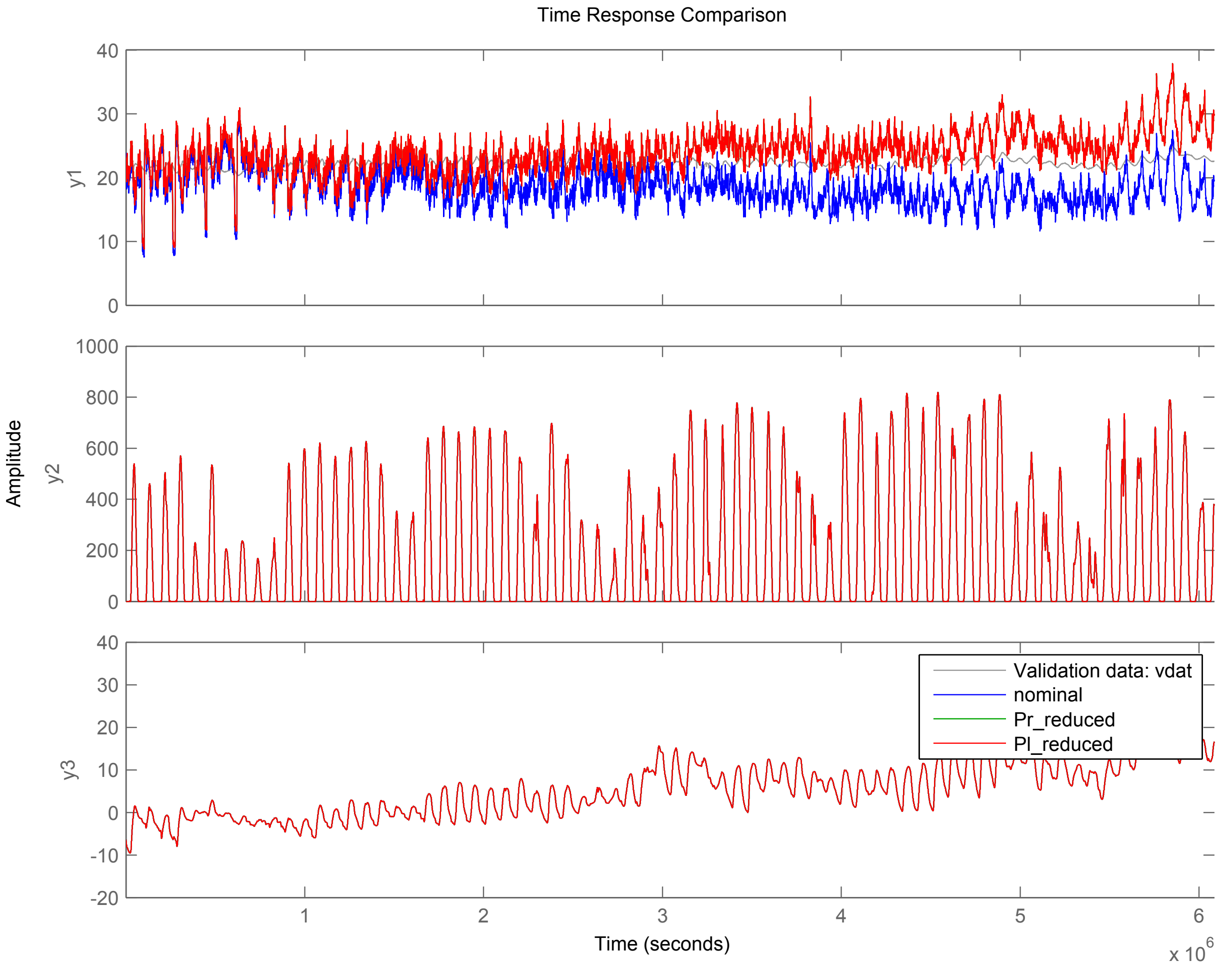

Fig. 8.5: Comparison of the obtained data with the predictions from the initial model and identified models. Output y1 is the indoor temperature, output y2 is the solar intensity and output y3 is the temperature outside. The gray line is the real measured data, the green and red lines are the data generated using the input sequence together with the identified plant with respectively the right and left coprime factorizations. The blue line is the input sequence together with the initial guess on the plant.

A bode plot of the initial guess on the plant and the identified plant is made to investigate the error. On Fig. 8.6 the bode plot of the initial guess and the identified plant is shown. It is noticed that the method have identified and error on input 2 and 3, while input 1 stays close to the initial guess. The bode plot shows that the identified model both amplify and delay the solar intensity through input 2.

It is noted that the identification method improves the indoor temperature prediction. However the model predict the indoor temperature to change faster than the data suggest, furthermore the predicted temperature is also a bit higher than what the measurements suggest. The fast change in the indoor temperature seems to come from the heat pump input, which is the only input which changes fast enough to cause this kind of behavior. To slow down the changes in the indoor temperature the initial guess on the mass of the floor is increased. With an increase in the floor mass the energy needed to change the temperature is increased. The mass of the air inside the house is increased as well to take into account that the house is filled with furniture made of other materials than air. A comparison plot of the plant and data with the new initial

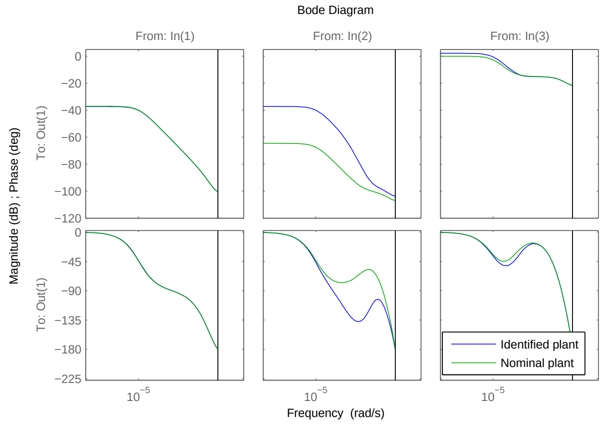

Fig. 8.6: Frequency response of the initial model guess and the identified plant. Input 1 is the energy input from the heat pump, input two is the solar intensity, input 3 is the temperature outside and output 1 is the temperature inside the house.

guess can be seen on Fig. 8.7. The predicted temperature now follows the measurements and is not fluctuating. The identification method is thus seen as working on the obtained data.

On Fig. 8.8 a sample of 5 days of the full sequence is studied to see the result of the identification. From the sample of 5 days it can be seen that the nominal plant suggest that the indoor temperature should change faster than it is observed. Through the identification both the error in phase and the gains are adjusted, which is also easy to see using the frequency and phase plot on Fig. 8.6.

8.3 Observations and Results

Analyzing S as a way improving the nominal model proved highly unintuitive. Rather, the improvements seen from tuning the nominal model came in large part by analyzing how the complete transfer function of the system changed as a function of S. Also, analyzing the response of both the identified and the nominal system compared to the real system gave some insight into how to improve the initial guess. For determining the temperature in the house 3 inputs were identified: the heat pump, the sun intensity and the temperature outside. The results suggest that these inputs are sufficient and no more are needed. The results of the identification seen in Fig. 8.5 and Fig. 8.7 show that the choice of nominal model have a big impact on the result of the identification. This suggests that significant improvements can be made by spending more time tuning the initial guess for the model. As the calculations necessary for the method are somewhat simple - the factorizations merely being a way of ordering the state space matrices and generation of x and z being simulations of a linear system - it may be possible to build an optimization algorithm on top of this method which optimizes the nominal model for the best post-identification result. Another method could be to use an identified model as the nominal model in an iterative fashion to arrive at a final model. However these options are not further explored in this project. Furthermore the proposed thermal model is able to capture the dynamics of the plant and it seems as a good initial guess. However the identification increased the order of the model by one, which suggest that the initial guess can be improved by adding one more state to the model.

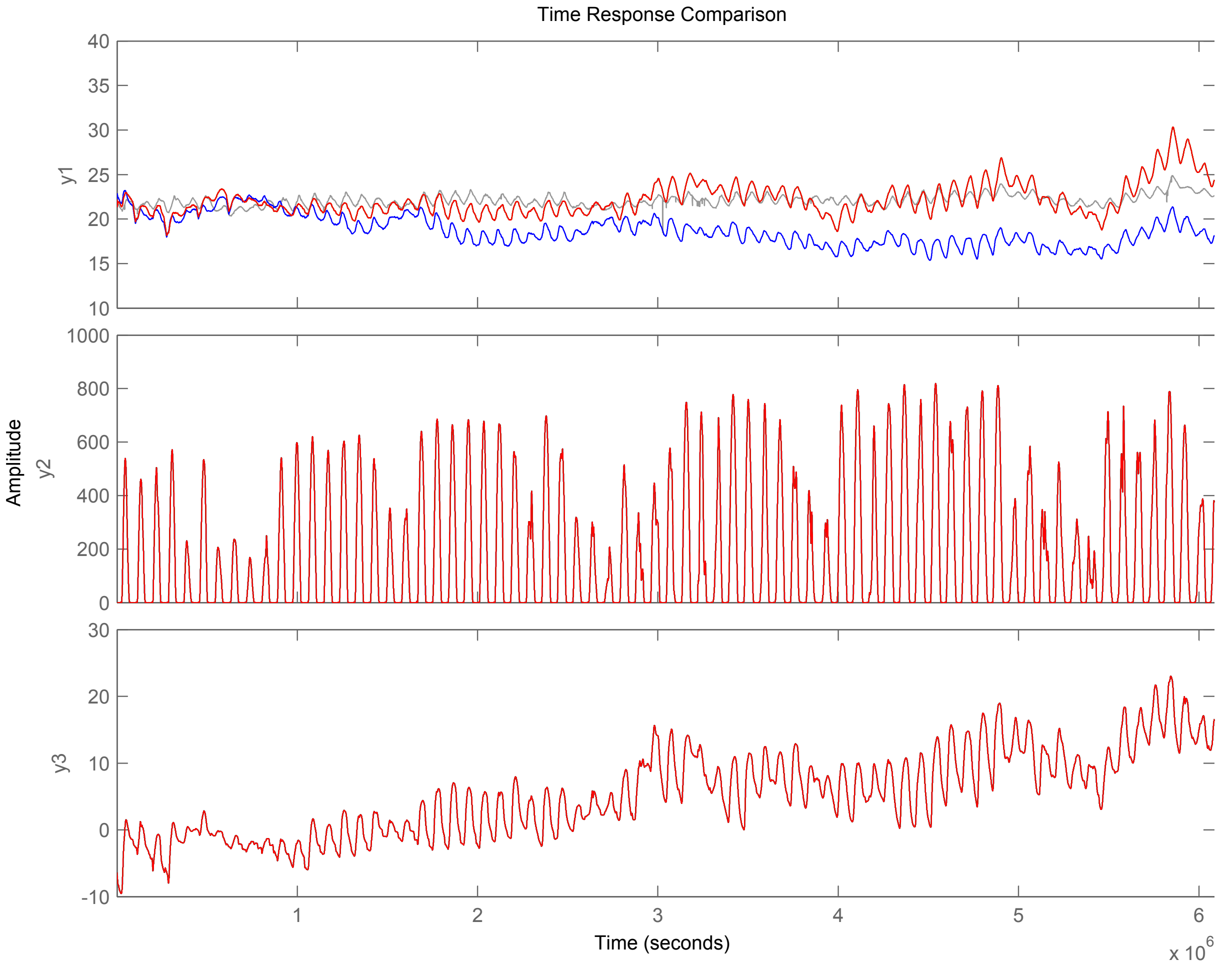

Fig. 8.7: Comparison of the obtained data with the predictions from the initial model with new starting parameters and identified models. Output y1 is the indoor temperature, output y2 is the solar intensity and output y3 is the temperature outside. The gray line is the real measured data, red line is the identified and the blue line is the nominal plant.

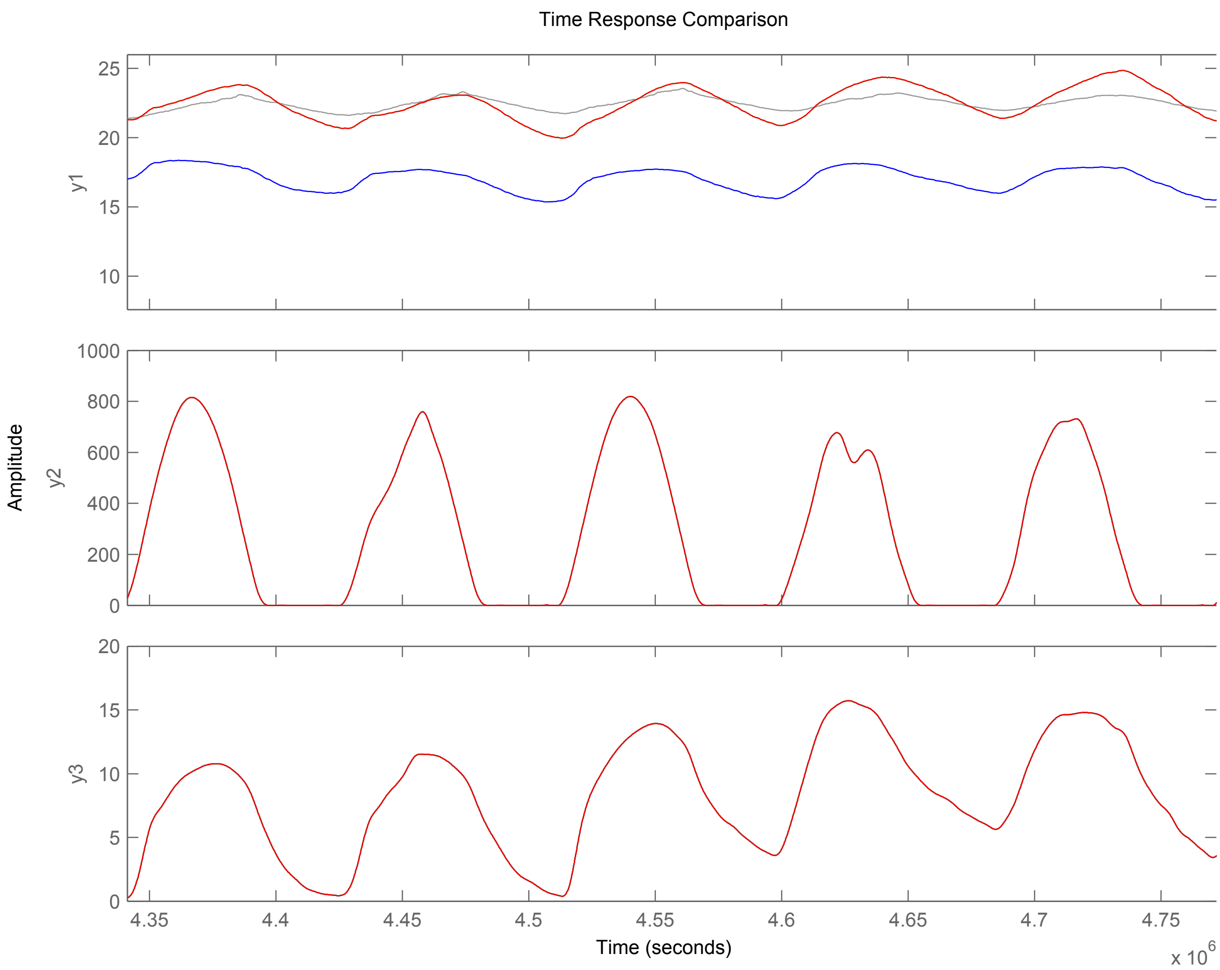

Fig. 8.8: Comparison of the obtained data with the predictions from the initial model with new starting parameters and identified models. Output y1 is the indoor temperature, output y2 is the solar intensity and output y3 is the temperature outside. The gray line is the real measured data, red line is the identified and the blue line is the nominal plant.

Conclusion 9

In this project the problem of heating a house using a heat pump was analyzed. Some of the primary inputs to the system were analyzed based on the availability of data which could be used for model identification.

A nominal model was developed based on estimates of the average house, with the objective of using this nominal model to better model an actual house. Further, a nominal controller was designed to stabilize this nominal model. The controller was designed with integral action to ensure a steady state error of 0. This was done to somewhat mimic the behavior of the heat pump controller, which also uses integrating action to reach its reference, although in a slightly different manner. Further, a reference feed forward was designed to allow the proportional and integral control to work towards the same target.

Adding reference feed forward and integral action meant that the standard coprime factorizations were no longer valid. For this reason it was necessary to investigate the mathematical foundations on which these factorizations rest and how adding additional terms might affect them. This resulted in the factorizations seen in chapter 7 and appendix F.

The primary contribution of this project is the expansion and explanation of the coprime factorizations of a system with integral action and a reference feed forward. The factorizations are proven analytically to be valid factorizations of the system and controller and are in turn tested with a simulation example to prove that the factorizations do indeed result in the system which was factorized, as expected.

Model identification is attempted using the nominal model. The initial attempts show that it is indeed possible to produce a better estimate than the nominal model through the Hansen Scheme using the factorizations. By analyzing the results of the initial identification it a significantly better model estimate is produced, which again is improved by the Hansen Scheme. This showed that the nominal model had a great impact on the identification result.

It can also be concluded that the houses participating in the project can be identified by the proposed method, as shown in chapter 8. The identified model was a 4th order model which suggests that the order of the initial guess was too low.

10 Discussion

While the model identification was successful there are still some things which could improve the end result. Most notably the Hansen Scheme assumes that the controller is fully known. This can be achieved by designing a controller and using this controller on the plant. This would further give the added value of being able to have a non-constant reference, which might better reveal how the dynamics of the system behaves.

Another method could be to use the Hansen Scheme to identify a "nominal" controller for heat pumps by using a fully known system with some sort of representative heat pump. Since the controller used by heat pumps isn't a linear controller it would only be possible to get an approximation. This approximation could however be sufficient for model identification purposes.

Further it could be interesting to analyze how the identification method behaves to different discrepancies between the real and the nominal model, such as the order of the model and the magnitude of the difference in system parameters.

While the nominal model used for identification was a third order model it was seen that the identified model was a 4th order model. Given this an identification using a 4th order nominal model might give a better result.

As for the factorizations, the method with which they were derived easily lends itself to other system configurations. One such configuration could be the addition of zero assignment through feed forward gain. Deriving these would be quite easy and may be useful for other applications, specifically if the controller is known to be of this structure.

Bibliography

[1] ForskEL. Slutrapport ForskEL 2010 - 10469 Intelligent Fjernstyring af Individuelle Varmepumper, 2010.

[2] Energinet.dk. Workshop netbelastninger - smart grid-projekter og løsninger. http://www.ea-energianalyse.dk/presentations/2012-11-05_netbelastning_smart_grid.pdf, 2012. [Online; accessed 29-May-2014].

[3] Energinet.dk. Fra vindkraft til varmepumper. https://styrdinvarmepumpe.dk/sites/default/files/Fra%20vindkraft%20til%20varmepumper_-_rapport_juli_2012.pdf, 2012. [Online, accessed 30-May-2014].

[4] Benjamin Biegel and Palle Andersen and Jakob Stoustrup and Mathias Madsen and Lars Hansen. Lumped thermal household model. In 4th IEEE PES Innovative Smart Grid Technologies Europe (ISGT Europe), 2013.

[5] Nord Pool Spot. The nordic electricity exchange and the nordic model for a liberalized electricity market.
http://www.nordpoolspot.com/Global/Download%20Center/Rules-and-regulations/The-Nordic-Electricity-Exchange-and-the-Nordic-model-for-a-liberalized-electricity-mar pdf. [Online, accessed 30-May-2014].

[6] T. S. Pedersen and P. Andersen and K. M. Nielsen and H.L. Stærmose and P.D. Pedersen. Using heat pump energy storages in the power grid. In 2011 IEEE International Conference on Control Applications (CCA), 2011.

[7] Linda McLaughlin and Zhe Yu, Liyan Jia and Mary C. Murphy-Hoye and Ellen G. Piccioli and Annabelle Pratt and Lang Tong. Thermal Dynamic Modeling for Home Energy Management: A Case Study, unknown.

[8] Danfoss. Maintenance Instructions: DHP-H Opti Pro, DHP-H, DHP-C, DHP-L, DHP-A, DHP-AL - VUBMA402, 2008.

[9] Lennart Ljung, editor. System Identification (2nd Ed.): Theory for the User. Prentice Hall PTR, Upper Saddle River, NJ, USA, 1999.

[10] Brian D. O. Anderson. From Youla-Kucera to Identification, Adaptive and Nonlinear Control, 1998.

[11] J. Bendtsen and K. Trangbæk and J. Stoustrup. Closed-loop System Identification with New Sensors, 2008.

[12] Paul Van den Hof. CLOSED-LOOP ISSUES IN SYSTEM IDENTIFICATION. http://www.sciencedirect.com/science/article/pii/S1367578898000169, 1998. [Online; accessed 27-May-2014].

[13] Fred Hansen and Gene Franklin and Robert Kosut. Closed-loop identification via the fractional representation: Experiment design. In Proc. American Control Conference, 1989.

[14] Murværk for KALK-OG TEGLVÆRKSFORENINGEN AF 1893 Teknologisk Institut. Varmeledningsevne. http://www.mur-tag.dk/index.php?id=554, 2008. [Online; accessed 19-May-2014].

[15] Miljøstyrrelsen. Dimensioneringsprogrammets forudsætninger. http://www2.mst.dk/udgiv/publikationer/2010/978-87-92708-16-8/html/kap03.htm, 2010. [Online; accessed 19-May-2014].

[16] The Engineering Toolbox. The Engineering Toolbox. http://www.engineeringtoolbox.com/specific-heat-capacity-d_391.html, 2008. [Online; accessed 19-May-2014].

[17] Vladimir Kucera. A method to teach the parameterization of all stabilizing controllers. In 18th IFAC World Congress, 2011.

[18] J. S. Freudenberg, C. V. Hollot, and D. P. Looze. A FIRST GRADUATE COURSE IN FEEDBACK CONTROL. ftp://barney.ecs.umass.edu/pub/hollot/control_system_design/syllabus%20+%20book/textbook.pdf, 2003. [Online; accessed 21-May-2014].

Energy Flow Check A

A.1 Objective

The objective of these simulations are to prove that the model of a house used throughout this project is realistic in the sense of how energy flows and the steady state values found for different types of input. The objective is therefore not to confirm if the model is able to fit the data obtained on houses used in the forskEL project nor to find parameters for the model. Instead the simulations are done with parameters assigned values that most certainly are unrealistic if looking on the dynamics of the house.

A.2 Procedure

The state space model tested is shown in Eq. (A.1) to (A.3) where it is noted that the model have 9 independent parameters. Some restrictions apply to the final parameters and using those restrictions some simple values are used for these simulations. All parameters are known to be positive and the COP factor is more than 1, while β has to be between 0 and 1. The COP factor is therefore chosen to be 2 while β is set to 0.5.

$$\mathbf{A}=\begin{bmatrix} -\frac{\alpha_{f,a}+\alpha_{w,a}}{M_a\cdot c_a} & \frac{\alpha_{w,a}}{M_a\cdot c_a} & \frac{\alpha_{f,a}}{M_a\cdot c_a} \\ \frac{\alpha_{w,a}}{M_w\cdot c_w} & -\frac{\alpha_{o,w}+\alpha_{w,a}}{M_w\cdot c_w} & 0 \\ \frac{\alpha_{f,a}}{M_f\cdot c_f} & 0 & -\frac{\alpha_{f,a}}{M_f\cdot c_f} \end{bmatrix} \tag{A.1}$$

$$\mathbf{B}=\begin{bmatrix} 0 & 0 & 0 \\ 0 & A\cdot\beta & \frac{\alpha_{o,w}}{M_w c_w} \\ \frac{COP}{M_f c_f} & A\cdot(1-\beta) & 0 \end{bmatrix} \tag{A.2}$$

$$\mathbf{C}=\begin{bmatrix} 1 & 0 & 0 \end{bmatrix} \tag{A.3}$$

In table A.1 the parameters used can be seen.

$\alpha_{f,a}$	450.8
$\alpha_{w,a}$	554.4
$\alpha_{o,w}$	117.6
$M_a\cdot c_a$	764.4
$M_w\cdot c_w$	87897.6
$M_f\cdot c_f$	764.4
A	196
COP	1.34
β	0.1

Fig. A.1: Parameters and their values for the simulations

With the parameters chosen 3 simulations with different input have been made. First simulation is done by setting all inputs except for the outdoor temperature to zero. That way all states are supposed to reach the same temperature as the one outside. The second simulation is done by having constant non zero input on the pump and the outdoor temperature, while keeping the solar intensity 0. The last simulation is done with all 3 inputs being a nonzero constant. All simulations have been run for 100 seconds and the initial states have been chosen to be 23 for the indoor temperature, 19 for the temperature in the wall and 27 for the floor temperature.

A.3 Results

On Fig. A.2 a plot of how the 3 states evolve when no energy is put into the house from the heat pump and the sun. The states are therefore supposed to all reach the same level equal to the temperature outside the house. The temperature outside the house is set to 5 which it can been seen all states also reach after some time. The model therefore satisfies that all states will reach the same level if no energy is added to the house from the heat pump and sun.

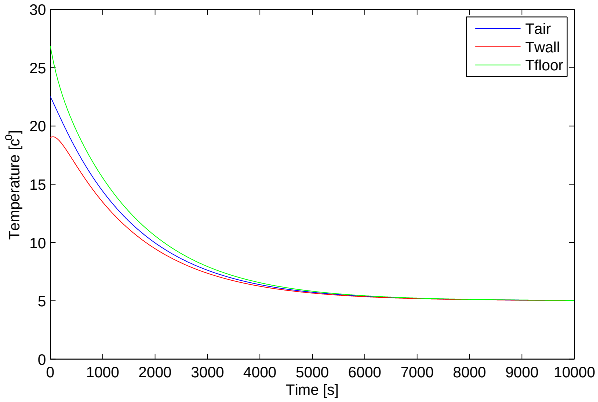

Fig. A.2: Plot of the 3 states with the pump and intensity inputs set to zero and the T_{out} set to 5.

In the second simulation a nonzero input from the heat pump is added. In this case the 3 states are supposed to find 3 different steady states, with the wall being the coldest and the floor being the warmest. The steady state temperatures on Fig. A.3 are all different with the floor temperature being the highest and the wall temperature the lowest. The energy flow through the house is therefore pointing the desired way, which was shown on Fig. 5.1.

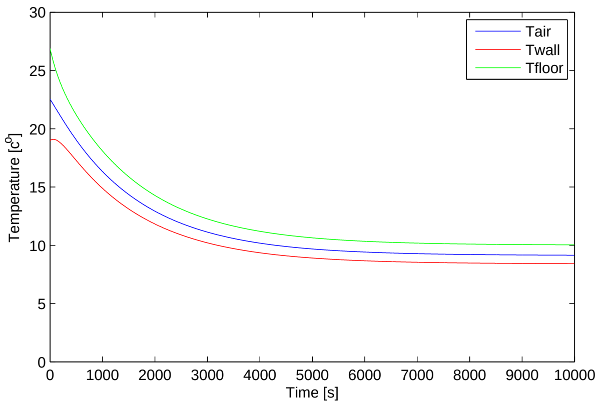

Fig. A.3: Plot of the 3 states with the intensity input set to zero and P_{pump} and T_{out} set to 5.

Lastly all inputs have been set to a nonzero constant and the steady state values are therefore supposed to be higher on Fig. A.4 than on Fig A.3. Since the state reach higher steady state values on Fig. A.4 the relationships between states and inputs have been confirmed to react in a realistic way.

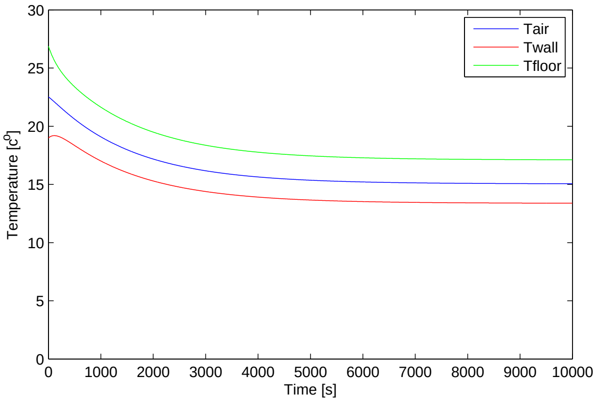

Fig. A.4: Plot of the 3 states with all inputs set to 5.

Coefficient of Performance B

B.1 Objective

As the Coefficient of Performance depends on many different conditions, most notably the source and sink temperature, but it is necessary with a single, linear model it is desirable to use a COP which is representative of the average case.

To calculate the COP it is necessary to know how much energy is put into the house as well as the amount of electrical energy used. However, since the pump will have to monitor when to pump it uses energy even when not running. This can result in a disproportionally large COP as there is still some mass flow due to the inertia of the system, even when the pump is not running.

To get a better picture of the how running the pump actually affects the system it might be more beneficial to look at a long period where the pump is running so it reaches a steady state value. However as the source and sink temperature are of importance an average COP should reflect several scenarios.

For this reason the average value of the COP at all times where the pump is on is used. *On* is in this case defined as any period where the electrical power usage of the pump exceeds 100W.

B.2 Procedure

The COP is defined as equation (B.1), as seen in equation (5.3) in section 5.2.

$$COP = \frac{\dot{m}_w \cdot c_w \cdot (T_{w,i} - T_{w,o})}{P_p} \tag{B.1}$$

To generate the COP it is important that the necessary data is synced. However, since some sensors will sometimes be offline or otherwise incapable of taking a measurement, two vectors of data points of the same length may not refer to the same instant in time. Luckily, for each data point there's an accompanying timestamp such that the data points can be correlated.

To generate the average COP, the COP is calculated for all times where all necessary data is there and the electrical power consumption is larger than 100W.

B.3 Results

With $c_w = 4180$ the average COP is calculated to be 1.364.

Identification Data C

C.1 Objective

The purpose of this Appendix is to identify which data is available and how it relates to the inputs and output of the system.

Data from the forskEL project styrdinvarmepumpe ("Control your heatpump") as well as data from DMI (The Danish Meteorological Institute) is used to generate the input and output vectors for model identification. The data is taken from a collection of 39 different houses in different parts of Denmark in the period 13:00 January 1st 2013 - 10:00 May 21st 2013.

The data from the styrdinvarmepumpe project contains the following measurements of interest with a sampling time of 5 minutes:

Variable name	Description	Unit
$HPpower$	Electrical power expended in the heat pump	[W]
$HPtin$	Inside temperature	[C]

While the meteorological data contains the following measurements of interest with a sampling time of 1 hour:

Variable name	Description	Unit
$Direct$	Direct sunlight hitting a given house	[W/m^2]
$Diffuse$	Diffuse sunlight hitting a given house	[W/m^2]
$Temp\_out$	Outside Temperature	[C]

Further it contains some different parameters for the houses, such as location and size.

C.2 Procedure

The meteorological data is interpolated such that the number of house and weather samples are equal. This gives a total of 40285 samples. Of these, the first 20000 are used for identification purposes while the remaining are used for verification.

The total sunlight hitting the house is defined as the sum of the direct and the diffuse sunlight. This gives the mapping seen in equation C.1.

$$
\begin{aligned}
u &= \begin{bmatrix} P_p \\ I_s \\ T_o \end{bmatrix} = \begin{bmatrix} HPpower \\ Direct + Diffuse \\ Temp\_out \end{bmatrix} \\
y &= \begin{bmatrix} T_i \\ I_s \\ T_o \end{bmatrix} = \begin{bmatrix} HPtin \\ Direct + Diffuse \\ Temp\_out \end{bmatrix} \\
r &= \text{mean}(HPtin)
\end{aligned} \tag{C.1}
$$

To generate the reference, the average of the indoor temperature of the entire 40285 samples is used.

The average size of the house is calculated as simply the mean of the sampled houses.

C.3 Results

The reference value is calculated to be 21.7523 °.

The average house size is calculated to be 196 m^2.

The remaining values can be fed directly into the identification algorithm and need no further changes.

Coprime Expansion D

In this chapter the logic behind the coprime factorizations are shown. When the two factorized systems are multiplied together, their internal components should cancel out, such that they are left with original system which was factorized. Here, it is graphically shown how each block can cancel another part of the system.

To achieve both left and right coprime factorization it is necessary to have an appropriate stable system which each define a pair of transfer functions.

Right coprime factorizing a plant produces $\tilde{D}$, the transfer function from r to u, and $\tilde{N}$, the transfer function from r to y, as seen on Fig. D.1.

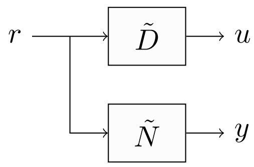

Fig. D.1: The $\tilde{N}$ and $\tilde{D}$ blocks map the reference to the output and input, respectively.

From this figure it is readily seen that the plant transfer function, the transfer function from u to y can be found by $P = \tilde{N}\tilde{D}^{-1}$ as seen on Fig. D.2.

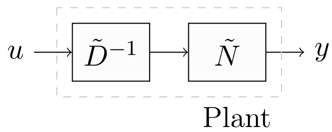

Fig. D.2: The plant can be found be going from u to y through ˜ and $\tilde{D}$.

A plant with no reference gain but a stabilizing state feedback, sees the reference directly on its input, $u = Fx + r$. In other words the reference enters the system through the B matrix as seen on Fig. D.3.

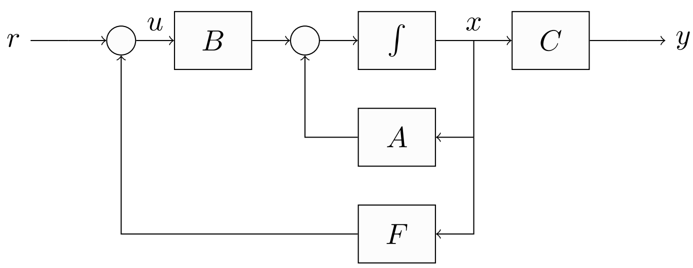

Fig. D.3: Without reference gain the reference can be considered simply an input to the system.

With the input defined the descriptions for both the states and the output is easily found, as seen in Eq. (D.1).

$$
\begin{aligned}
u &= Fx + r \\
\dot{x} &= (A + BF)x + Br \\
y &= (C + DF)x + Dr
\end{aligned}
\tag{D.1}
$$

With $D = 0$ the right coprime factorization can be made:

$$
\tilde{D} = \left[\begin{array}{c|c} A+BF & B \\ \hline F & I \end{array}\right], \qquad \tilde{N} = \left[\begin{array}{c|c} A+BF & B \\ \hline C & 0 \end{array}\right]
\tag{D.2}
$$

$$
\tilde{D}^{-1} = \left[\begin{array}{c|c} A & B \\ \hline -F & I \end{array}\right]
\tag{D.3}
$$

Fig. D.4 shows how these systems interact when they are connected.

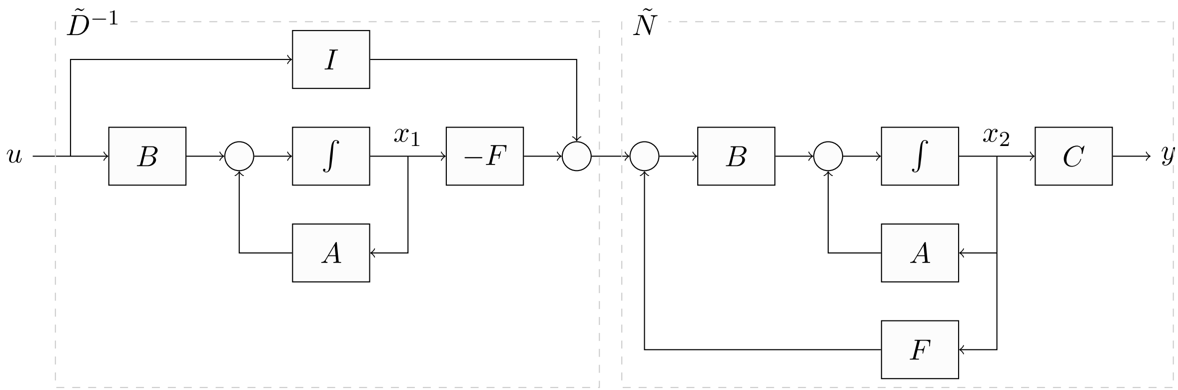

Fig. D.4: The combined plant when $\tilde{D}^{-1}$ and $\tilde{N}$ are in series.

Verifying that $P = \tilde{N}\tilde{D}^{-1}$:

$$
\tilde{N}\tilde{D}^{-1} = \left[\begin{array}{c|c} A+BF & B \\ \hline C & 0 \end{array}\right] \left[\begin{array}{c|c} A & B \\ \hline -F & I \end{array}\right] = \left[\begin{array}{cc|c} A & 0 & B \\ -BF & A+BF & B \\ \hline 0 & C & 0 \end{array}\right]
\tag{D.4}
$$

To verify that this is indeed equal to the plant we first calculate the difference in derivatives between the two states:

$$
\dot{x}_1 - \dot{x}_2 \Rightarrow Ax + Bu - (-BFx_1 + Ax_2 + BFx_2 + Bu) \Rightarrow (A + BF)(x_1 - x_2)
\tag{D.5}
$$

In other words: The derivatives are equal when the states are equal. This implies that the states will always be equal as the system is stable so both states converges towards the same value.

Given that $x_1 = x_2$, $\dot{x}_1 = \dot{x}_2$ and $\dot{x}_1 = Ax_1 + Bu$ then $\dot{x}_2 = Ax_2 + Bu$. This then gives the system

$$
\tilde{N}\tilde{D}^{-1} = \left[\begin{array}{cc|c} A & 0 & B \\ 0 & A & B \\ \hline 0 & C & 0 \end{array}\right]
\tag{D.6}
$$

This system has an unobservable state x_1 and can therefore be simplified to

$$\tilde{N}\tilde{D}^{-1} = \left[\begin{array}{c|c} A & B \\ \hline C & 0 \end{array}\right] \tag{D.7}$$

Reference Feedforward

The case of reference feedforward is a simple expansion of the current system, where any reference signal has a gain of R, where it previously has I. In other words, $u = Fx + Rr.$, as seen on Fig. (D.5).

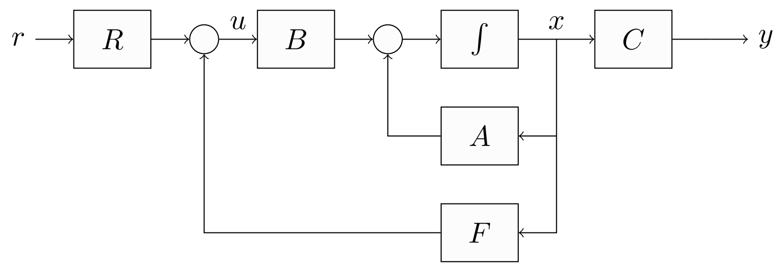

Fig. D.5: Without reference gain the reference can be considered simply an input to the system.

The factorization is straight forward:

$$\tilde{D} = \left[\begin{array}{c|c} A+BF & BR \\ \hline F & R \end{array}\right], \qquad \tilde{N} = \left[\begin{array}{c|c} A+BF & BR \\ \hline C & 0 \end{array}\right] \tag{D.8}$$

$$\tilde{D}^{-1} = \left[\begin{array}{c|c} A & -B \\ \hline R^{-1}F & R^{-1} \end{array}\right] = \left[\begin{array}{c|c} A & B \\ \hline -R^{-1}F & R^{-1} \end{array}\right] \tag{D.9}$$

Connecting these gives the total system as seen on Fig. D.6.

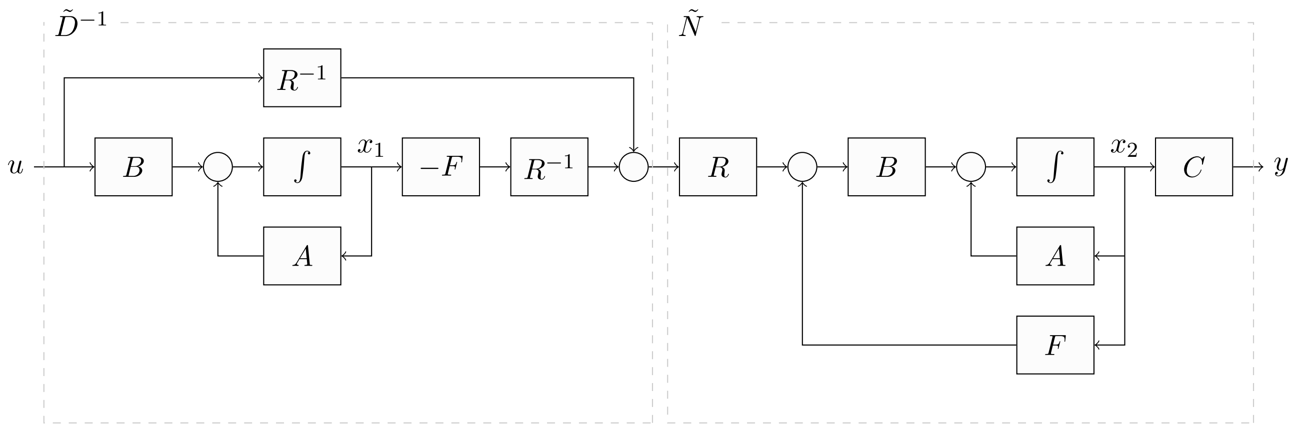

Fig. D.6: The combined plant when $\tilde{D}^{-1}$ and $\tilde{N}$ are in series.

$$\tilde{N}\tilde{D}^{-1} = \left[\begin{array}{c|c} A+BF & BR \\ \hline C & 0 \end{array}\right] \left[\begin{array}{c|c} A & B \\ \hline -R^{-1}F & R^{-1} \end{array}\right] \tag{D.10}$$

$$= \left[\begin{array}{cc|c} A & 0 & B \\ -BRR^{-1}F & A+BF & BRR^{-1} \\ \hline 0 & C & 0 \end{array}\right] \tag{D.11}$$

$$= \left[\begin{array}{cc|c} A & 0 & B \\ -BF & A+BF & B \\ \hline 0 & C & 0 \end{array}\right] \tag{D.12}$$

Which is equivalent to the previous system and can therefore also be reduced to equal P.

Integral Control

When adding integral control, which adds additional states, the factorization should still reduce to the original plant.

The factorization is derived by looking at the previous factorizations and noting that the output from $\tilde{D}^{-1}$ negates the feedback through F in $\tilde{N}$ and that the states will always be equal. The same thing should happen with the integral gain - The states should be equal and never diverge and the integrating controller in $\tilde{D}^{-1}$ should exactly cancel the effect of the integrating controller in $\tilde{N}$. In other words the input to the integrators should always be equal, such that the integrators will always be equal, given equal starting conditions.

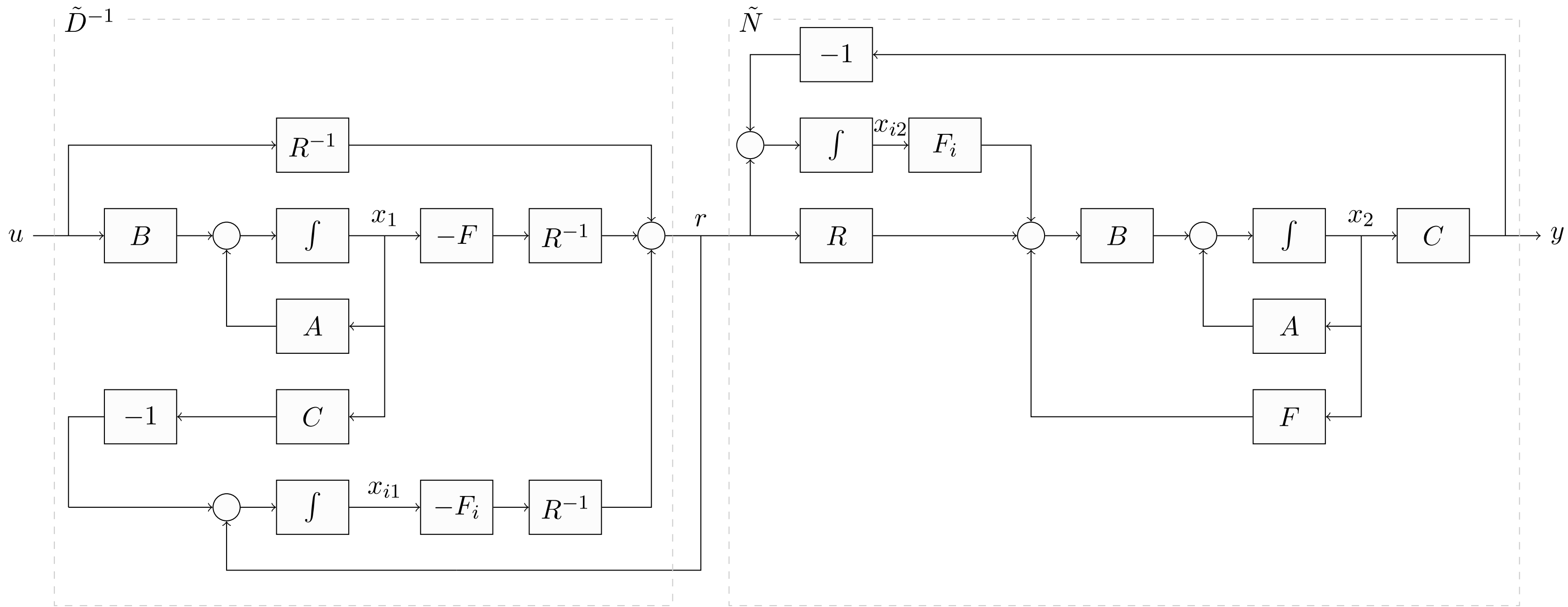

Fig. D.7: Coprime factorization with integral control.

From Fig. D.7 the total state space representation of the system can be derived.

$$\tilde{D} = \left[\begin{array}{cc|c} A+BF_x & BF_i & BR \\ -C & 0 & I \\ \hline F_x & F_i & R \end{array}\right] \qquad \tilde{N} = \left[\begin{array}{cc|c} A+BF_x & BF_i & BR \\ -C & 0 & I \\ \hline C & 0 & 0 \end{array}\right]$$

$$\tilde{D}^{-1} = \left[\begin{array}{cc|c} A & 0 & B \\ -C-R^{-1}F_x & -R^{-1}F_i & R^{-1} \\ \hline -R^{-1}F_x & -R^{-1}F_i & -R^{-1} \end{array}\right]$$

$$\tilde{N}\tilde{D}^{-1} = \left[\begin{array}{cccc|c} A & 0 & 0 & 0 & B \\ -C-R^{-1}F_x & -R^{-1}F_i & 0 & 0 & R^{-1} \\ -BF_x & -BF_i & A+BF_x & BF_i & B \\ -R^{-1}F_x & -R^{-1}F_i & -C & 0 & R^{-1} \\ \hline 0 & 0 & C & 0 & 0 \end{array}\right]$$

For the case $x_1 = x_2$, $x_{i1} = x_{i2}$ the controller input is canceled out, leaving $\tilde{N}\tilde{D}^{-1} = \left[\begin{array}{c|c} A & B \\ \hline C & 0 \end{array}\right]$. Therefore this is a valid right coprime factorization of a system with integral control.

Simulation Example E

The purpose of this appendix is to show that the proposed method will be able to successfully identify a known system in a closed loop setting. The factorizations are shown to be valid factorizations of the system and the necessary steps of the method are outlined. Further, the method is shown to be superior to direct open loop identification of a closed loop system, as expected.

With the theory behind the identification method outlined in 4.2 an example is used to show how the identification method can be applied to the data obtained from the forskEL project. Throughout this project it is assumed that the heat pump is controlled by some unknown PI controller. The example will therefore be controlled by an state estimator and integral control as seen on Fig. E.1. The whole example is divided into subproblems that are described individually. For the simulation example 200 seconds have been simulated with a step length of 0.1 seconds.

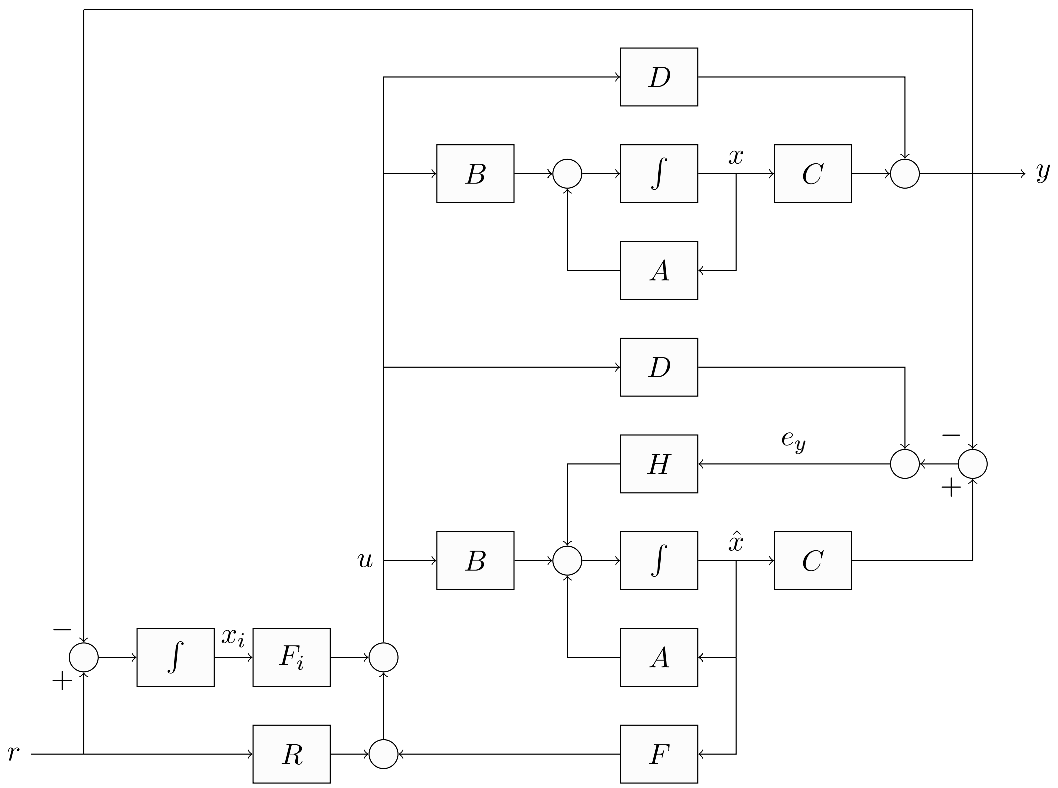

Fig. E.1: Full system representation.

Incomplete Model of Plant

The plant tried to identify in the example is the house model described in 5 which consist of 3 inputs, 3 states and 3 outputs. The plant is thus square which is necessary for the identification method. To identify the plant a nominal plant is needed. It is chosen to set the heat transfer coefficient from the wall to the air to 0.9 of the true value. The real plant system matrix is shown in Eq. (E.1) and the nominal plant's system matrix is shown in Eq. (E.2).

$$A = \begin{bmatrix} -0.5000 & 0.1000 & 0.4000 \\ 30.0000 & -70.0000 & 0 \\ 1.0000 & 0 & -1.0000 \end{bmatrix} \tag{E.1}$$

$$\hat{A} = \begin{bmatrix} -0.4900 & 0.0900 & 0.4000 \\ 27.0000 & -67.0000 & 0 \\ 1.0000 & 0 & -1.0000 \end{bmatrix} \tag{E.2}$$

Because the heat transfer coefficient from the wall to the air only affects the system matrix the input, output and the feedthrough matrices are same for the nominal and the real plant. The input matrix is in Eq. (E.3), the output matrix is in (E.4) and the feedthrough matrix is in (E.5).

$$B = \begin{bmatrix} 0 & 0 & 0 \\ 0 & 15 & 40 \\ 0.1667 & 0.125 & 0 \end{bmatrix} \tag{E.3}$$

$$C = \begin{bmatrix} 1 & 0 & 0 \\ 0 & 0 & 0 \\ 0 & 0 & 0 \end{bmatrix} \tag{E.4}$$

$$D = \begin{bmatrix} 0 & 0 & 0 \\ 0 & 1 & 0 \\ 0 & 0 & 1 \end{bmatrix} \tag{E.5}$$

To design the total controller a feedback and an observer gain are found using the lqr command in matlab. The feedback gain found is shown in Eq. (E.6), while the observer gain is shown in Eq. (E.7). Both the feedback gain and the observer gain have been set to 0 for input two and three since they are uncontrollable.

$$F = \begin{bmatrix} -1.0582 & -0.0014 & -0.4171 & 0.1000 \\ 0 & 0 & 0 & 0 \\ 0 & 0 & 0 & 0 \end{bmatrix} \tag{E.6}$$

$$L = \begin{bmatrix} -0.328 & 0 & 0 \\ -0.1313 & 0 & 0 \\ -0.2568 & 0 & 0 \end{bmatrix} \tag{E.7}$$

The feed forward gain, R, is found using the closed loop nominal system without the integral state and is calculated to be as shown in Eq. (E.8).

$$R = \begin{bmatrix} 2.3 & 0 & 0 \\ 0 & 1 & 0 \\ 0 & 0 & 1 \end{bmatrix} \tag{E.8}$$

Simulation of Plant

A system consisting of 3 states, 1 controllable input, 2 uncontrollable inputs and 3 outputs is used for the simulation example. The system is extended with an observer adding 3 observer states and integral feedback adding an integral state to the system matrix.

The closed loop system can thus be describes as in Eq. (E.9). The reference is used instead of input one, while the two uncontrollable inputs are seen as independent of the controller and are therefore independent of any controller reference.

$$
\begin{aligned}
\begin{bmatrix} \dot{x} \\ \dot{\hat{x}} \\ \dot{x}_i \end{bmatrix} &= \begin{bmatrix} A & BF_x & BF_i \\ -LC & \hat{A} + BF_x + LC & BF_i \\ -C & 0 & 0 \end{bmatrix} \begin{bmatrix} x \\ \hat{x} \\ x_i \end{bmatrix} + \begin{bmatrix} BR \\ BR \\ I \end{bmatrix} \begin{bmatrix} r \\ u_2 \\ u_2 \end{bmatrix} \\
y &= \begin{bmatrix} C & 0 & 0 \end{bmatrix} \begin{bmatrix} x \\ \hat{x} \\ x_i \end{bmatrix} + \begin{bmatrix} DR \end{bmatrix} \begin{bmatrix} r \\ u_2 \\ u_2 \end{bmatrix}
\end{aligned}
\tag{E.9}
$$

The system is discretized in order to simulate 200 seconds with a time step of 0.1 second. The system is discretized using the c2d command in matlab. The states are updated as shown in Eq. (E.10) where the controllable input is substituted with the reference and disturbance is directly feed into the two uncontrollable inputs.

$$
\begin{aligned}
\begin{bmatrix} x_1[k+1] \\ x_2[k+1] \\ x_3[k+1] \\ \hat{x}_1[k+1] \\ \hat{x}_2[k+1] \\ \hat{x}_3[k+1] \\ x_i[k+1] \end{bmatrix} &= \begin{bmatrix}
0.9566 & 0.0014 & 0.0372 & -0.0003 & -0.0000 & -0.0001 & 0.0000 \\
0.4121 & 0.0015 & 0.0138 & -0.0001 & -0.0000 & -0.0000 & 0.0000 \\
0.0926 & 0.0001 & 0.9067 & -0.0160 & -0.0000 & -0.0065 & 0.0016 \\
0.0311 & 0.0000 & 0.0006 & 0.9252 & 0.0013 & 0.0365 & 0.0000 \\
0.0126 & 0.0000 & 0.0002 & 0.3749 & 0.0017 & 0.0126 & 0.0000 \\
0.0246 & 0.0000 & 0.0005 & 0.0517 & 0.0001 & 0.8996 & 0.0016 \\
-0.0978 & -0.0001 & -0.0019 & 0.0000 & 0.0000 & 0.0000 & 1.0000
\end{bmatrix} \begin{bmatrix} x_1[k] \\ x_2[k] \\ x_3[k] \\ \hat{x}_1[k] \\ \hat{x}_2[k] \\ \hat{x}_3[k] \\ x_i[k] \end{bmatrix} \\
&+ \left[\begin{array}{c|cc}
0.0007 & 0.0020 & 0.0048 \\
0.0002 & 0.2148 & 0.5726 \\
0.0374 & 0.0119 & 0.0002 \\
0.0007 & 0.0020 & 0.0048 \\
0.0002 & 0.2148 & 0.5726 \\
0.0374 & 0.0119 & 0.0002 \\
0.1000 & 0 & 0
\end{array}\right] \begin{bmatrix} r[k] \\ u_2[k] \\ u_3[k] \end{bmatrix}
\end{aligned}
\tag{E.10}
$$

The output is updated using Eq. (E.11).

$$
y[k] = \begin{bmatrix} 1 & 0 & 0 & 0 & 0 & 0 & 0 \\ 0 & 0 & 0 & 0 & 0 & 0 & 0 \\ 0 & 0 & 0 & 0 & 0 & 0 & 0 \end{bmatrix} \begin{bmatrix} x_1[k] \\ x_2[k] \\ x_3[k] \\ \hat{x}_1[k] \\ \hat{x}_2[k] \\ \hat{x}_3[k] \\ x_i[k] \end{bmatrix} + \begin{bmatrix} 0 & 0 & 0 \\ 0 & 1 & 0 \\ 0 & 0 & 1 \end{bmatrix} \begin{bmatrix} r[k] \\ u_2[k] \\ u_3[k] \end{bmatrix}
\tag{E.11}
$$

With Observer gain and and feedback designed an simulation of 200 seconds have been done in order to verify that the system is indeed stabilized and to create a data sequence to identify the system with. The controllable input, u_1 have zero noise, while the two uncontrollable input have been given a noise signal generated using a normal distribution with a mean of 0 and a variance of 1. The reference was set to 20 and output 1 were tracked. The result can be seen on Fig. E.2.

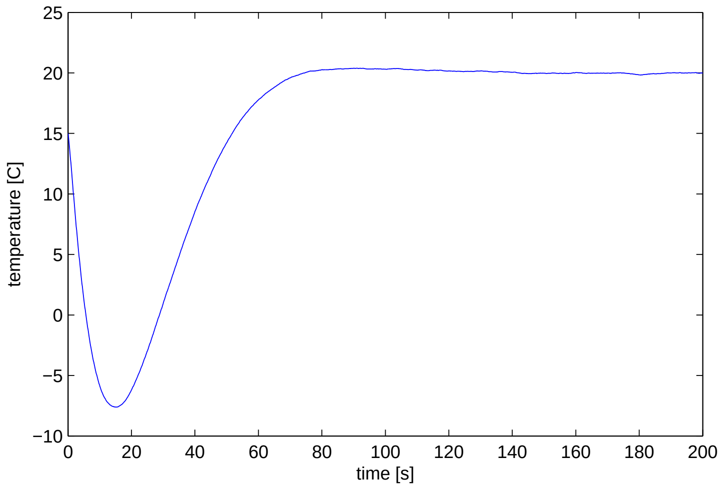

Fig. E.2: Simulated output for 200 seconds.

The integral state is shown on Fig. E.3, which is seen to go towards a steady state to compensate for the observer error.

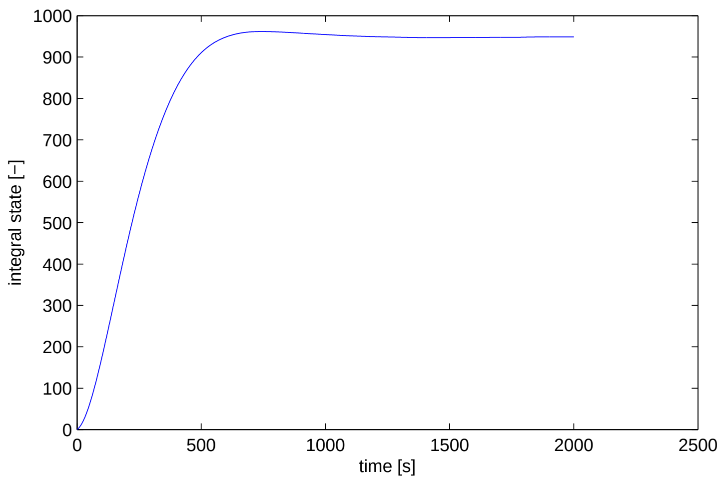

Fig. E.3: Simulated integral state for 200 seconds.

Data Creation

A data sequence needed to identify the plant is generated using the real plant and the controller designed. The states are initialized with the vector shown in Eq. (E.12), and the input vector at each time step is calculated using Eq. (E.13).

$$\begin{bmatrix} x_1 \\ x_2 \\ x_3 \end{bmatrix} = \begin{bmatrix} 15 \\ 10 \\ 12 \end{bmatrix} \tag{E.12}$$

$$u(k) = F \cdot \begin{bmatrix} \hat{x} \\ x_i \end{bmatrix} + R \cdot \begin{bmatrix} r \\ u_2 \\ u_3 \end{bmatrix} \tag{E.13}$$

The simulation was run for 200 seconds with a step time of 0.1 second. The two uncontrollable inputs were simulated with as white noise with zero mean and a standard deviation of 1. The 3 input signals are shown on Fig. E.4

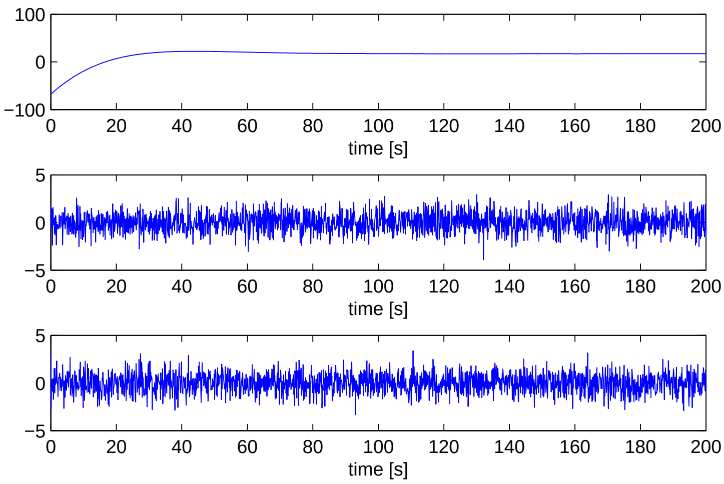

Fig. E.4: Plot of the 3 input signals generated by simulations with the real plant and the controller designed to stabilize it.

E.1 Coprime Factorization

Using the coprime factorizations derived in 7 the frequency response of the plant is compared with the right, ND^{-1}, and left, $\bar{D}^{-1}\bar{N}$, coprime factorizations of the plant. As seen in Fig. E.5 the frequency response is the same for all 3 plants as expected. The factorization method is therefore working as intended.

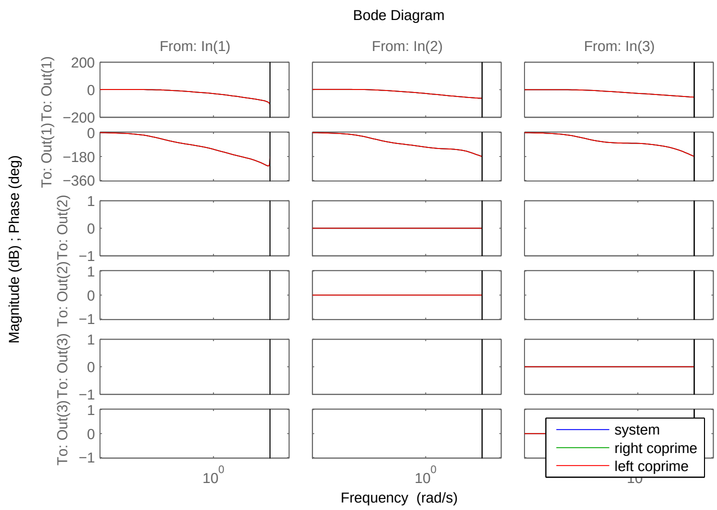

Fig. E.5: Bode plot of the plant to be identified and the respective right and left coprime factorizations of the plant. Each have its own color with the plant color being blue, the right coprime being green and the left coprime being red.

With the corpime factorization of the plant verified the left and right coprime factorizations of the plant are investigated. The controller consist of the observer and the integral state which can be shown to be the state space representation in Eq. (E.14).

$$
\begin{bmatrix} \dot{\hat{x}} \\ \dot{x}_i \end{bmatrix} = \begin{bmatrix} A + HC + BF_x + HDF_x & BF_i + HDF_i \\ 0 & 0 \end{bmatrix} \begin{bmatrix} \hat{x} \\ x_i \end{bmatrix} + \begin{bmatrix} -H \\ -I \end{bmatrix} y
$$

$$
u = \begin{bmatrix} F_x & F_i \end{bmatrix} \begin{bmatrix} \hat{x} \\ x_i \end{bmatrix} \tag{E.14}
$$

On Fig. E.6 the dynamics of the controller are compared with the right and left coprime factorizations. It is seen that all 3 plots are equal and the factorization of the controller is thus verified.

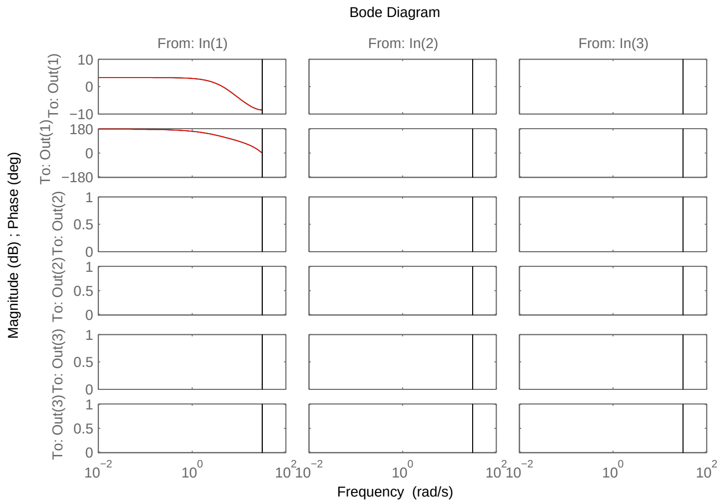

Fig. E.6: Bode plot of the controller and the respective right and left coprime factorizations. Each have its own color with the controller color being blue, the right coprime being green and the left coprime being red.

With the factorization of the plant and controller verified and initial guess made the open loop error can be found.

E.2 Error Calculation

The unidentified plant is not directly found when using the Youla-Kucera method for system identification. Instead a fit for the open loop error block, S is found. Knowing the true plant and the nominal model might therefore not give an intuitive idea of what the S-block is supposed to be. It is however possible to find out what S should approximate towards when using a known plant and knowing the nominal plant and nominal controller as well. The plant can be described as in Eq. (E.15).

$$
P = (N + YS)(D - XS)^{-}1 \tag{E.15}
$$

It is possible to isolate S by some simple matrix manipulations. The S-block can therefore be determined using Eq. (E.18)

$$
\begin{aligned}
P(D - XS) &= N + YS && \text{(E.16)}\\
PD - N &= PXS + YS = (PX + Y)S && \text{(E.17)}\\
(PX + Y)^{-1}(PD - N) &= S && \text{(E.18)}
\end{aligned}
$$

A bode plot of the S that map from the nominal to the real plant can be seen on Fig. E.7. It is worth to notice that the gain is zero between all inputs and output 2 and 3 due to the full knowledge of these two systems.

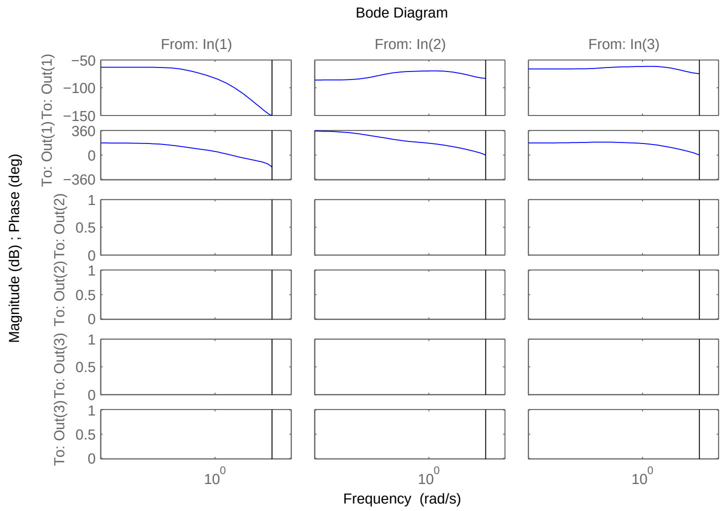

Fig. E.7: Bode plot of the open loop error.

E.3 Identification

Hansen scheme is used to identify the S-block and thus the real system. The Hansen scheme explained in 4.2 is showed as a block diagram in Fig. E.8.

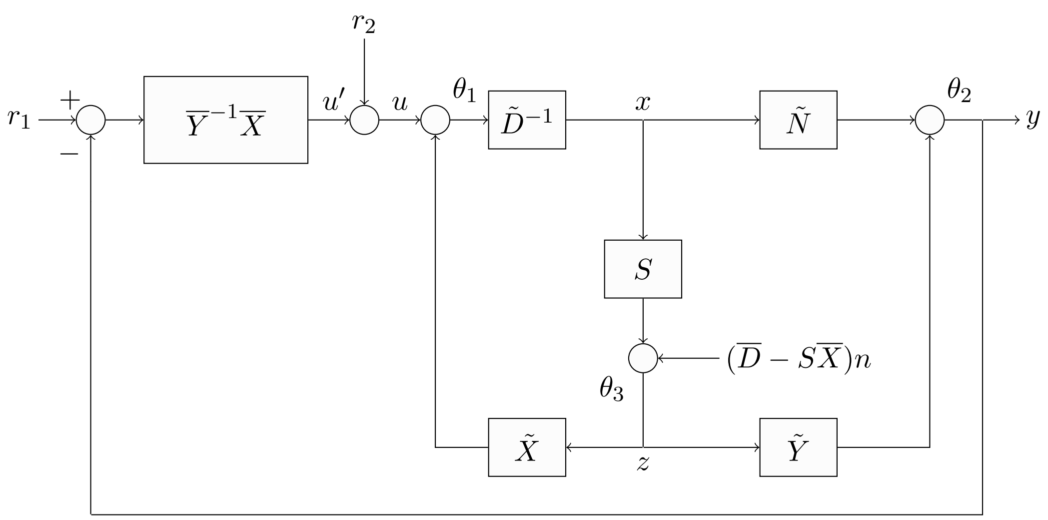

Fig. E.8: Block diagram of the Hansen scheme.

To identify the S-block using the Hansen scheme the two sequences x and z need to be calculated using Eq. (E.19) and Eq. (E.20).

$$x = \bar{X}r_1 + \bar{Y}r_2 \tag{E.19}$$
$$z = \bar{D}y - \bar{N}u \tag{E.20}$$

The two unknown sequences, r_1 and r_2 are seen respectively as the reference and the reference in feed forward together with the two unknown input signals. A block diagram of how r_1 and r_2 is determined is shown in Fig. E.9.

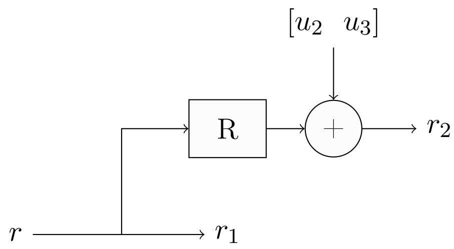

Fig. E.9: Calculation method of r_1 and r_2.

The identification process is conducted using the *n4sid* command in matlab and a bode plot of the S-block can be seen in fig. E.10 together with the open loop error block calculated using Eq. (E.18).

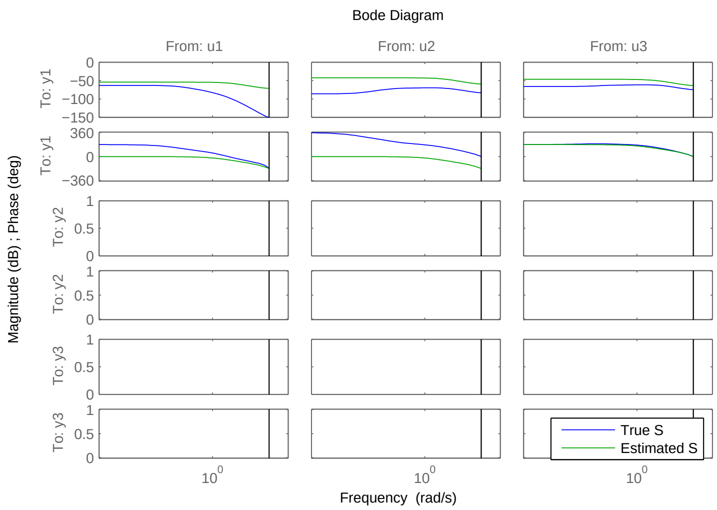

Fig. E.10: Bode plot of the open loop error.

The plant can be found using the open loop error block in Eq. (E.21) or in Eq. (E.22) [10].

$$P_{right} = (N + YS)(D - XS)^{-1} \tag{E.21}$$
$$P_{left} = (\bar{D} - S\bar{X})^{-1}(\bar{N} + S\bar{Y}) \tag{E.22}$$

E.4 Model Reduction

A side effect of the identification method is that the identified plant often contains many non important states. Before looking at the step response a pole zero plot of the identified plant is investigated. For the rest of the example the method will be shown for the right coprime factorization, but the method is equivalent for the left coprime factorization. To find out how many states can be reduced from the system while keeping the same dynamics the Hankel singular values of the plant are calculated. On Fig. E.11 the singular values can be seen and it is easy to spot that two states contain more energy than the rest.

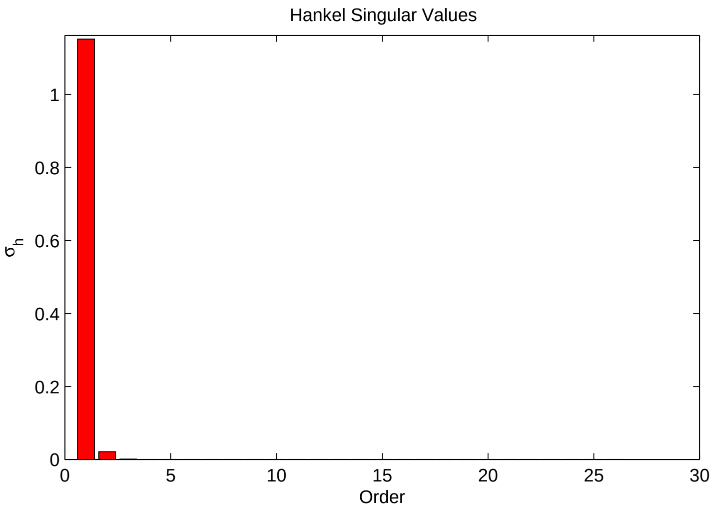

Fig. E.11: Hankel singular values of the identified plant.

The number of states to throw away can also be seen on Fig. E.12 where the pole zero plot of the identified plant is shown. The right figure is a zoom of the left and it is clear to see that the right most pole is not canceled out while there are two poles together with the left zero and one of those should therefore also not be removed.

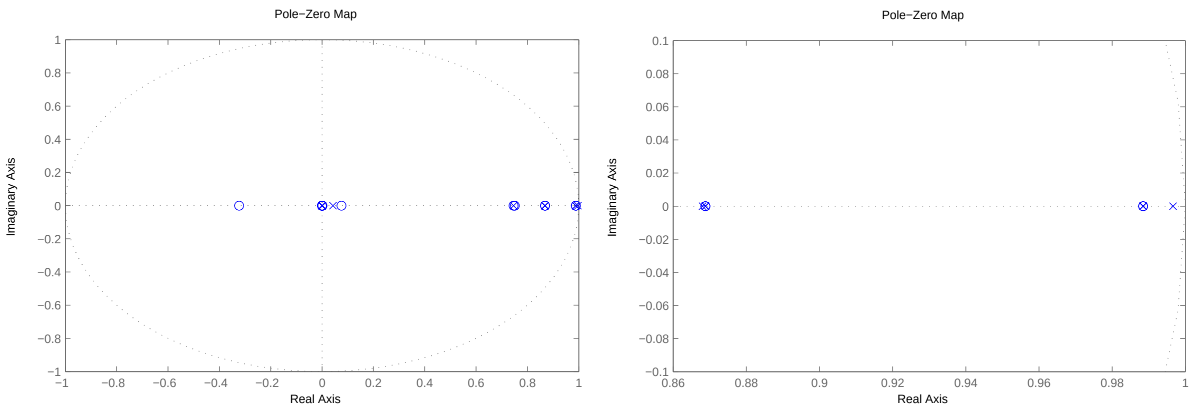

Fig. E.12: Pole zero plot of the identified system. On the left is a pole zero plot of all the poles and zeros shown while a plot of the two important poles are shown on the right.

With the use of the balreal function in matlab the two states are identified and using the modred function the model is reduced to only containing two states that were found to have the highest "energy". The zero pole plot of the reduced system can be seen together with the system tried to identify on Fig. E.13. It is worth to notice that the model were reduced to two states although the real plant had 3. The reason that this is possible can be found on Fig. E.13 where it is noticed that the third state is removed by a zero and therefore not important to identify.

The model reduced left and right coprime factorized plant have been compared with the bode

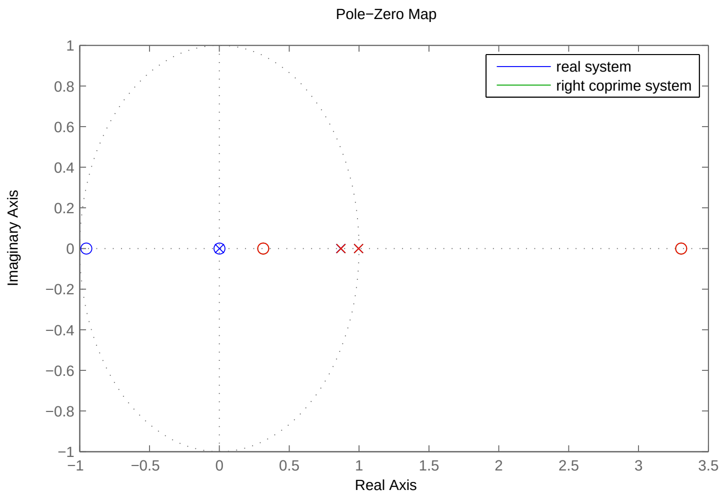

Fig. E.13: Zero pole plot for the reduced model and for the plant tried to identify.

plot of the real plant and the bode plot of an direct identification using the *n4sid* directly on the input and output data generated in the simulation. The result can be seen in Fig. E.14. It can be seen that the direct identification method have a 180 degree phase shift from input 2 to output 1 and the gain is off too for input 2 and 3.

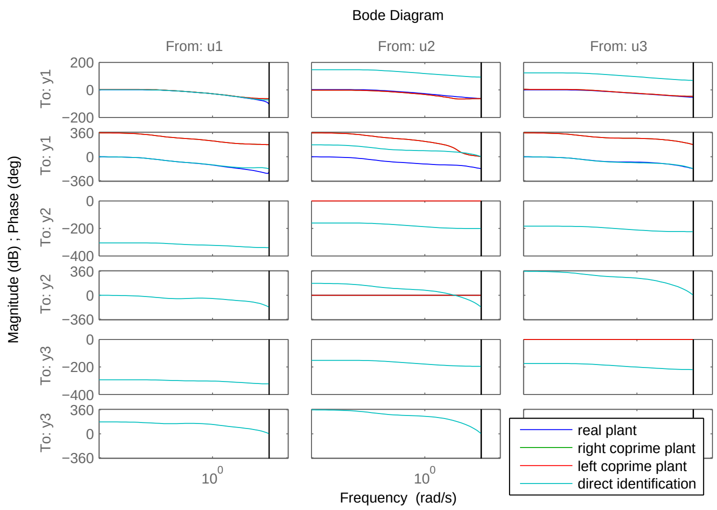

Fig. E.14: Bode plot of the real plant, and the identified plants.

Verification

A verification sequence have been generated to investigate how well the model fit. The verification sequence was generated by let input one be 15 and let the plant reach steady state. With the plant in steady state input one were stepped to 20 and a verification sequence of 100 seconds were generated.

The 4 models (nominal plant, left coprime factorized plant, right factorized plant, directly identified plant) have been compared with the input and output data using the compare function in matlab. The result can be seen on Fig. E.15 where the direct identification have been left out because the inability to follow the real output made it impossible to see the other data.

The normalized root mean square error (NRMSE) seen in Eq. (E.23) is used to compare the

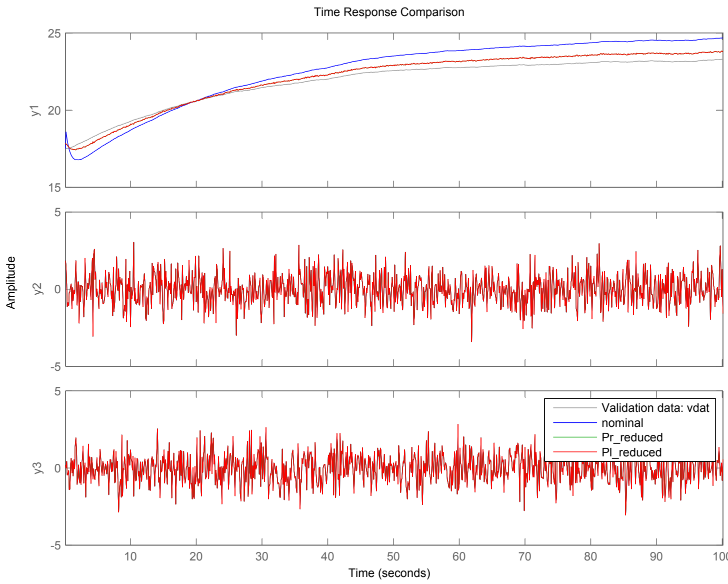

Fig. E.15: Comparison of output for the 3 models together with the real output data.

goodness of the fit. Here $\hat{y}$ is the estimated output using the model with the input, while y is the output given by the simulation.

$$\phi = 100 \cdot \left(1 - \frac{|\hat{y} - y|}{|\hat{y} - mean(\hat{y})|}\right) \tag{E.23}$$

The NRMSE for the nominal plant is 6 % while the right and left coprime factorized plants have an NRMSE of 67 % which is an significant improvement.

F Coprime Factorizations

In this chapter the coprime factorizations are simply listed for easy reference.

$$\tilde{N} = \left[\begin{array}{cc|c} A+BF_x & BF_i & BR \\ -C-DF_x & -DF_i & I-DR \\ \hline C+DF_x & DF_i & DR \end{array}\right] \tag{F.1}$$

$$\tilde{D} = \left[\begin{array}{cc|c} A+BF_x & BF_i & BR \\ -C-DF_x & -DF_i & I-DR \\ \hline F_x & F_i & R \end{array}\right] \tag{F.2}$$

$$\bar{N} = \left[\begin{array}{cc|c} A+HC & 0 & B+HD \\ -R^{-1}F_x & -R^{-1}F_i & R^{-1} \\ \hline -C & 0 & -D \end{array}\right] \tag{F.3}$$

$$\bar{D} = \left[\begin{array}{cc|c} A+HC & 0 & -H \\ -R^{-1}F_x & -R^{-1}F_i & -I \\ \hline C & 0 & -I \end{array}\right] \tag{F.4}$$

$$\tilde{X} = \left[\begin{array}{cc|c} A+BF_x & BF_i & H \\ -C-DF_x & -DF_i & I \\ \hline -F_x & -F_i & 0 \end{array}\right] \tag{F.5}$$

$$\tilde{Y} = \left[\begin{array}{cc|c} A+BF_x & BF_i & H \\ -C-DF_x & -DF_i & I \\ \hline C+DF_x & DF_i & -I \end{array}\right] \tag{F.6}$$

$$\bar{X} = \left[\begin{array}{cc|c} A+HC & 0 & -H \\ -R^{-1}F_x & -R^{-1}F_i & -I \\ \hline -R^{-1}F_x & -R^{-1}F_i & 0 \end{array}\right] \tag{F.7}$$

$$\bar{Y} = \left[\begin{array}{cc|c} A+HC & 0 & B+HD \\ -R^{-1}F_x & -R^{-1}F_i & R^{-1} \\ \hline -R^{-1}F_x & -R^{-1}F_i & R^{-1} \end{array}\right] \tag{F.8}$$